

**NIR SPECTROSCOPIC AND LASER INDUCED
FLUORESCENCE STUDIES OF SOME ORGANIC
MOLECULES**

Thesis Submitted to
Gochin University of Science and Technology
in partial fulfilment of the requirements
for the award of the degree of
DOCTOR OF PHILOSOPHY

By

Sunny Kuriakose

Department of Physics
Cochin University of Science and Technology
Cochin 682 022 India.

November 2003

Not on my merits... but on His grace...

.....Dedicated to my parents and family



Department of Physics
Cochin University of Science and Technology
Cochin 682 022

CERTIFICATE

Certified that the work presented in this thesis entitled “ **NIR Spectroscopic and Laser Induced Fluorescence studies of some organic molecules**” is based on the bonafide research work done by Mr. Sunny Kuriakose under my guidance in the Department of Physics Cochin University of Science and Technology, Cochin 682 022, and has not been included in any other thesis submitted previously for the award of any degree.

Cochin- 22
07-10-2003

Dr. T.M Abdul Rasheed
(Supervising guide)
Reader, Dept. of Physics
CUSAT, Kochi-22

Present Affiliation:
Assistant professor
Department of Physics
King Faisal University
Damam, Saudi Arabia



Department of Physics
Cochin University of Science and Technology
Cochin 682 022

CERTIFICATE

Certified that the work presented in this thesis entitled “ **NIR Spectroscopic and Laser Induced Fluorescence studies of some organic molecules**” is based on the bonafide research work done by Mr. Sunny Kuriakose under my guidance in the Department of Physics, Cochin University of Science and Technology, Cochin 682 022 and has not been included in any other thesis submitted previously for the award of any degree.


Cochin- 22
10-10-2003

K.P. Rajappan Nair
Prof. K.P Rajappan Nair
(Co-guide)
Dean, Faculty of Science
CUSAT, Cochin-22

DECLARATION

I hereby declare that the present work entitled “NIR SPECTROSCOPIC AND LASER INDUCED FLUORESCENCE STUDIES OF SOME ORGANIC MOLECULES” is based on the original work done by me under the guidance of Dr. T. M. Abdul Rasheed, Reader, Department of Physics and under the co-guidance of Prof. K. P. Rajappan Nair, Dean, Faculty of Science, Cochin University of Science and Technology, Kochi 22 and has not been included in any other thesis submitted previously for the award of any degree.

Kochi – 22
Date: 25-11-2003


Sunny Kuriakose

Acknowledgement

With great pleasure I express my deepest gratitude to my guide Dr. T.M Abdul Rasheed Reader, Dept. of Physics, Cochin University of science and technology for his excellent guidance and constant encouragement.

My sincere thanks are not less to, Dr. K.P.Rajappan Nair, Dean Faculty of sciences Cochin University of science and technology for his valuable suggestions and directions during this course of work.

I am thankful to Prof K.P Vijay Kumar, Head, Dept. of Physics, Cochin University of Science and Technology and Prof. M. Sabir, Prof. Elizabeth Mathai former Heads of the department and Dr. M.K. Jayaraj for providing the necessary facilities. And I thank all the teaching and non-teaching staff of the Dept. of physics for their sincere co-operation.

I am extremely grateful to Dr.S.Shaji, Dr.Shibu.M.Eappen and Ms Jyotsna Ravi for the valuable help extended to me during the course of this work. I owe a lot to Mr.K.K.Vijayan, Ms.B.Syamalakumari, Ms.T.Nandini, Mr. Thomas.P.Zachzria and Ms.Usha John, my colleagues in the Laser spectroscopy Lab.

I thank Ms.K.Bindu, Mr.S.Thomas Lee, Ms. Denny Mathew, Mr. K.Raveendranath, Mr. R.Manoj, Mr. Alex Mathew and Mr. Jimmy Paul for their timely help.

I remain thankful to Principal, Maharajas College, Ernakulam and all staff members in the Dept. of Physics, for their kind advice and encouragement.

I am grateful to all faculty members, General section, Govt. Polytechnic, Kalamassery for their co-operation during the period of the work.

I must thank the university grants commission for granting the teacher fellowship, the Higher education department of Kerala for permitting to proceed on leave and the Cochin University of Science and Technology for providing me the facilities.

I am extremely grateful to my parents, wife, children and all other members of family for their support, love and encouragement.

Sunny Kuriakose

CONTENTS

PREFACE	Page
Chapter 1 NIR Vibrational overtone spectroscopy of polyatomic molecules	
1.1 Introduction	1
1.2 Vibrational spectroscopy	3
1.3 Vibrational energy of a diatomic molecule	4
1.4 Normal modes of vibration of polyatomic molecules	6
1.5 Anharmonicity	7
1.6 Vibrational overtone excitation of polyatomic molecules in the ground electronic state	8
1.7 Local mode treatment of higher excited vibrational levels	9
1.8 Refinements in local mode model	13
1.9 Applications of overtone spectroscopy in molecular structural studies	17
1.10. Intramolecular vibrational energy redistribution (IVR) dynamics	22
1.11 Intensity aspects in overtone spectra	25
References	27
Chapter 2 NIR Analysis of some aromatic molecules	
2.1 Introduction	33
2.2 Experimental	34
2.3 Results and discussion	35
2.3.1 Analysis of the overtone spectra of benzaldehyde and salicylaldehyde	35
2.3.2 Aldehydic CH overtones	42
2.3.3 Aryl CH overtones	45
2.3.4 Analysis of the overtone spectrum of phenyl hydrazine	47
2.3.5 Analysis of the vibrational overtone spectra of phenol, <i>o</i> -chlorophenol and <i>p</i> -chlorophenol	53
References	73
Chapter 3 NIR analysis of some aliphatic molecules	
3.1 Introduction	75
3.2 Experimental	76

3.3	Results and Discussion	76
3.3.1	Analysis of the overtone spectra of formamide	76
3.3.2	Analysis of overtone spectra of allyl alcohol and allyl chloride	83
3.3.3	Analysis of CH overtone absorption spectrum of nitromethane using local mode picture	91
	References	99

Chapter 4 Pulsed LIF and Raman Studies of some organic molecules

4.1	Introduction	101
4.2	Fluorescence	102
4.2.1	Fluorescence properties of aliphatic compounds	103
4.2.2	Fluorescence properties of aromatic compounds	103
4.3	LIF in molecular structural studies – some recent works	106
4.4	Raman spectroscopy	108
4.5	Laser Raman Spectroscopy in molecular structural studies – some recent works	111
4.6	The present experimental setup	112
4.7	Experimental considerations	114
4.8	Preparation of the polymer thin film of <i>o</i> -chloroaniline	115
4.9	Laser induced fluorescence spectrum of N,N diethylaniline and polymerized <i>o</i> - chloroaniline.	116
4.10	Pulsed laser Raman spectrum of <i>p</i> -chlorotoluene, nitromethane, <i>o</i> - chlorophenol and <i>m</i> -toluidine	117
4.10.1	Pulsed laser Raman spectrum of <i>p</i> -chlorotoluene	119
4.10.2	Pulsed Raman spectrum of nitromethane	121
4.10.3	Pulsed laser Raman spectrum of <i>o</i> -chlorophenol	123
4.10.4	Pulsed laser Raman spectrum of <i>m</i> -toluidine	125
4.11	Conclusions	127
	References	128

**Chapter 5 High-resolution TDL and conventional spectroscopic
study of 2-propanol in the NIR region**

5.1 Tunable Diode laser Absorption Spectroscopy	131
5.2 High resolution overtone spectroscopy – some reported works	132
5.3 Earlier measurements of OH overtone spectra in alcohols	133
5.4 The Tunable diode laser experimental set up	134
5.4.1 Tunable Diode Laser	135
5.4.2 Beam splitter	135
5.4.3 Multipass cell	135
5.4.4 Detector	136
5.5 Experimental procedure	136
5.6 High resolution spectrum of 2-propanol in the second overtone region	138
5.7 Absorption spectrum of liquid phase 2-propanol in NIR region	141
5.8 Conclusions	148
References	149
Summary & Conclusions	151

PREFACE

Vibrational overtone spectroscopy of molecules containing X-H oscillators ($X = C, N, O...$) has become an effective tool for the study of molecular structure, dynamics, inter and intramolecular interactions, conformational aspects and substituent effects in aliphatic and aromatic compounds. In the present work, we studied the NIR overtone spectra of some liquid phase organic compounds. The analysis of the CH, NH and OH overtones yielded important structural information about these systems. In an attempt to get information on electronic energy levels, we studied the pulsed Nd:YAG laser induced fluorescence spectra of certain organic compounds. The pulsed laser Raman spectra of some organic compounds are also studied. The novel high resolution technique of near infrared tunable diode laser absorption spectroscopy (TDLAS) is used to record the rotational structure of the second OH overtone spectrum of 2-propanol. The spectral features corresponding to the different molecular conformations could be identified from the high resolution spectrum.

The whole work described in this thesis is divided into five chapters. The first chapter presents an introduction and review of the area of vibrational overtone spectroscopy of X-H containing molecules ($X=C, N, O...$). It gives an outline of the local mode theory that has been used as a tool to analyse vibrational transitions in molecules in the NIR region. The vibrational overtone spectroscopic studies can yield a lot of valuable information, such as the molecular structure, intra and intermolecular interactions, radiationless transitions, intramolecular vibrational relaxations, multiphoton excitations and chemical reactivities. The general applications of vibrational overtone spectroscopy, with emphasis on deriving molecular structural details are also outlined.

The second chapter contains the details of the analysis of NIR vibrational overtone spectra of some aromatic molecules, namely benzaldehyde, salicylaldehyde, phenyl hydrazine, phenol, o-chlorophenol and p-chlorophenol. The inhibition of indirect lone pair trans effect in benzaldehyde and inhibition of

direct lone pair trans effect in salicylaldehyde are confirmed by the analysis of the overtone spectra. The observed differences in aldehydic CH local mode parameters in these compounds with respect to acetaldehyde are due to the difference in intramolecular environment present in the molecules. The presence of two non-equivalent NH oscillators in phenyl hydrazine is established. The analysis reveals the mutual lone pair interaction between the NH bond and the lone pair of the adjacent nitrogen. The overtone spectra of phenol, o-chlorophenol and p-chlorophenol are compared and the presence of intramolecular hydrogen bonding in o-chlorophenol is confirmed. In o-chlorophenol solution, as the concentration is decreased from high (saturated) values, the population of the trans form of the molecule increases, thus causing the formation of cis-trans dimer (due to intermolecular hydrogen bonding) to become dominant. This causes a decrease in the strength of the intramolecular hydrogen bonding originally present in the cis form. The weakening of intramolecular bonding causes a decrease in the electron density of the OH bond and hence an increase in the mechanical frequency value of the OH oscillator.

The third Chapter contains the details of present investigations on the overtone spectra of some aliphatic compounds namely allyl chloride, allyl alcohol, formamide and nitromethane. The possible factors influencing the local mode parameters of the vinyl CH and methylene CH in allyl chloride and allyl alcohol are discussed. The analysis of overtone spectra of formamide confirms the inhibition of lone pair trans effect. The large value of CH mechanical frequency observed in formamide with respect to the aldehydic CH mechanical frequency in acetaldehyde is explained as due to the inhibition of lone pair trans effect due to intermolecular hydrogen bonding and lone pair interaction between carbonyl oxygen and NH_2 . The CH overtone spectrum of nitromethane is analyzed using a coupled local mode Hamiltonian under C_{3v} symmetry. The observed pure local mode overtones and local-local combinations in the $\Delta V=2-5$ regions are found to agree with the peak positions predicted by the model Hamiltonian.

The fourth chapter gives the details of the Nd:YAG laser based experimental set up used for recording the LIF spectra and pulsed laser Raman spectra of some organic compounds, namely, polymerized o-chloroaniline, liquid N,N diethyl aniline, nitromethane, o-chlorophenol, p-chlorotoluene and m-toluidine. The analysis of the LIF spectra of polymerized o-chloroaniline and liquid N,N diethyl aniline and the pulsed laser Raman spectra of nitromethane, o-chlorophenol, p-chlorotoluene and m-toluidine are discussed. The characteristic fluorescence and Raman peaks for the respective groups of these molecules are identified. The observed Raman spectra show some new lines corresponding to low-lying vibrational states.

The fifth chapter demonstrates the utility of a near infrared TDL high-resolution spectrometer in recording the second overtone band of the –OH group in 2-propanol. The observed high resolution spectrum shows features corresponding to the trans and gauche conformations of the molecule. The local mode analysis of the methyl CH and OH overtone bands of liquid phase 2-propanol is also included in this chapter.

The summary and conclusions of the present study are given towards the end of the thesis.

CHAPTER 1

NIR VIBRATIONAL OVERTONE SPECTROSCOPY OF POLYATOMIC MOLECULES

1.1 Introduction

Molecular spectroscopy deals with the measurement of the interaction of light with matter, usually in the form of absorption or emission of radiant energy as a function of wavelength [1,2]. In the infrared region (IR spectroscopy) the vibrational modes in irradiated molecules are activated. Absorption bands occur in the IR spectra generally due to the normal modes in the mid-infrared (MIR) region ($400 - 4000 \text{ cm}^{-1}$) and their overtones and/or combinations in the near infrared (NIR) region ($4000 - 14000 \text{ cm}^{-1}$). In contrast to strong and sharp absorption peaks in MIR, near infrared spectra show less intensity and broad bands caused by overlapping vibrational modes.

Over the last many years, near-infrared (NIR) spectroscopy has rapidly developed into an important and extremely useful method of analysis and much exciting progress has brought it to the attention of spectroscopists working in various scientific fields. In fact, for certain research areas and applications, ranging from material science via chemistry to life sciences, it has become an indispensable tool because this fast and cost-effective type of spectroscopy provides qualitative and quantitative information not available from other analytical techniques [3-5].

A near-infrared spectrum represents combination bands and overtone bands that are harmonics of absorption frequencies in the mid-infrared. Because near-infrared bands are much less intense, more of the sample can be used to produce spectra and with near infrared, sample preparation activities are greatly reduced or eliminated. In addition, long path lengths and the ability to sample through glass in the near-infrared allows samples to be measured in common media such as culture tubes, cuvettes and reaction bottles. This is unlike mid-

infrared where very small amounts of a sample produce a strong spectrum; thus sample preparation techniques must be employed to limit the amount of the sample that interacts with the beam. Like the mid-infrared, combination bands and overtone bands correspond to the frequencies of vibrations between the bonds of the atoms making up the material. Because each different material is a unique combination of atoms, no two compounds produce the exact same near-infrared spectrum. Therefore, near-infrared spectroscopy can result in a positive identification (qualitative analysis) of each different material. In addition, the size of the peaks in the spectrum is a direct indication of the amount of material present. With modern software algorithms, near infrared is an excellent tool for quantitative analysis.

The near infrared region of the spectrum contains a great wealth of spectral data primarily concerned with hydrogenic (CH, NH, OH..) stretching vibrations, where absorptions corresponding to overtones and combinations of the fundamental vibrational transitions occur. The relative accessibility of the near infrared region of the spectrum to measurement makes this region attractive for analytical purposes as well as for molecular structure studies. The hydrogenic stretching vibrations are highly characteristic, the fundamental and overtone bands occurring at remarkably constant frequencies. These absorptions occur at considerably higher frequencies than other common fundamental absorption bands so that there is little ambiguity in the assignment of fundamental and overtone bands. In molecular structure studies, the near infrared region is particularly useful through observation of the shift or perturbation of absorption bands due to interactions of molecular groups (hydrogen bonding).

A number of advantages for quantitative analysis are offered by NIR although there are limitations in its use in structural studies. The inherent instrumental advantages of NIR are that since the emission maximum of the source is close to the region of interest, a high energy throughput and low stray radiation result. This, combined with the availability of sensitive solid state detectors, leads to a signal to noise ratio, which is typically 10000:1. Cheap and robust materials such as glass or quartz are transparent to NIR radiation and are therefore available for optical components and cells. Extremely rapid analyses are

possible since the detectors have response times measured in microseconds. However, probably the most important advantage arises from the fact that absorptivities for NIR bands are lower by at least an order of magnitude for each successive overtone. Therefore, moderately concentrated samples and more convenient path lengths compared with mid-IR may be used. This means that quantitative NIR transmission spectra of intractable materials such as plastics or protein fibres may be obtained, possibly without sample preparation or destruction of the samples. The absorptivities of solvents, including water, are sufficiently low as to cease to pose a serious problem in the NIR.

In brief, the major advantages of NIR spectroscopy are- it is quick, non destructive, remote sampling with low cost fiber optics, easy to use and can be performed on site without any lengthy sample preparation.

1.2 Vibrational spectroscopy

One of the best methods of studying internal energy changes of molecules is through spectroscopy. Of the different types of energies of a molecule possesses, the vibration of its atoms with respect to each other has the next larger energy level spacing after the rotation of the molecules. Transitions between the vibrational levels result in the vibrational spectra that give an insight in to the discrete motion of the atoms in the molecular systems. Once the vibrational frequencies are obtained, valuable information regarding molecular structure, symmetry, bond strength, inter and intramolecular interactions etc can be derived [6-9].

There are two types of spectroscopy that involve vibrational transitions – Infrared spectroscopy and Raman spectroscopy. A mode of vibration of a molecule will be infrared active if a changing dipole moment occurs during the vibration. On the other hand a mode of vibration will be Raman active if a changing polarizability results during the corresponding vibration [10,11].

At room temperature, almost all molecules reside in their lowest vibrational energy levels with quantum number $V = 0$. For each normal mode, the

most probable vibrational transition is from this level to the next highest level ($V = 0 \rightarrow 1$). These transitions result strong IR or Raman bands that are called fundamental bands. Other transitions to higher excited states result in overtone bands. Overtone bands are much weaker than fundamental bands.

1.3 Vibrational energy of a diatomic molecule

Consider the vibrations of a system of two masses m_1 and m_2 connected by a spring, which is the analogue of a diatomic molecule. If the spring is compressed and released, the system executes simple harmonic motion with fundamental frequency of the harmonic oscillator with mass m replaced by the reduced mass μ of the system

$$\nu_0 = \frac{1}{2\pi} \sqrt{\frac{k}{\mu}} \quad (1)$$

Where k is the force constant and

$$\mu = \frac{m_1 m_2}{m_1 + m_2} \quad (2)$$

Quantum mechanically, the vibrational energy of such a harmonic system is given by

$$E_V = (V+1/2) h\nu_0 \quad (3)$$

$V = 0, 1, 2, \dots$ Where 'V' is the vibrational quantum number.

Expressing the energy in cm^{-1} , we get

$$\epsilon_V = \frac{E_V}{hc} = \left(V + \frac{1}{2} \right) \frac{\nu_0}{c} = \left(V + \frac{1}{2} \right) \bar{\nu}_0 \quad (4)$$

where $\bar{\nu}_0$ is the frequency in cm^{-1} units. These energy levels are equally spaced and the energy of the lowest scale

$$\epsilon_0 = \frac{1}{2} \bar{\nu}_0 \text{cm}^{-1} \quad (5)$$

is called the zero point energy. That is, the vibrational energy is not zero even at the lowest vibrational level, indicating that a molecule must vibrate always.

In diatomic molecules, the actual potential energy curve is not of the simple harmonic type but is generally modelled by

$$U = D_{eq} [1 - \exp \{a (r_{eq} - r)\}]^2 \quad (6)$$

Where D_{eq} is the dissociation energy, a is a constant for the given molecule and r_{eq} is the internuclear distance at the minimum energy. This potential energy function is called the Morse function. With the potential in the above equation, the Schrodinger equation of such an anharmonic oscillator gives the allowed vibrational energy eigen values.

$$\varepsilon_v = \left(V + \frac{1}{2}\right) \bar{\nu}_e - \left(V + \frac{1}{2}\right)^2 x_e \bar{\nu}_e + \left(V + \frac{1}{2}\right)^3 y_e \bar{\nu}_e + \dots \quad (7)$$

Here $\bar{\nu}_e$ is the oscillation frequency of the anharmonic system in cm^{-1} , x_e and y_e are anharmonicity constants which are very small and positive for band stretching vibrations.

Retaining the first anharmonic term, we get

$$\varepsilon_v = \left(V + \frac{1}{2}\right) \bar{\nu}_e - \left(V + \frac{1}{2}\right)^2 x_e \bar{\nu}_e \text{cm}^{-1}, v = 0, 1, 2, 3 \quad (8)$$

As x_e is positive, the effect of anharmonicity is to crowd more closely the vibrational levels. These energy levels are shown in fig. 1.1. The exact zero point energy is,

$$\varepsilon_0 = \frac{1}{2} \left(1 - \frac{1}{2} x_e\right) \bar{\nu}_e \quad (9)$$

Rewriting equation (8)

$$\varepsilon_v = \left[1 - \left(V + \frac{1}{2} x_e\right)\right] \left(V + \frac{1}{2} x_e\right) \bar{\nu}_e \quad (10)$$

and equating it to that given in equation (4), we obtain

$$\bar{\nu}_0 = \bar{\nu}_e \left[1 - \left(V + \frac{1}{2} x_e\right)\right] \quad (11)$$

Here $\bar{\nu}_0$ is the oscillation frequency of the harmonic oscillator having the same vibrational energy as the anharmonic one. In other words, the anharmonic oscillator behaves like the harmonic oscillator but with an oscillation frequency that decreases with increasing v . If we set $V = 1/2$, $\varepsilon_v = 0 = 0$ and $\bar{\nu}_e = \bar{\nu}_0$. Therefore

$\bar{\nu}_e$ is considered as the (hypothetical) equilibrium oscillation frequency of the anharmonic system.

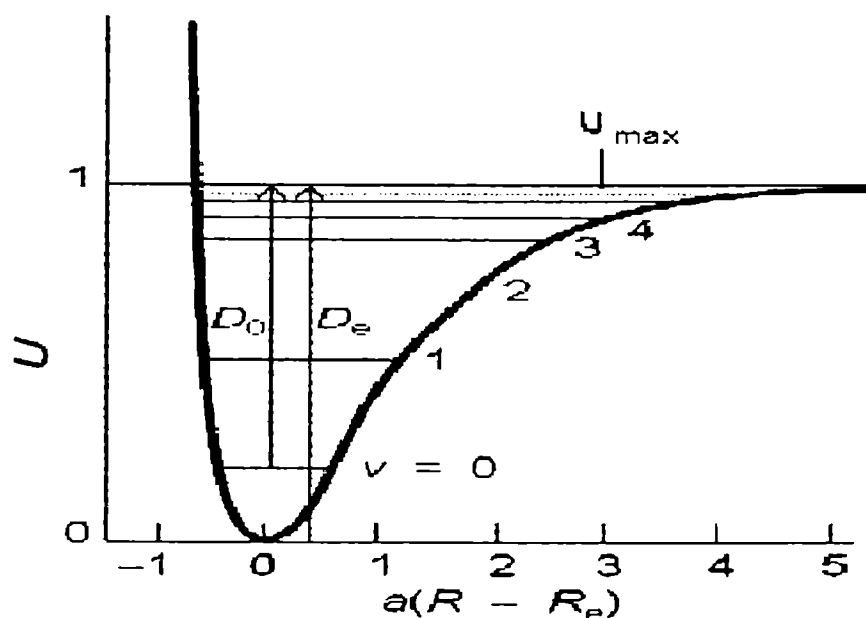


Fig1.1 Energy levels of an anharmonic oscillator

1.4 Normal modes of vibration of polyatomic molecules

A non-linear molecule with N atoms has $(3N-6)$ vibrational degrees of freedom, whereas for a linear molecule, there are $(3N-5)$ vibrational degrees of freedom. The $(3N-6)/ (3N-5)$ vibrations are called the internal vibrations or normal vibrations or fundamental vibrations of the molecule. A normal vibration is defined as a molecular motion in which all the atoms move in phase and with the same frequency, but generally with different amplitudes. Each normal mode of vibration is equivalent to a quantum mechanical harmonic oscillator with characteristic frequency. During a normal vibration, the centre of gravity of the

molecule remains unchanged. Any general vibrational motion of a molecule can be considered as a superposition of $(3N-6)/(3N-5)$ normal modes of vibrations [2].

1.5 Anharmonicity

The result of anharmonicity in a single oscillator is that the period of the oscillation varies with amplitude. The effect of this on the vibrational energy levels of a molecule undergoing vibration is to cause them to be unequally spaced. In a diatomic molecule the effect of anharmonicity is to cause the energy levels to close up smoothly with increasing value of the vibrational quantum number V and the separations of adjacent levels becomes zero at the limit of dissociation.

Whatever the form of the potential function for a particular vibration, the energy levels are always, to a quarter or lesser extent, anharmonic. The effect is often, but not always to cause the levels to close up smoothly with increasing quantum number V , rather as they do in a diatomic molecule.

Anharmonicity is taken account of in the Schrodinger equation by modifying the harmonic oscillator potential function of equation

$$V = \frac{1}{2} \sum_{i=1}^{3N-6} \sum_{j=1}^{3N-6} K_{ij} R_i R_j \quad (12)$$

When V is the Potential energy, K_{ij} the force constant, R_s can be expressed as functions of the cartesian co-ordinates,

$$R_i = f_i (x, y, z, \dots, x_{3N}, y_{3N}, z_{3N}) \quad (13)$$

or the cartesian coordinates as functions of the internal coordinates

$$x_j = f_j (R_1, R_2, \dots, R_{3N-6}) \quad (14)$$

to

$$V = \frac{1}{2} \sum_{i \leq j} K_{ij} R_i R_j + \sum_{i \leq j \leq k} K_{ijk} R_i R_j R_k + \sum_{i \leq j \leq k \leq l} K_{ijkl} R_i R_j R_k R_l + \dots \quad (15)$$

Where it is conventional to use the K symbols for force constants when sums over i, j are restricted by $i \leq j$, An alternative formulations is

$$V = \frac{1}{2!} \sum_{ij} f_{ij} R_i R_j + \frac{1}{3!} \sum_{ijk} f_{ijk} R_i R_j R_k + \dots \quad (16)$$

the f , force constants are used when the sum over i, j , is unrestricted. The first term in the potential is the quadratic term of the harmonic force field. The second and third terms correspond to the cubic and quartic contributions to the force field. Higher terms are not normally taken into account.

The solution of the Schrodinger equation for a molecule in which all vibrations are non-degenerate gives the vibrational term values

$$\sum G(V_i) = \sum \omega_i \left(V_i + \frac{1}{2} \right) + \sum_{i \neq j} x_{ij} \left(V_i + \frac{1}{2} \right) \left(V_j + \frac{1}{2} \right) + \dots \quad (17)$$

Where ω_i are the fundamental vibration wave numbers for infinitely small displacement from the equilibrium configuration. The x_{ij} are anharmonic constants.

1.6 Vibrational overtone excitation of polyatomic molecules in the ground electronic state

During the last several years, much attention was focussed on the study of the different aspects of higher excited vibrational levels of the ground electronic states of polyatomic molecules containing X-H (X=C, N, O) oscillators [12-15]. The major reasons for the motivation of this interest are the following; first, it is recognized in the study of nonradiative electronic transitions that higher excited levels of hydrogen atom based vibrations play a key role in accepting the excited electronic energy [16-19]. Second, the normal mode or harmonic description, so successful in describing the fundamental vibrations of molecules, fails to provide a satisfactory description of the anharmonic overtones. Third, an understanding of higher vibrational levels is essential in the development of the theory of multiphoton photochemistry as well as bond selective chemistry [20-22]. Finally, The spectroscopic studies of higher vibrational states are concerned with excitation of bonds to a significant fraction of their bond dissociation energies, and this can provide a link between chemical reactivity and spectroscopic properties. The development of techniques like intra cavity dye laser

photoacoustic spectroscopy has produced dramatic improvements in resolution and applicability.

The validity of the local mode (LM) description of the highly excited X-H vibrations in polyatomic molecules is now well established. The LM model is being used extensively to provide a satisfactory understanding of the appearance of high overtone absorption spectra. Theoretical treatments of the LM model have provided a strong justification for the description of the vibrationally excited molecule in terms of individual anharmonic X-H oscillators (X= C, N, O...). An outline of the theoretical basis of local mode model is given in the following section.

1.7 Local mode treatment of higher excited vibrational levels

Normal modes of vibration, with their corresponding normal coordinates are satisfactory in describing the low-lying vibrational levels, usually those with $V=1$ or 2 which can be investigated by traditional infrared absorption or Raman Spectroscopy. For certain types of vibration, particularly stretching vibrations involving more than one symmetrically equivalent terminal atom, this description becomes much less satisfactory as the vibrational quantum number V increases.

The local mode model (LM) introduced by Henry and Siebrand is used for the description of higher excited vibrational levels [23,24]. In their attempt to model nonradiative electronic transition in polyatomic molecules [17,25] they found that the Franck Condon factors for $T_1 \rightarrow S_0$ and $S_1 \rightarrow S_0$ transitions are governed by the anharmonicity of the CH stretching modes. They also found semi quantitative agreement between the anharmonicity parameter in the Franck-Condon factors and the known anharmonicity of the CH molecule. This led the authors to find the relation between the CH anharmonicity constant in the CH molecule and that in a hydrocarbon molecule. The local mode model is the outcome of these investigations.

The concept of normal modes arises from the analysis of vibrational motion for infinitesimal amplitudes where the molecule is considered as $3N-6$ (non-linear) or $3N-5$ (linear) uncoupled harmonic oscillators [26,27]. This model

is found to be successful in explaining the fundamental and the lower overtone spectra of polyatomic molecules. However, it cannot be valid under every condition. Consider the CH stretching vibrations of benzene. Since there are six identical C-H bonds there are six CH stretching vibrations. If we excite the molecule with sufficiently high energy, it will eventually dissociate losing six hydrogen atoms in the process.



This seems reasonable when we think only in terms of normal vibrations but intuition suggests that, since the dissociation in equation (18) would require something like six times the C-H bond dissociation energy, the process



is surely more likely to occur. The difficulty here is that no normal vibration of benzene leads to CH stretching being localised in only one bond. These considerations together with a very early observation of overtone bands up to eight quanta of CH stretching in benzene, led to the concept of a local mode of vibration.

In diatomic molecules, there is a clear-cut relation between the anharmonicity constant X and the dissociation energy D . For e.g., if Morse potential is assumed this relation takes the following form

$$X = -\frac{\omega^2}{4D} \quad (20)$$

In polyatomic molecules the relation between normal mode anharmonicity constants X_{KL} , bond dissociation energies D_i and normal mode dissociation energies D_k , is not obvious. For those normal modes in which the vibrational energy is evenly distributed among a number of equivalent chemical bonds, the dissociation energy D_k refers to the sum of all bond energies D_i , $D_k = \sum D_i$. This implies a large value of D_k and thus a small value of the diagonal normal mode anharmonicity constant X_{kk} . As mentioned earlier the physically important dissociation is the rupture of a single chemical bond. The vibration associated with this rupture is not a normal mode but it is termed as a local mode. Its dissociation energy is much smaller than the normal mode dissociation energy; $D_i \ll D_k$ so that the corresponding anharmonicity constant X_{ii} will be much larger

than X_{kk} . In other words for high vibrational quantum levels, the vibrational energy become increasingly more diagonal in a local mode representation than in a normal mode representation, that is the molecule will oscillate in a pattern close to a local mode rather than a normal mode.

Henry and co-workers used these local mode ideas to obtain normal mode anharmonicity constants. They described the overtone spectra of molecules like NH_3 , C_6H_6 , CH_2Cl_2 etc. in terms of the components of normal mode anharmonicity constants. It was concluded from these studies that higher vibrational levels of X-H (X=C, N, O) containing molecules cannot be described in terms of a set of symmetry allowed normal mode components but instead by a relatively small number of most anharmonic motions namely, localised excitations of bond modes [23,28]. Swofford et al in their study of the fifth overtone spectra of benzene and its deuterated analogues using thermal lens technique [29] have given a quantum mechanical description of the one dimensional (single bond based) appearance of CH overtone spectra with particular application to benzene. This theory forms the basis of the local mode treatment of any molecule.

The number of symmetry allowed states increases dramatically with quantum number [27], if the conventional normal mode description is used. The total number of vibrational levels increases much more rapidly with the quantum number. This is given by Bose statistics by which there are ${}^{V+N-1}C_V$ ways of distributing V quanta over N sites. Thus there are 462 CH based levels for benzene at $V=6$. Of these, 150 states are allowed. These are the 75 doubly degenerate states with E_1 symmetry. However experimental observations show only a single broad peak in the aryl CH $\Delta V=6$ region for benzene, deuterated benzenes and substituted benzenes. This clearly demonstrates the success of the local mode model of uncoupled anharmonic oscillators localized on individual CH bonds.

The energy levels of one dimensional anharmonic oscillator is given by the perturbation theory [27] as

$$\Delta E_{V,0} = -1/2 (X_1 + \frac{1}{2} X_2) + (V + \frac{1}{2}) X_1 + (V + \frac{1}{2})^2 X_2 \quad (21)$$

Ellis [30,31] fitted the observed overtone bands of benzene to equation

$$\Delta E_{V,0} = AV + BV^2 \quad (22)$$

Hamiltonian to analyse the overtone spectrum of 2-butanone. They showed that the CH₃ group away from the carbonyl maintains C_{3v} symmetry whereas that adjacent to the carbonyl loses C_{3v} symmetry due to anisotropic environments created by lone pair and π electrons. Our analysis of the CH overtone spectrum of nitromethane has shown that the observed pure CH local mode overtones and local local combinations are well predicted by a C_{3v} coupled oscillator Hamiltonian (Chapter 3). The general form of the coupled local mode Hamiltonian used for an XH_n system is [58-63]

$$\begin{aligned}
 H = \omega \sum V_i + \omega_x \sum (V_i + V_i^2) + \frac{\omega}{2} \sum_{i=1}^n \sum_{j=1}^n \phi (a_i^+ - a_i) (a_j^+ - a_j) \\
 + \frac{\omega}{2} \sum_{i=1}^n \sum_{j=1}^n \gamma (a_i^+ + a_i) (a_j^+ + a_j)
 \end{aligned}
 \tag{23}$$

Here the first two terms represent the unperturbed local mode energy and the last two terms represent the harmonic coupling between the local modes. Here ω and ω_x are respectively the mechanical frequency (X_1) and anharmonicity ($-X_2$) of the X-H bonds, V_i and V_j are the quantum numbers for the i th and j th X-H bond respectively. The parameter γ characterises the kinetic energy coupling between the different XH oscillators and ϕ , the corresponding potential energy coupling. These coupling parameters are related to Wilson G and F matrix elements respectively

$$\gamma = -\frac{1}{2} \frac{G_{ij}}{G_{ii}}
 \tag{24}$$

$$\phi = +\frac{1}{2} \frac{F_{ij}}{F_{ii}}
 \tag{25}$$

The operators a^+ and a are related to the normalised momentum and coordinate variables through

$$p = (a^+ - a)
 \tag{26}$$

$$q = (a^+ + a) \quad (27)$$

and have the usual raising and lowering properties in the harmonic oscillator limit [64].

$$\langle V+1 | a^+ | V \rangle = (V+1)^{1/2} \quad (28)$$

$$\langle V-1 | a | V \rangle = V^{1/2} \quad (29)$$

These properties are shown to be valid to a good approximation even for Morse oscillators [58]. This is called Ladder approximation. Since manifolds corresponding to different values of the total quantum number ($\sum V_i$) are well separated in energy, intermanifold couplings are neglected. With these two approximations the Hamiltonian matrix elements are calculated for the symmetrised basis sets relevant to the problem. Table 1.1 shows the Hamiltonian matrices for XH_3 groups [63]. The details of the calculation of overtone spectra using these Hamiltonian matrices are given in chapter 3 where our work on nitromethane is presented.

V=1	$\langle 100;A_1 $	$\omega - 2\omega x + 2\lambda$			
	$\langle 100;E $	$\omega - 2\omega x - \lambda$			
V=2	$\langle 200;A_1 $	$2\omega - 6\omega x$	$2\sqrt{2}\lambda$		
	$\langle 110;A_1 $	$2\sqrt{2}\lambda$	$2\omega - 4\omega x + 2\lambda$		
	$\langle 200;E $	$2\omega - 6\omega x$	$-\sqrt{2}\lambda$		
	$\langle 110;E $	$-\sqrt{2}\lambda$	$2\omega - 4\omega x - \lambda$		
V=3	$\langle 300;A_1 $	$3\omega - 12\omega x$	$\sqrt{6}\lambda$	0	
	$\langle 210;A_1 $	$\sqrt{6}\lambda$	$3\omega - 8\omega x + 3\lambda$	$2\sqrt{3}\lambda$	
	$\langle 111;A_1 $	0	$2\sqrt{3}\lambda$	$3\omega - 6\omega x$	
	$\langle 210;A_2 $	$3\omega - 8\omega x - 3\lambda$			
	$\langle 300;E $	$3\omega - 12\omega x$	$\sqrt{6}\lambda$	0	
	$\langle 210;1E $	$\sqrt{6}\lambda$	$3\omega - 8\omega x$	$-\sqrt{3}\lambda$	
	$\langle 210;2E $	0	$-\sqrt{3}\lambda$	$3\omega - 8\omega x$	
V=4	$\langle 400;A_1 $	$4\omega - 20\omega x$	$2\sqrt{2}\lambda$	0	0
	$\langle 310;A_1 $	$2\sqrt{2}\lambda$	$4\omega - 14\omega x + \lambda$	$2\sqrt{3}\lambda$	$\sqrt{6}\lambda$
	$\langle 220;A_1 $	0	$2\sqrt{3}\lambda$	$4\omega - 12\omega x$	$2\sqrt{2}\lambda$
	$\langle 211;A_1 $	0	$\sqrt{6}\lambda$	$2\sqrt{2}\lambda$	$4\omega - 10\omega x + 4\lambda$
	$\langle 310;A_2 $	$4\omega - 14\omega x - \lambda$			
	$\langle 400;E $	$4\omega - 20\omega x$	$2\sqrt{2}\lambda$	0	0
	$\langle 310;1E $	$2\sqrt{2}\lambda$	$4\omega - 14\omega x + \lambda$	0	$-\sqrt{3}\lambda$
	$\langle 310;2E $	0	0	$4\omega - 14\omega x - \lambda$	3λ
	$\langle 220;E $	0	$-\sqrt{3}\lambda$	3λ	$4\omega - 12\omega x$
	$\langle 211;E $	0	$\sqrt{6}\lambda$	0	$-\sqrt{2}\lambda$
					$4\omega - 10\omega x - 2\lambda$

Table 1.1 Hamiltonian matrices for CH₃ for the overtone manifolds V=1 to 4

Here $\lambda = -\omega \gamma = -\omega (\gamma - \phi)$, which is the effective coupling parameter. The values of ω , the mechanical frequency and ω_x , the anharmonicity for CH bonds are obtained from Birge-Sponer plot of the overtone transition energies at various quantum levels. The effective coupling parameter $\omega \gamma$ is related to the energy difference between A₁ (symmetric) and E (antisymmetric) states of the fundamental CH transitions through the relation $3 \omega \gamma = E(|100\rangle_E) - E(|100\rangle_{A_1})$

where A and B are constants and V is the overtone level. This empirical equation of Ellis follows directly from the theory of one dimensional anharmonic oscillator whose energy levels are given by equation (21). The empirical constants A and B in equation (22) are related to equation (21) as $X_1 = A-B$ (Mechanical frequency) and $X_2 = B$ (anharmonicity). X_1 and X_2 are related to conventional spectroscopic parameters through $X_1 = \omega_e$ and $X_2 = -\omega_e x_e$.

The local mode model has been widely used for the interpretation of overtone spectra of a wide variety of molecules [32-47]. Additional weak features are observed in many overtone spectra, in addition to pure overtones, which are combination bands arising from excitation of more than one local mode (local-local combinations) or excitation of low frequency vibrations of the molecule along with a pure local mode (local-normal combinations). The appearance of these combination bands in overtone spectra implies the presence of non-zero couplings between local modes and between local and normal modes. However, the magnitudes of these couplings are found to be much smaller than the diagonal local mode anharmonicity values. This allows the local mode description to be used as a good zero order picture to start within the calculations of higher vibrational spectra.

When the absorption spectra of benzene and benzene d_5 at $\Delta V = 6$ are compared, the band shape or peak energy of the two molecules show no significant difference which is in contrast to the predictions of the strongly coupled normal mode model. However, the similarity in the observed spectra was well predicted by the local mode model, which established its applicability in benzene molecule.

Observations on a number of molecular systems led Henry and co-workers to propose the following empirical rules relating to overtone spectra. (1) Local mode overtones involving high frequency oscillators are most intense but fall off rapidly in intensity with increasing vibrational quantum number. (2) Local-local and local-normal combinations occur generally with much less intensity than pure local mode overtones. (3) Combination bands fall off more quickly in intensity than do the pure overtones with increase in quantum number.

1.8 Refinements in local mode model

Many workers suggested refinements by inclusion of the terms neglected in the zero order local mode model. Wallace [48-50] used Morse oscillator potential for CH oscillator and included potential energy cross terms of the form $F_{ij} Q_i Q_j$ in the Hamiltonian. Halonen [51] calculated the CH and CD overtone spectra in benzene and deuterobenzene using a model in which anharmonic local mode oscillators are coupled through kinetic energy (Wilson G Matrix cross terms) to the C-C framework. Sage and Jortner [13,52-54] used Morse oscillator function to model the CH bond potential and included the Wilson G. matrix cross terms involving CH bending and stretching vibrations in the Hamiltonian.

When more than one hydrogen atom share a common X atom, the symmetry effects in the spectra are produced due to coupling between the oscillators. The effects of local mode picture were briefly discussed by Swofford et.al. [24]. Gelbart et.al [55] pointed out that symmetry adaptation is completely compatible with energy localization. The analysis of the states of water molecule using the local mode picture by Moller and Mortensen [56] showed that the symmetry effects arising from the equivalence of the two CH bonds are important. In the local mode picture, the local mode model is used as the starting point and considers the interaction between the equivalent oscillators in terms of kinetic and potential coupling. The resulting Hamiltonian is used to interpret the entire spectra down to first overtone level. This approach is used by Henry and co workers for the analysis of spectra of water [57], dihalomethanes [58] and deuterated dihalomethanes [59]. A C_{2v} model Hamiltonian containing inter oscillator coupling terms is shown to predict the full overtone spectra of these compounds. Rasheed et al [60] analysed the overtone spectra of 1,2 dihaloethanes in the near infrared region and observed the symmetry effects. They showed that the model Hamiltonian used for dihalomethanes can be used to interpret the overtone spectra of 1,2 dihaloethanes. Henry and co-workers analysed the overtone spectra of neopentane [61, 62] using a C_{3v} model Hamiltonian that is an extension of the C_{2v} Hamiltonian. Halonen and Child have given a local mode theory of C_{3v} molecules like CH_3D , CHD_3 , SiH_3D and $SiHD_3$ [63]. Rasheed et.al. used the C_{3v} local mode

1.9 Applications of overtone spectroscopy in molecular structural studies

The most important application of overtone spectroscopy is the characterisation of CH bonds in organic compounds. The CH stretching overtone spectra are characterised by one peak for each of the non-equivalent oscillators in a molecule and can be interpreted within the local mode model of molecular vibrations [65]. The infrared spectral study of vibrational fundamentals generally does not give information on the influence of environment on a particular CH oscillator. There are a number of additional advantages for overtone spectral studies. First is the practical reason that one can avoid dependence on deuterated samples, which are often not readily available and also difficult to prepare. The overtone bands are quite well resolved even for very similar oscillators. Second, the CH stretching parameters obtained from fitting a number of sequential overtones for each local mode oscillator promise higher precision than single measurements in the infrared. Finally, the overtone spectra also give the anharmonicity values of the local mode oscillators, which determine the shape of the corresponding potential curves, whereas the infrared fundamentals of deuterated samples give only the frequencies of isolated CH bonds.

Overtone spectroscopy and the local mode model provide a valuable probe of molecular structure and molecular conformation. The local mode parameters X_1 and X_2 are characteristics of the particular CH oscillator and thus give rise to distinct absorption peaks corresponding to the distinct non-equivalent CH oscillators in the molecule. The non-equivalence of CH oscillators can arise from different reasons. The alkyl and aryl CH bonds are nonequivalent due to the difference in states of carbon hybridisation. Nonequivalent primary, secondary and tertiary CH bonds are present in alkanes. Conformational origin, inter and intramolecular environmental origin etc. also cause non-equivalence among CH bonds.

Alkyl and aryl CH bonds in toluene and xylenes display distinguishable peaks in their overtone spectra, as do the primary, secondary and tertiary CH bonds in

alkanes [66-68]. The development of laser based techniques like thermal lens effect and photoacoustic effect have produced dramatic improvements in resolution and applicability of overtone spectroscopy. The highly sensitive determination of bond length changes led to an understanding of substituent effects on CH bonds in aryl systems [69]. Extensive studies in the aryl CH overtones of substituted benzenes have shown that an electron-withdrawing group when substituted in the benzene ring causes an increase in the ring CH mechanical frequency while an electron-donating group causes a decrease in the mechanical frequency. Mizugai et.al. [70] and Gough et.al.[67,69] in their study of substituted benzenes, noted a correlation between the shift in CH overtone frequencies and change in CH bond lengths with respect to benzene. The bond length – overtone shift correlation can conveniently be used to determine the CH bond lengths in substituted benzenes from that in benzene (1.084\AA), and the overtone frequency shift relative to benzene $\Delta\bar{\nu}$ for a given overtone ΔV_{CH} . Clearly the overtone method gives a means of determining change in CH bond length rather than the absolute values [71]. The correlation between the two reads as

$$r_{\text{CH}}^{\text{LM}}(\text{\AA}) = 1.084 - \left[\frac{\Delta\bar{\nu}}{11\Delta V_{\text{CH}}} \right] 0.001 \quad (30)$$

This relation is used to determine CH bond lengths from the CH bond length in benzene and the overtone frequency shift $\Delta\bar{\nu}$ (cm^{-1}) from benzene for a given overtone ΔV_{CH} .

Katayama et. al. [72] studied the fifth overtone spectra of the CH stretching vibrations of pyridine and its related compounds and found that the chemical shifts in proton magnetic resonance roughly correlate with the frequencies of the overtones. The observation of the high overtones of the C-H vibrations thus gives valuable information concerning various properties of the C-H bonds in molecules. Kjaergaard et.al [73] carried out the overtone spectral investigations on the difference in C-H bond length values in pyridine. The peaks corresponding to three non-equivalent CH stretching local modes were assigned in the vapour phase overtone spectra. Absolute oscillator strengths were obtained from the conventional spectra and the relative oscillator strengths between

observed peaks within a given overtone from the photoacoustic spectra. Oscillator strengths were calculated with an anharmonic oscillator local mode model and ab initio dipole moment functions.

The importance of mass, electronegativity and steric influences of halogens have been revealed by the studies on halomethanes [74,75] in determining the local mode parameters of the CH bonds in these compounds. Our work on the overtone spectrum of allyl chloride [76] has shown that the vinyl CH mechanical frequency is greater than that in ethylene (Chapter 3)

Overtone spectroscopy is widely used to detect and characterise conformationally non-equivalent CH bonds in many molecules. In *o*-fluorotoluene and *o*-xylene, two peaks are observed in methyl region with an intensity ratio of 2:1. The studies on *o*-fluorotoluene [77] and *o*-xylene [78] revealed that the most stable conformer is the planar ones, where methyl groups have one CH bond in ring plane and the two at 60°. The in plane CH bond is shorter than the two out of plane at 60° and from spectral splitting this difference amounts to 0.003 Å. These results are found to agree with ab initio calculations. Two well resolved series of peaks are observed in the gas phase overtone spectra of toluene and xylenes at $\Delta V_{CH} = 3$ and 4, one set corresponding to aryl CH bonds and the other to methyl CH bonds. In these molecules [67] methyl substitution causes the aryl CH bond lengths to increase (mechanical frequency to decrease) with respect to benzene, which results from the electron donating nature of the methyl group. There are two aryl peaks for toluene also, one at a lower frequency and the other at the same frequency as the corresponding peak in benzene. The frequency separation between these aryl peaks corresponds to a bond length difference of 0.002 Å.

Rai et al [79] reported the CH and OH vibrational spectra of normal, secondary and tertiary butanol, where the fundamentals and a large number of overtone and combination bands were assigned. The anharmonicity constant and dissociation energy for the CH and OH bonds in the molecules were also obtained. Xu et.al [80] reported the OH stretching overtone spectra of isobutyl alcohol at $\Delta V = 3, 4$ and 5 levels as measured using cavity ring-down spectroscopy (CRDS), where the three observed bands for OH overtones are assigned as due to the three

kinds of conformations of the hydroxyl group. Fang et.al reported the vibrational overtone spectra of gaseous alcohols [81]. The overtone absorption spectra of gaseous 1-propanol, 2-propanol and tert butyl alcohol were measured with ICL-PAS and FTIR spectroscopy. The prominent features in the spectra are assigned as OH and CH stretching overtones within the local mode model. The remaining features are assigned as combinations involving a local mode overtone and lower frequency motions of the molecules. Fedorov et al [82] described a direct correlation method for OH, NH and CH local modes. The vibrational overtone spectra of gaseous biphenyl, anthracene, isobutanol, 2-chloro ethanol and ethylene diamine at $\Delta V=4$ region were recorded by ICL-PAS and assigned using the local mode model. An internal coordinate Hamiltonian was constructed by Hanninen et al [83] to model the torsional motion in the OH stretching vibrational overtone region of methanol. The model includes harmonic couplings between OH and CH stretching vibrations and Fermi resonance interactions between OH stretches and COH bends and between CH stretches and CH_2 bends.

Fang et al reported the overtone spectra of gas-phase methyl, dimethyl amine and hydrazine [84] as measured by intracavity photoacoustic and FTIR spectroscopy. The prominent features in the spectra are assigned as N-H and C-H stretching overtones within the local mode model of loosely coupled, anharmonic vibrations. In diethyl amine, C-H overtone bands arising from more than one conformation are observed. In dimethyl amine, C-H stretching frequencies are observed that correspond to the methyl C-H bond trans to the other methyl, trans to the hydrogen or trans to the electron lone pair on nitrogen. The N-H overtones in hydrazine also show distinct bands arising from conformationally non-equivalent oscillators. Our analysis of the overtone spectra of benzaldehyde and salicylaldehyde [85] has revealed evidence for the inhibition of indirect and direct lone pair trans effects (chapter 2).

Sowa et al [86] analysed the CH stretching overtone spectra of furan and several thiophenes in regions where there is spectral evidence for vibrational state interactions. The interactions appear to behave differently in furan and in thiophenes. However, in both molecules, the interactions are dominated by distinct resonances rather than by purely statistical interactions with the large

density of vibrational states. In thiophenes, these distinct resonances give rise to energy shifts and transition intensity redistribution in the spectra. The vibrational overtone spectra of gaseous pyridine, 3-fluoropyridine and 2,6-difluoropyridine were recorded and analysed by Snavely et al [87] using photoacoustic absorption spectroscopy. The pyridine, 3-fluoropyridine and 2,6-difluoropyridine overtone spectra exhibit two local mode progressions. The appearance of these two progressions in the difluorinated compound results from a splitting of the C(3,5)-H and C(4)-H stretches which overlapped in pyridine.

Vibrational overtone spectroscopy is established to be an effective tool in studying inter and intramolecular hydrogen bonding also. The presence of inter and intramolecular hydrogen bonding is reflected in the mechanical frequency and hence the energy values of the overtone transitions. Shaji et al [88] analysed the overtone spectra of anilines and chloroanilines and established the presence of intramolecular bonding in *o*-chloroaniline. Eappen et al [89] analysed the aryl CH and OH overtone spectrum of α -naphthol and observed the existence of intramolecular hydrogen interaction between the hydroxyl group and aromatic nucleus. Vineet Kumar et al [90] studied the overtone spectra of aniline and its *o*- and *m*-chloro derivatives dissolved in carbon tetrachloride at different concentrations. The vibrational frequencies and the anharmonicity constants for the C-H stretch vibration and for the symmetric and asymmetric N-H stretch vibrations were determined. The presence of intermolecular hydrogen bonding in all the three molecules and intramolecular hydrogen bonding involving N-H...Cl in *o*-chloroaniline were detected.

We have studied the overtone spectra of phenol, *o*-chlorophenol and *p*-chlorophenol. The presence of intramolecular bonding in *o*-chlorophenol is confirmed by the overtone spectroscopic method. The analysis of overtone spectrum of *o*-chlorophenol at different concentrations shows that, two different conformations with intra and intermolecular bonding are present in *o*-chlorophenol along (chapter 2).

To mention a typical work on high resolution overtone transitions, Zhan et al [91] investigated the rotations and local modes in stannane using a Ti: Sapphire ring laser based intracavity photoacoustic technique. The Doppler limited

rotational structure of the fifth and seventh stretching vibrational overtone bands of a monoisotopic stannane sample were recorded and analysed. Yang et al [92] recorded the vibrational overtone transitions of OCS in the near infrared region using photoacoustic technique. The observed transitions were well assigned and the spectra was analysed using molecular parameters.

The rich literature available on overtone absorption spectroscopy indicates that it has become a well-established and valuable probe for drawing structural information on polyatomic molecules.

1.10. Intramolecular vibrational energy redistribution (IVR) dynamics

Understanding intramolecular energy flow in polyatomic molecules is one of the important goals of chemical physics. A large number of studies have shown that, in high state density regions where chemical reactions occur, intramolecular vibrational energy redistribution (IVR) is a rapid and nearly universal phenomenon [93-97].

Vibrational overtone spectroscopy is a valuable tool to obtain insight into the intramolecular dynamics of energized species. Extensive experimental and theoretical studies of relatively small molecules have shown that the vibrational energy initially localised in a CH (or OH) stretch overtone relaxes rapidly through Fermi resonance phenomena with strongly coupled combination states of modes involving motion of a common or proximate atom (CH bend for example). More generally, IVR dynamics appear as largely uncorrelated to the total state density and primarily controlled by specific details of the coupling between different vibrational modes [96-98]. Several studies have suggested that some structural characteristics of the molecule can control the extent of vibrational mode coupling [96, 97, 99-101]. The presence of a low barrier hindered methyl group attached to aromatic rings has been experimentally evidenced as promoting IVR in the first excited electronic state [102-105]. Theoretical arguments ascribe this substantial influence on IVR dynamics to the strong interaction of the methyl internal rotation

with ring vibrations [103, 106]. The vibrational contribution to the effective internal rotation potential, due to the coupling of the CH stretch and the quasi free internal rotation, determines most of the spectral features and induces a relative localisation of the CH stretch vibrational energy [107].

The CH overtone spectra of flexible molecules have not been extensively studied. They generally exhibit, even in the gas phase, complex and broad features [101, 108-110]. The methyl spectral profiles of gaseous compounds have been explained both as due to conformationally non-equivalent methyl CH bonds and unresolved methyl rotational structure, possibly perturbed by alkyl CH stretch-bend Fermi resonance [109,110]. A theoretical treatment involving a weak coupling between the anharmonic CH vibration and the hindered internal rotation reproduces the principal features of the experimental profiles and concludes to a conformational insensitivity of the nearby free internal methyl rotors. The study on nitromethane, which is a small molecule possessing nearly free methyl rotation, provides a theoretical framework for the analysis of the overtone spectra of quasi free methyl internal rotors [111, 112]. The vibrational contribution to the effective internal rotation potential, due to the coupling of the CH stretch and the quasi free internal rotation determines most of the spectral features, and induces a relative localisation of the CH stretch vibrational energy.

Benzene and its deuterated derivatives are the most extensively studied molecules, both experimentally and theoretically. Local mode line shapes also have been investigated in neopentane and its deuterated analogues, deuterated methanes, tetramethyl dioxetane, durene and naphthalene [113]. It is generally agreed that intramolecular processes determine the gas phase local mode line shapes for relatively large molecules; but there is much disagreement over the identity of the kind of coupling mechanisms causing IVR. There are two general types of intramolecular line broadening mechanisms; one is lifetime broadening, which is due to decay of the excited state population. Several coupling schemes have been proposed to account for the population decay of the initially prepared state. The second type of broadening mechanism is dephasing in which line broadening arises due to modulation of the overtone absorption frequency by the other vibrational modes of the molecules. For pure dephasing no population decay

occurs. Both the mechanisms, dephasing and lifetime broadening have been applied to benzene to interpret the line width data. However there are two general arguments against the significant contribution of dephasing to overtone linewidths. The first objection is that dephasing predicts a general increase in overtone linewidths with increase of the vibrational quantum number V . However experimental observations show that this need not be true. Secondly, dephasing predicts that the line widths should be very sensitive to temperature and should become very narrow at low temperatures; due to the depopulation of the lower frequency modes. However, recent experiments have shown that overtone line widths are insensitive to changes in temperature, down to very low temperatures. The $\Delta V_{CH} = 5$ overtone spectrum of tetramethyl dioxetane, which was obtained in a seeded supersonic expansion, was found to be essentially the same as the room temperature photoacoustically detected spectrum. The low temperature overtone spectrum of crystalline benzene was found to show line widths similar to that observed in the gas phase at room temperature [113,114]

Similar to dephasing, another process, in which no population decay of excited state occurs, but can cause line broadening has also been suggested. This process for neopentane, can be represented as $|V,0,0\rangle \rightarrow |0,V,0\rangle \rightarrow |0,0,V\rangle \rightarrow |V,0,0\rangle \rightarrow$ where 'V' vibrational quanta hop from one CH oscillator to another oscillator in the same methyl group. While this process may be important for small molecules such as water, it will be a slow process in large molecules like neopentane, benzene etc. From these arguments and observations it is concluded that in almost all cases the major contribution of overtone line widths in gas-phase as well as in low temperature arise from homogeneous broadening due to the decay of excited state population. The decay of excited state occurs due to coupling of this state with other vibrational motions.

The mechanism of overtone relaxation as the coupling of CH overtone states to combinations involving overtones of CH deformation is also considered in the theoretical studies of Hutchinson et al [115] and high resolution spectroscopic experimental studies of Quack et al [116, 117]. Hutchinson et al modelled both classically and quantum mechanically the CH overtone relaxation in HC_n chains ($n=4-8$). Their analysis showed that ultra fast (50-100 fs)

irreversible vibrational energy transfer due to sequential nonlinear resonance occurs in even small hydrocarbons.

1.11 Intensity aspects in overtone spectra

In a molecule with a set of equivalent X-H oscillators, the intensities of the X-H overtone peaks depend on (1) the functional dependence of the dipole moment of the electronic ground state on the local co-ordinates (2) the matrix elements of the powers of the coordinates between the Morse oscillator wave functions and (3) the mixing of pure local mode states among themselves or with other normal modes [ref].

Stannard et al [118] carried out a detailed calculation of overtone intensities in water molecule. The result of their studies indicated that the most important source of overtone and combination intensity arises from diagonal and off diagonal terms higher than linear in the electric dipole moment operator, i.e., intensity borrowing due to off-diagonal terms in the local coordinate vibrational Hamiltonian is relatively unimportant. Henry and co-workers presented a theoretical description of the overtone intensities in dihalomethanes, where the functional dependence of dipole moment of the local coordinates is determined from CNDO calculations and numerical differentiation techniques [119].

Overtone intensity decreases by approximately a factor of 10 at each higher overtone level so the transition become extremely weak towards higher quantum levels. Kjaergaard et al presented calculations of O-H stretching vibrational intensities of hydrogen peroxide within a harmonically coupled anharmonic local mode model for the O-H stretching vibrational wave functions along with ab initio calculations to obtain the dipole moment function. They have also calculated vibrational fundamental and overtone band intensities of water [120]. The intensities were determined from a dipole moment function expanded in the three internal bond coordinates. The vibrational wave functions were calculated from a three-dimensional harmonically coupled anharmonic oscillator (HCAO) model.

Kjaergaard et al reported the intensities of local mode overtone spectrum of propane [121]. The gas phase vibrational overtone spectrum of propane was measured using conventional near infrared spectroscopy for $\Delta V_{CH} = 2-5$ regions and intracavity dye laser photoacoustic spectroscopy for $\Delta V_{CH} = 5$ and 6 regions. The peaks are assigned in terms of the local mode model and the experimental oscillator strengths are compared to calculated values for C-H stretching components of the spectra. Philips et.al measured the intensities of several OH vibrational overtone bands in vapour phase methanol, ethanol and isopropanol [122]. The trends in intensities as a function of the excitation level were modelled by two empirical approaches, yielding intensity predictions for the higher overtone transitions up to $7\nu(OH)$. Niefer et al [123] reported the intensities of C-H and N-H stretching transitions in the vapour phase overtone spectra of cyclopropylamine as measured using conventional absorption spectroscopy for lower overtones and intracavity laser photoacoustic spectroscopy for higher overtones.

References

1. C.N.Banwell and E.M.McCash; "*Fundamentals of Molecular spectroscopy*" Tata McGraw-Hill publishing company limited New Delhi,1995.
2. G.M.Barrow; "*Introduction to Molecular spectroscopy*" McGraw-Hill Kogakousha, LTD.1962.
3. W.Kaye; *Spectrochim. Acta.* Vol. 6 (1954) 257-287.
4. N.Coggeshall; "*Organic Analysis*", Vol.1 (1953) 403-450, New york, Interscience Publishers.
5. S.A.Francis; *Anal.Chem.*,25 (1953)1466.
6. R.S.McDonald; *Anal.Chem.*, 54 (1982) 1250-1275.
7. L.Lang; "*Absorption Spectra in the infrared region*" Vol.5 Ed.Akademiai, Budapest, Hungary, 1980.
8. L.J.Bellamy and D.W.Mayo; *J.Phys.Chem.*, 80 (1976) 1217.
9. D.C.Mckean, J.L.Duncan and L.Batt; *Spectrochim.Acta.* A 29 (1973) 1037.
10. G.Aruldas; *Molecular Structure and Spectroscopy*, Prentice-Hall of India, Pvt.Ltd., New Delhi,2001.
11. D.Wolverson: "*An Introduction to Laser Spectroscopy*", Ed. D.L.Andrews and Demidov, Plenum press, New York, 1995.
12. B R Henry; "*Vibrational spectra and structure*", ed. J.R Durig (Elsevier Amsterdam.), 10 (1981) 269.
13. M S Child and L. Halonen; *Adv. Chem. Phys.*,57 (1984) 1.
14. R J Hayward, B R Henry; *J. Mol. Struct.* 57 (1975) 221.
15. B R Henry; *Acc. Chem. Res.*, 20 (1987) 429.
16. J.B. Birks; "*Photophysics of Aromatic molecules*" (Wiley, New York, 1970).
17. B.R.Henry and W.Siebrand; *J. Chem. Phys.*, 49 (1968) 5369.
18. E.W.Schlag, S.Schneider and S.F.Fischer; *Ann. Rev. Phys. Chem.*, 22 (1971) 465.
19. B.R. Henry and M.Kasha; *Ann. Rev.. Phys. Chem.*,19 (1968) 161.

20. M.Quack; *Adv. Chem. Phys.*, 50 (1982) 395.
21. N. Bloembergen; *Opt. commun.* 15 (1975) 416.
22. R.V.Ambartzumian and V.S Letokhov; *Acc. Chem. Res.* 10 (1977) 61.
23. B.R. Henry; *Acc. Chem. Res.*, 10 (1977) 207.
24. R.L. Swofford, M.E.Long and A.C. Albrecht; *J. Chem. Phys.*, 65 (1976) 179.
25. W.Siebrand and D.F. Williams; *J.chem..Phys.*, 49(1968) 1860.
26. G. Herzberg; "*Infrared and Raman Spectra of Polyatomic molecules*", (Van Nostrand, New York, 1945.
27. E.B. Wilson, Jr. J.C. Decius and P.C. Gross; *Molecular Vibrations*, Mc. Graw Hill, New York 1955.
28. B.R. Henry; *J.Phys.Chem.*, 80 (1976) 2160.
29. R.L. Swofford, M.E. Long and A.C. Abrecht; *J.Chem.Phys.*, 65 (1976) 179.
30. J.W. Ellis; *Phys.Rev.*, 33 (1929) 27.
31. J.W. Ellis; *Trans. Faraday. Soc.*, 25 (1929) 888.
32. B.R. Henry and J.A.Thomson; *Chem. Phys. Lett.*, 69(1980) 275.
33. W.R.A.Greenlay and B.R.Henry; *Chem. Phys. Lett.*, 53 (2) (1978) 325.
34. B.R.Henry and J.A.Thomson; *Chem. Phys. Lett.*, 69 (1980) 275.
35. B.R.Henry, M.A.Mohammadi and J.A.Thomson; *J. Chem. Phys.*, 75 (1981) 3165.
36. R.Nakagaki and I.Hanazaki; *Chem. Phys. Lett.*, 83 (1981) 512.
37. H.L.Fang and R.L.Swofford; *Appl. Opt.*, 21 (1982) 55.
38. K.M.Gough and B.R.Henry; *J.Phys.Chem.*, 87 (1983) 3433.
39. A.W.Tarr and B.R.Henry; *Chem. Phys. Lett.*, 112 (1984) 295.
40. H.L.Fang and R.L.Swofford, M.McDevitt and A.R.Anderson; *J. Phys. Chem.*, 89 (1985) 225.
41. M.K.Ahmed, D.J.Swanton and B.R.Henry; *J. Phys. Chem.*, 91 (1987) 293.
42. M.K.Ahmed, and B.R.Henry, *J. Phys. Chem.*, 91 (1987) 3741.
43. M.K.Ahmed, and B.R.Henry, *J. Phys. Chem.*, 91 (1987) 5194.
44. M.G.Sowa, B.R.Henry and Y.Mizugai; *J. Phys. Chem.*, 97 (1993) 809.
45. H.G.Kjaergaard and B.R.Henry; *J. Phys. Chem.*, 99 (1995) 899.

46. D.M.Turnbull, M.G.Sowa, and B.R.Henry; *J. Phys. Chem.*, 100 (1996) 13433.
47. H.G.Kjaergaard, D.M.Turnbull, and B.R.Henry; *J. Phys. Chem.*, 101 (1997) 2589.
48. R. Wallace; *Chem. Phys.*, 11 (1975) 189.
49. J.Bron and R. Wallace; *Can. J. Chem.*, 55 (1977) 2292.
50. R. Wallace and A.A. Wu; *Chem Phys.*, 39 (1979) 221.
51. L.Halonen; *Chem. Phys. Lett.*, 87 (1982) 221.
52. M.L. Sage; *Chem. Phys.*, 35 (1978) 375.
53. M.L. Sage and J.Jortner; *Chem. Phys Lett.* 62 (1979) 451.
54. M.L. Sage; *J. Phys Chem.*, 83 (1979) 1455.
55. W.M. Gelbart, P.R. Stannard and M.L. elert; *In. J. Quantum.chem.*, 14 (1978) 703.
56. H.S. Moller and O.S. Mortensen; *Chem. Phys. Lett.*, 66 (1979) 539.
57. I.A. Watson, B.R. Henry and I.G. Ross; *Spectrochim. Acta, Part A*, 37 (1981) 857.
58. O.S. Mortensen, B.R. Henry and M.A. Mohammadi; *J. Chem. Phys.*, 75 (1981) 4800.
59. M.K. Ahmed and B.R. Henry; *J. Phys. Chem.*, 90(1986) 1081.
60. T.M.A. Rasheed, V.P.N. Nampoori and K. Sathianandan; *Chem. Phys.*, 108 (1986) 349.
61. B.R. Henry, A.W. Tarr, O.S. Mortensen, W.F. Murphy and D.A.C. Compton; *J.Chem.Phys.*, 79 (1983) 2583.
62. A.W. Tarr and B.R. Henry; *J. Chem. Phys.*, 84, (1986) 1355.
63. L. Halonen and M.S. Child; *J.Chem. Phys.*, 79 (1983) 4355.
64. L.I. Shiff; "*Quantum Mechanics*" 3rd edition, McGraw Hill, 1968 p.182.
65. H.G. Kjaergaard, D.M. Turnbull and B.R. Henry; *J. Phys. Chem.*, 101(1997) 2589.
66. M.S. Burberry, J.A. Morrel, A.C. Albrecht and R.L. Swofford; *J.Chem. Phys.*, 70 (1979) 5522.
67. K.M. Gough and B.R. Henry; *J.Phys. Chem.* 88(1984)1298.
68. J.S. Wong and C.B. Moore; *J. Chem. Phys.*, 77 (1982) 603.

92. X.Yang and C.Noda; *J. Mol. Spectrosc.*, 183 (1997)151.
93. F.F. Crim; *Annu. Rev. Phys. Chem.* 44 (1993) 397.
94. M.Quack; *Annu. Rev. Phys.Chem.* 41 (1990) 839.
95. M. Quack; *J.Mol. Struct*, 292 (1993) 171.
96. K.K. Lehman, B.H. Pates and G. Scoles; *Annu. Rev.Phys.Chem.*, 45 (1994) 241.
97. G.A. Bethardy, X. Wang and D.S. Perry; *Can. J. Chem.*, 72 (1994) 652.
98. C.Lung and C.Leforestier; *J. Chem. Phys.* 97(1992)2481.
99. H.Li, C.Cameron Miller and L.A. Philips; *J. Chem. Phys.*, 100 (1994) 8590.
100. A. McIlroy and D.J. Nesbitt; *J. Chem. Phys.* 101 (1994) 3421.
101. L.Lespade, S. Rodin, D. Cavagnat and S.Abbate; *J. Phys.Chem.*, 97 (1993) 6134.
102. V.A. Watters, S.D. Colson, D.L. Snavely, K.B. Wiberg and B.M. Jamison; *J. Phys. Chem.*, 89 (1985) 3857.
103. D.B. Moss, C.S. Parmenter and G.E. Ewing; *J. Chem. Phys.*, 86 (1987) 51.
104. D.B. Moss, C.S. Parmenter; *J. Chem. Phys.*, 98 (1993) 6897.
105. P.J.Timbers, C.S. Parmenter and D.B.Moss; *J.Chem.Phys.*100 (1994) 1028.
106. C.C. Martens and W.P. Reinhardt; *J. Chem. Phys.*, 93 (1990) 5621.
107. D. Cavagnet, L.Lespade and C.Lapouge; *J. Chem Phys.* 103 No.24 (1995) 10502.
108. S. Rodin-Bercion, D.Cavagnat, L.Lespade and P. Maraval; *J. Phys. Chem.*, 99 (1995) 3005.
109. K.M. Gough and B.R. Henry; *J. Phys. Chem.*, 88 (1984) 1298.
110. M.G. Sowa and B.R. Henry; *J. Chem. Phys.*, 95 (1991) 3040.
111. L. Anastasakos and T.A. Wildman; *J. Chem. Phys.*, 99 (1993) 9453.
112. D. Cavagnat and L.Lespade; *J. Chem. Phys.*, 106 (1997) 7946.
113. R.G.Bray and M.J.Berry; *J.Chem. Phys.*, 71 (1979) 4909.
114. K.V.Reddy, D.F.Heller and M.J.Berry; *J.Chem. Phys.*, 76 (1982) 2814.
115. J.S. Hutchinson, W.P. Reinhardt and J.T. Hynes; *J. Chem. Phys.* 79 (1983) 4247.

116. H.R. Dubal and M.Quack; *J.Chem. Phys.*, 81 (1984) 3779.
117. J.E. Baggot, M.C. Chuang, R.N. Zare, H.R. Dubal and M.Quack; *J. Chem. Phys.*, 82 (1985) 1186.
118. P.R. Stannard, M.L. Elert and W.M. Gelbart; *J. Chem. Phys.*, 74 (1981) 6050.
119. O.S. Mortensen, M.K. Ahmed, B.R. Henry and A. W. Tarr; *J. Chem. Phys.*, 82 (1985) 3903.
120. H.G. Kjaergaard, B.R. Henry, H. Wei, S. Lefebvre, T. Carrington Jr., O.S. Mortensen and M.L. Sage; *J. Chem. Phys.*, 100 (1994) 6228.
121. H.G. Kjaergaard, H.Yu, B.J. Schattka, B.R. Henry and A.W. Tarr; *J. Chem Phys.*, 93 (1990) 6239.
122. J.A. Philips, J.J. Orlando, G.S. Tyndall and V. Vaidya; *Chem. Phys. Lett.* 296 (1998) 377.
123. B.I. Niefer, H.G. Kjaergaard and B.R. Henry; *J. Chem. Phys.*, 99 (1993) 5682.

CHAPTER II

NIR OVERTONE SPECTRAL ANALYSIS OF SOME AROMATIC MOLECULES

2.1 Introduction

As described in detail in chapter 1, vibrational overtone spectroscopy of molecules containing X-H oscillators (X = C, N, O, Si...) has become an effective tool for the study of molecular structure, dynamics, inter and intramolecular interactions, conformational aspects and substituent effects, in aliphatic and aromatic compounds [1-4]. The local mode model in which the X-H bonds are considered to be loosely coupled anharmonic oscillators has been widely used for the interpretation of overtone spectra. To a first approximation, the overtone transitions obey the relation

$$\Delta E_{0 \rightarrow v} = AV + BV^2,$$

where V is the quantum level of excitation, $A/B=X_1$ is the mechanical frequency and B/X_2 is the anharmonicity of the X-H bond. The bond dissociation energy of the local oscillator is given by $D = -A^2/4B$. The local mode parameters X_1 and X_2 distinguish between both chemically nonequivalent X-H oscillators and conformationally nonequivalent X-H oscillators and are sensitive to the inter/intramolecular environment in which the X-H oscillator resides. Vibrational overtone spectral studies in organic compounds containing methyl CH oscillators subjected to anisotropic environments created by lone pair and π electrons have yielded important structural details [5-8].

This chapter describes the analysis of the NIR vibrational overtone spectra of liquid phase benzaldehyde and salicylaldehyde, phenyl hydrazine, phenol, ortho- and para- chlorophenols. The analysis of the spectra of benzaldehyde and salicylaldehyde shows that the observed differences in aldehydic CH local mode parameters in these compounds with respect to acetaldehyde are due to the difference in intramolecular environment present in the molecules. In particular, the large value of aldehydic CH mechanical frequency observed in

69. K.M. Gough and B.R. Henry; *J. Am. Chem. Soc.*, 106 (1984) 2781.
70. Y. Mizugai and M. Katayama; *Chem. Phys. Lett.*, 73 (1980) 240.
71. B.R. Henry, K.M. Gough and M.G. Sowa; *Int. Rev. Phys. Chem.* 5 (1986) 133.
72. M. Katayama, K. Itaya, T. Nasu, J. Sakai; *J. Phys. Chem.* 95 (1991) 10592.
73. H.G. Kjaergaard, R.J. Proos, D.M. Turnbull and B.R. Henry; *J. Phys. Chem.*, 100 (1996) 19273.
74. B.R. Henry and I-Fu Hang; *chem. phys.*, 29 (1978) 465.
75. H.L. Fang and R.L. Swofford; *J. Chem. Phys.*, 72 (1980) 6382.
76. Sunny Kuriakose, K.K. Vijayan, Shibu.M. Eappen, S. Shaji, K.P.R. Nair and T.M.A. Rasheed; *Asian Journal of Physics*, 11 (2002) 70.
77. J. Susskind; *J. chem. phys.*, 53 (1970) 2492.
78. H.D. Rudolph, K. Walzer and I. Krutzik; *J. Mol. Spectrosc.*, 47 (1973) 314.
79. S.B. Rai and P.K. Srivastava; *Spectrochim. Acta A.*, 55 (1999) 2793.
80. S.Xu, Y.Liu, J.Xie, G.Sha and C.Zhang; *J. Phys. Chem. A.*, 105 (2001) 6048.
81. H.L. Fang and D.A.C. Compton; *J. Phys. Chem.* 92 (1988) 6518.
82. A.V. Federov and D.L. Snavely; *Chem. Phys.*, 254 (2000) 169.
83. V. Hanninen, M. Horn and L. Halonen; *J. Chem. Phys.*, 111 (1999) 3018.
84. H.L. Fang, R.L. Swofford and D.A.C. Compton; *Chem. Phys. Lett.*, 108 (1984) 539.
85. Sunny Kuriakose, K.K. Vijayan, T.M.A. Rasheed, *Asian Journal of Spectroscopy*; 1 (2001) 17.
86. M.G. Sowa, B.R. Henry and Y. Mizugai; *J. Phys. Chem.*, 97 (1993) 809.
87. D.L. Snavely, J.A. Overly and V.A. Walters; *Chem. Phys.*, 201 (1995) 567.
88. S. Shaji and T.M.A. Rasheed; *Spectrochim. Acta. A.* 57 (2001) 337.
89. S.M. Eappen, S. Shaji and K.P.R. Nair; *Asian. J. Spectrosc.* 2 (2001) 89.
90. Vineet Kumar Rai, S.B. Rai and D.K. Rai; *Spectrochim. Acta. A.*, 59 (2003) 1299.
91. X. Zhan, M. Halonen, L. Halonen, H. Burger and O. Polanz; *J. chem. Phys.*, 102 (1995) 3911.

salicylaldehyde is explained as due to the inhibition of lone pair trans effect due to the strong intramolecular hydrogen bond present in the molecule. This observation gives an additional evidence for the originally present lone pair trans effect in aldehydes. The aryl CH local mode parameters in the two compounds agree with the nature of substituents on the ring. The analysis of the observed CH and NH local mode mechanical frequency values of phenyl hydrazine shows that mutual lone pair interaction occur between the NH bond and the lone pair of the adjacent nitrogen. This observation supports the conclusion drawn by Bellamy et al from their Infrared frequency studies [9]. The analysis of the observed aryl CH and OH local mode mechanical frequency values of liquid phase phenol, *o*-chlorophenol and *p*-chlorophenol confirms the presence of intramolecular hydrogen bonding between the OH group and the chlorine atom in *o*-chlorophenol. This observation supports the conclusion drawn from the electronic spectroscopic studies reported earlier [10]. The presence of intramolecular hydrogen bonding in *o*-halophenols is also well supported by the DFTB3YLP and MP2 calculations [11]. The analysis of the near infrared overtone spectra of carbon tetrachloride solutions of *o*-chlorophenol at different concentrations indicate that the intramolecular bonding present in *o*-chlorophenol at higher concentrations is weakened in lower concentrations due to the increased population of the trans conformer favoring the formation of intermolecular hydrogen bonding.

2. 2 Experimental

High purity (>99%) benzaldehyde, salicylaldehyde and phenyl hydrazine from Central Drug House Pvt. Ltd, Bombay (India) and phenol, *o*-chlorophenol and *p*-chlorophenol from Sisco Research Laboratories, Bombay (India) are used for the present experiments. The near infrared (2000-700nm) absorption spectra at room temperature (26±1°C) are recorded using a Hitachi UV-VIS-NIR dual beam spectrophotometer, which uses a tungsten lamp as the near infrared source. The spectra of the compounds except phenol and chlorophenols are recorded from pure liquid samples of 1 cm path length with air as reference. The absorption spectra of phenol and *p*-chlorophenol are recorded from a near saturated solution

in spectrograde carbon tetrachloride. The spectra of *o*-chlorophenol are recorded from carbon tetrachloride solutions of different concentration values.

2.3 Results and discussion

2.3.1 Analysis of the overtone spectra of benzaldehyde and salicylaldehyde

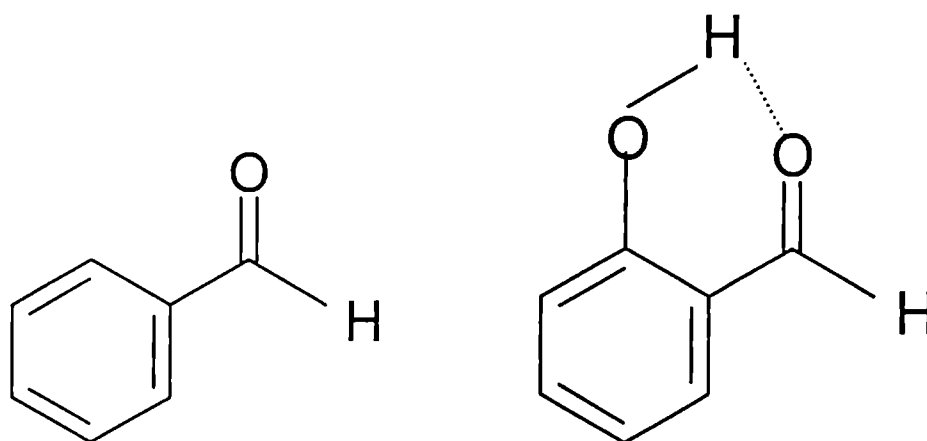


Fig. 2.1 The molecular structures of benzaldehyde and salicylaldehyde

The observed overtone absorption spectra of the two compounds in the aryl ($\Delta V=2-5$) and aldehydic ($\Delta V=2-4$) CH local modes are shown in figures 2.2 – 2.10. The $\Delta V=2$ and $\Delta V=4$ regions show multiple peaks arising from combination bands, but we could assign the pure overtone peaks from the structure as those giving good least square fit for the Birge-Sponer plot with the pure overtone peaks in the other regions. The transition energies, local mode parameters obtained from the Birge-Sponer relation and the bond dissociation energies are given in table 2.1. The Birge-Sponer plots for ring CH and aldehydic CH overtones for benzaldehyde and salicylaldehyde are shown in figures 2.11 and 2.12. The CH local mode parameters reported for liquid benzene [12] are also given in the table 2.1. The aldehydic CH local mode parameters in benzaldehyde are slightly larger than those reported earlier [13]. The aldehydic CH mechanical frequency and

anharmonicity values in benzaldehyde are less than those in acetaldehyde by ~ 16 cm^{-1} and ~ 10 cm^{-1} respectively. The aldehydic CH mechanical frequency value in salicylaldehyde is larger than that in acetaldehyde by ~ 73 cm^{-1} whereas the anharmonicity value is close to that in acetaldehyde. The aryl CH mechanical frequency values in benzaldehyde and salicylaldehyde are larger than that in benzene by 24 cm^{-1} and 13 cm^{-1} respectively.

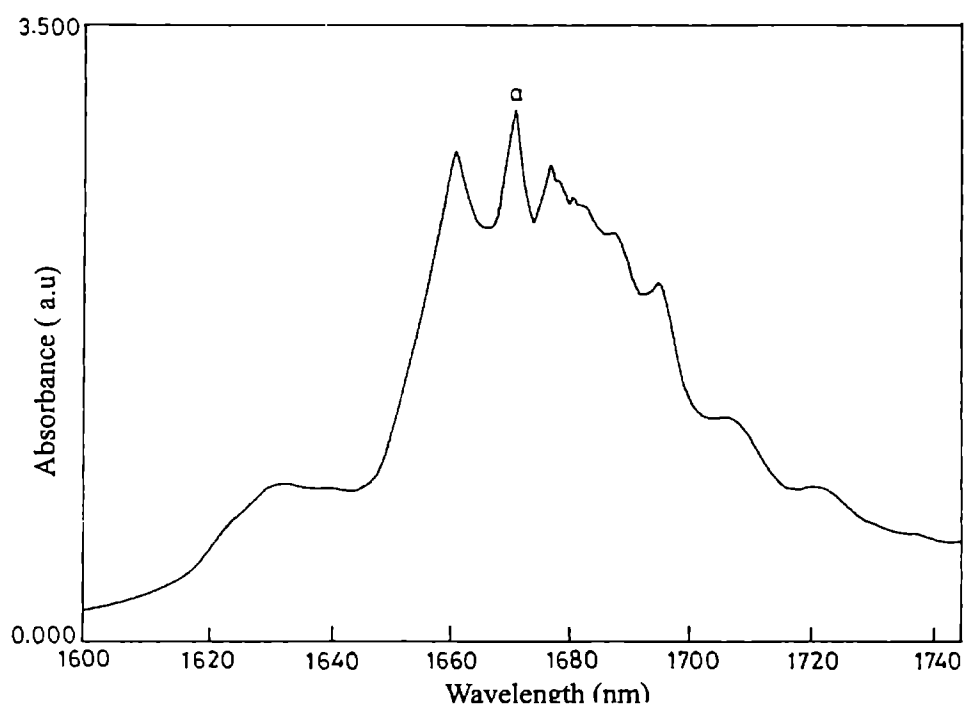


Fig. 2.2 Aryl CH band structure of benzaldehyde in the $\Delta V=2$ region. The pure overtone peak is marked as 'a'

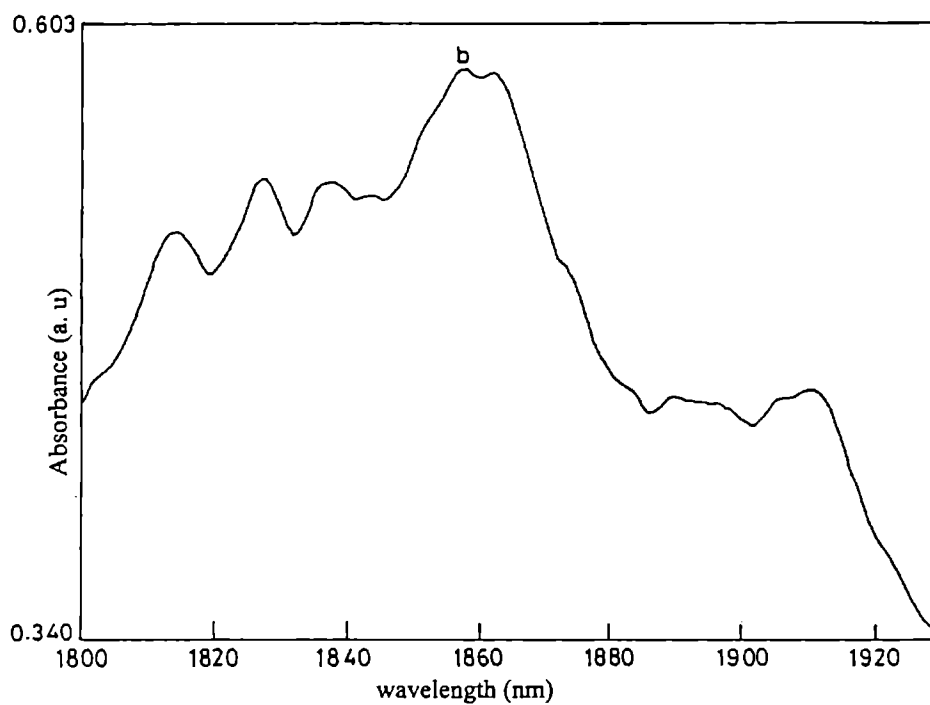


Fig. 2.3 Aldehydic CH band structure of benzaldehyde in the $\Delta V=2$ region. The pure overtone peak is marked as 'b'

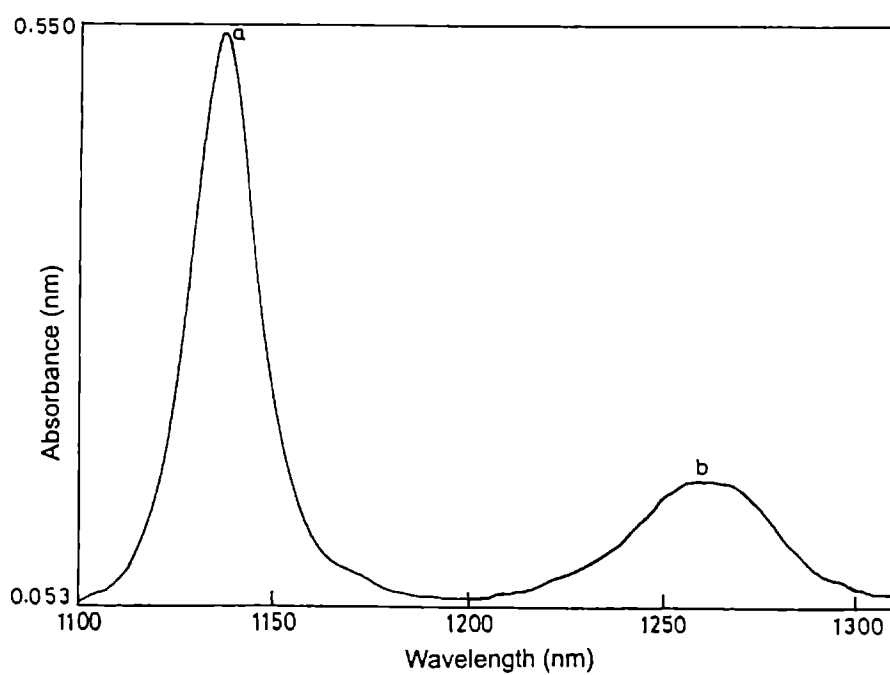


Fig. 2.4 Aryl ('a') and aldehydic ('b') CH overtone peaks of benzaldehyde in the $\Delta V=3$ region

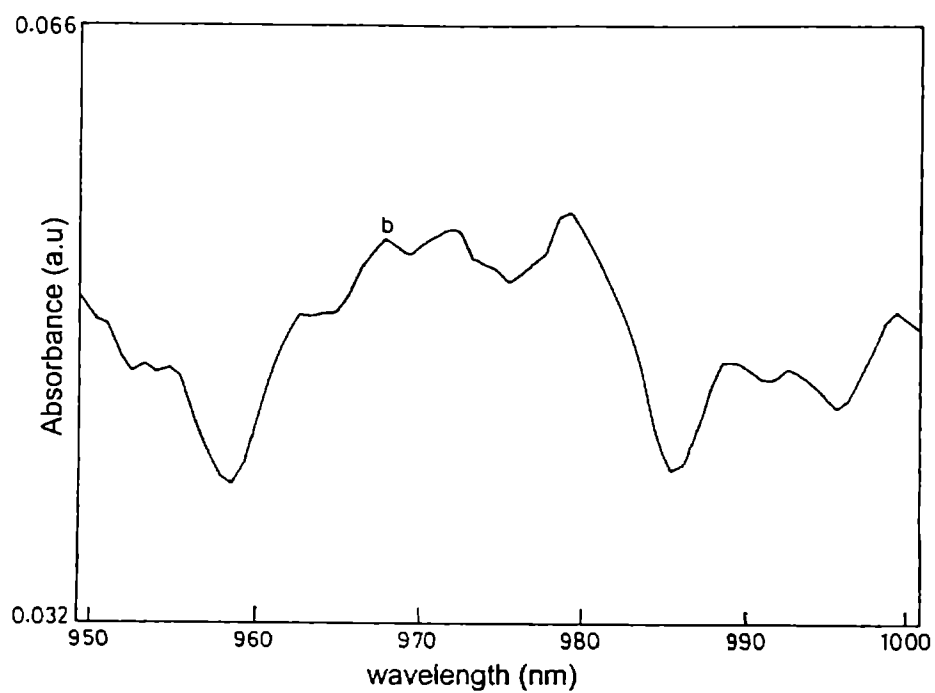


Fig. 2.5 Aldehydic CH band structure of benzaldehyde in the $\Delta V=4$ region. The pure overtone peak is marked as 'b'

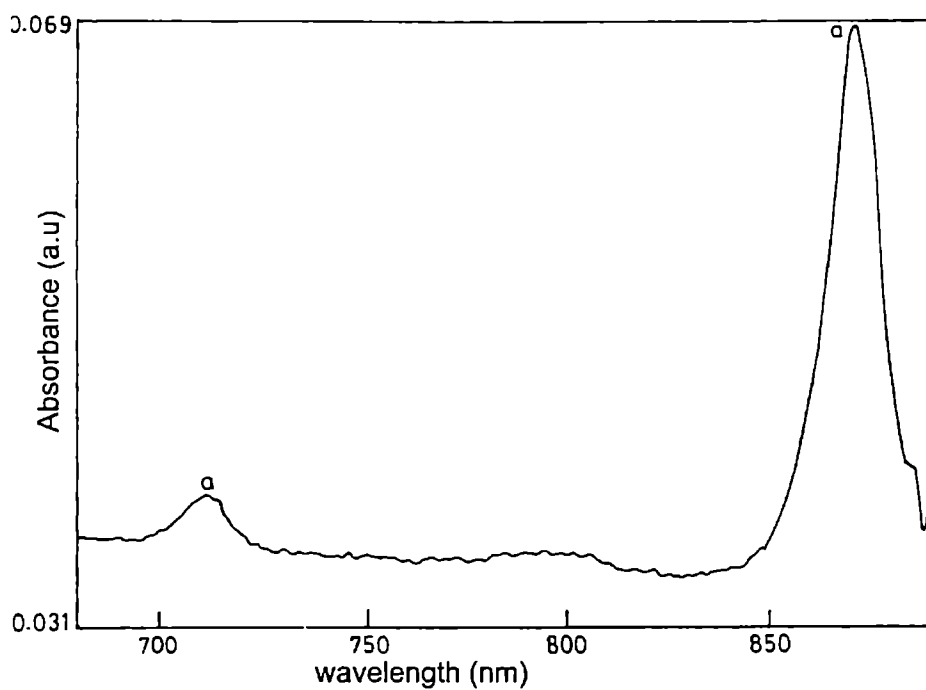


Fig. 2.6 Aryl CH overtone peaks of benzaldehyde in the $\Delta V=4$ and $\Delta V=5$ regions.

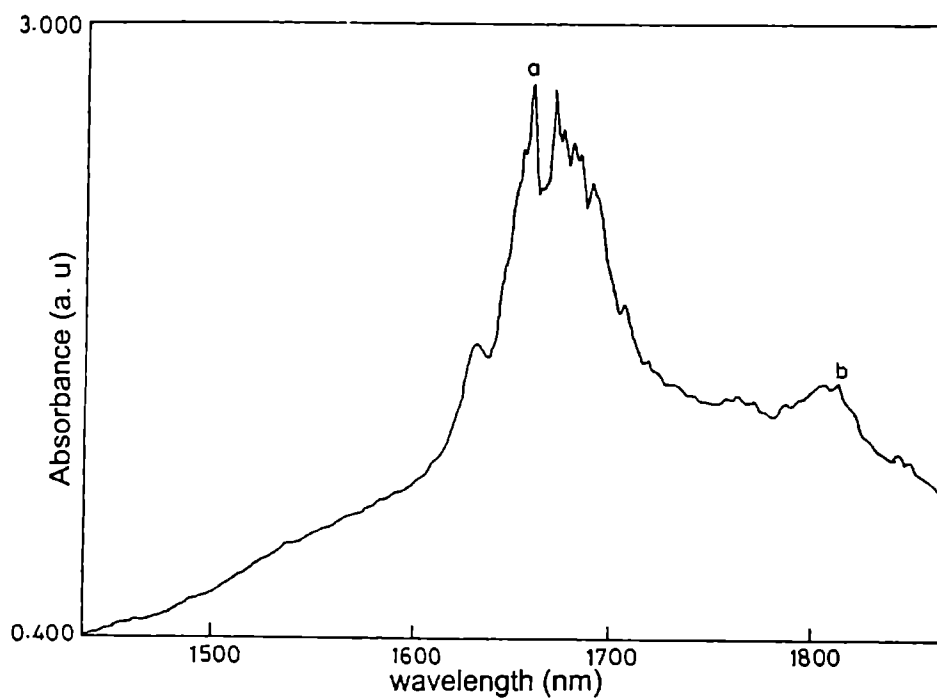


Fig. 2.7 Aryl and aldehydic CH bands of salicylaldehyde in the $\Delta V=2$ region. The pure overtone peak is marked as 'a' and 'b' respectively.

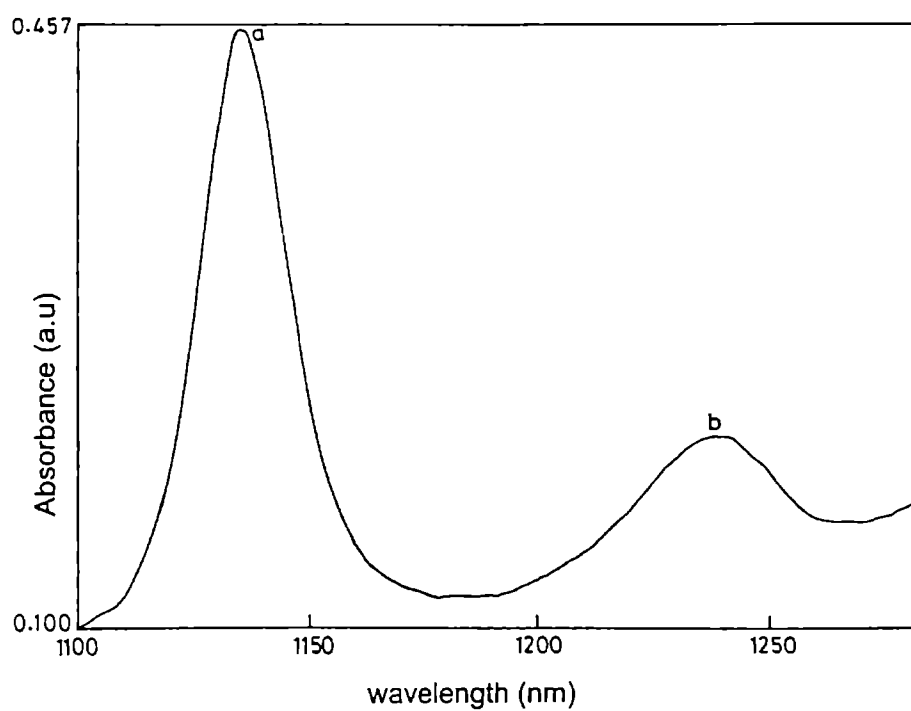


Fig. 2.8 Aryl ('a') and aldehydic ('b') CH overtone peak of salicylaldehyde in the $\Delta V=$ region.

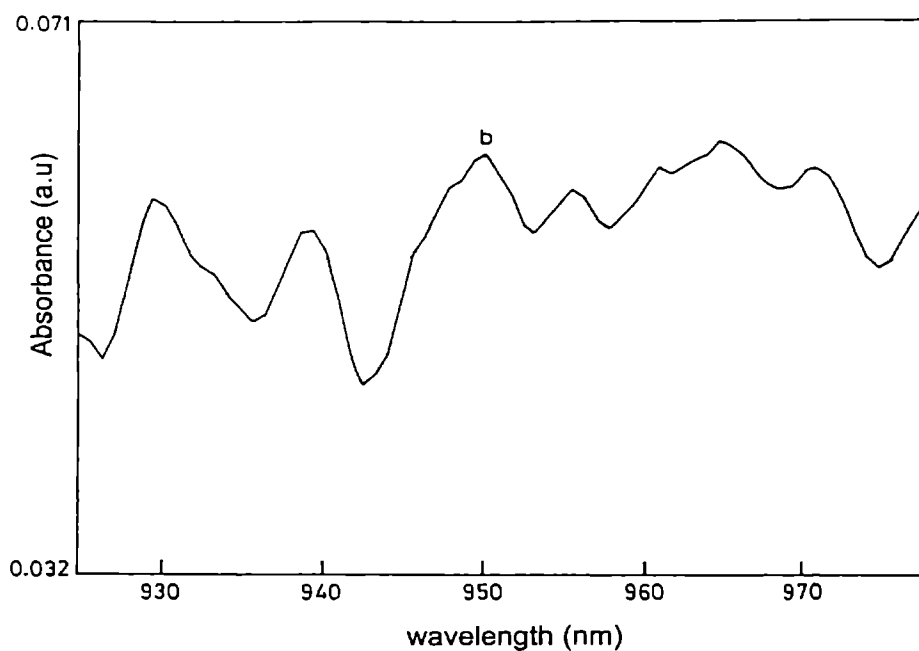


Fig. 2.9 Aldehydic CH band structure of salicylaldehyde in the $\Delta V=4$ region. The pure overtone peak is marked as 'b'

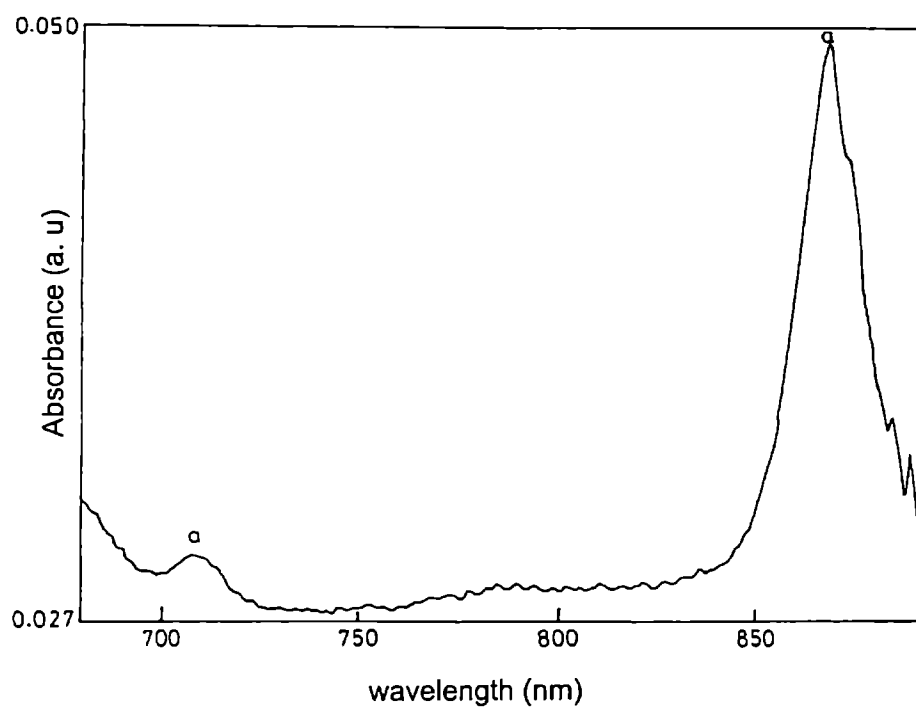


Fig. 2.10 Aryl CH overtone peaks of salicylaldehyde in the $\Delta V=4$ and $\Delta V=5$ regions.

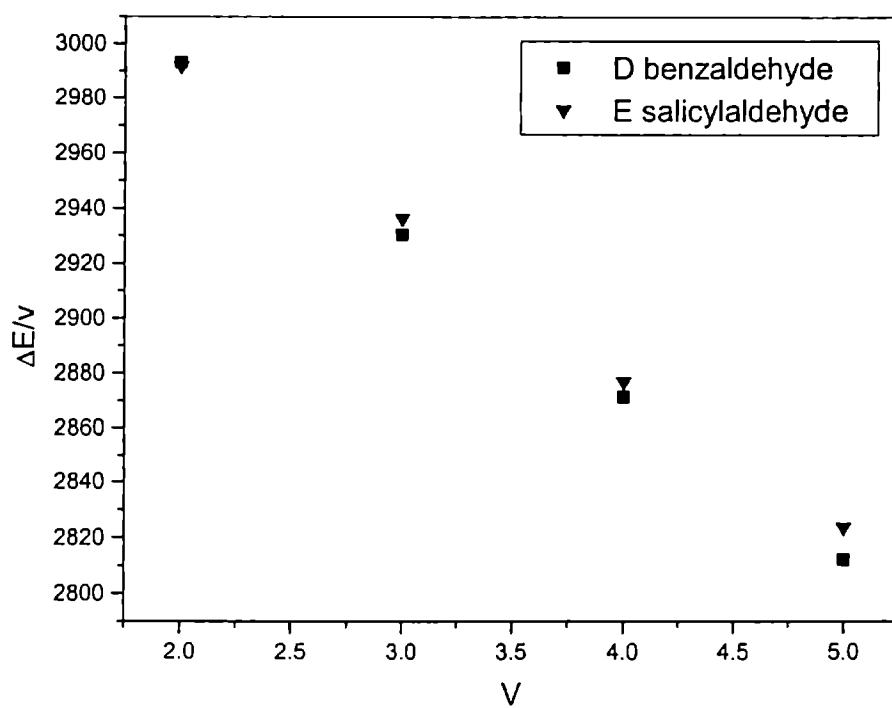


Fig. 2.11. Birge-Sponer plots for ring CH overtones in benzaldehyde and salicylaldehyde.

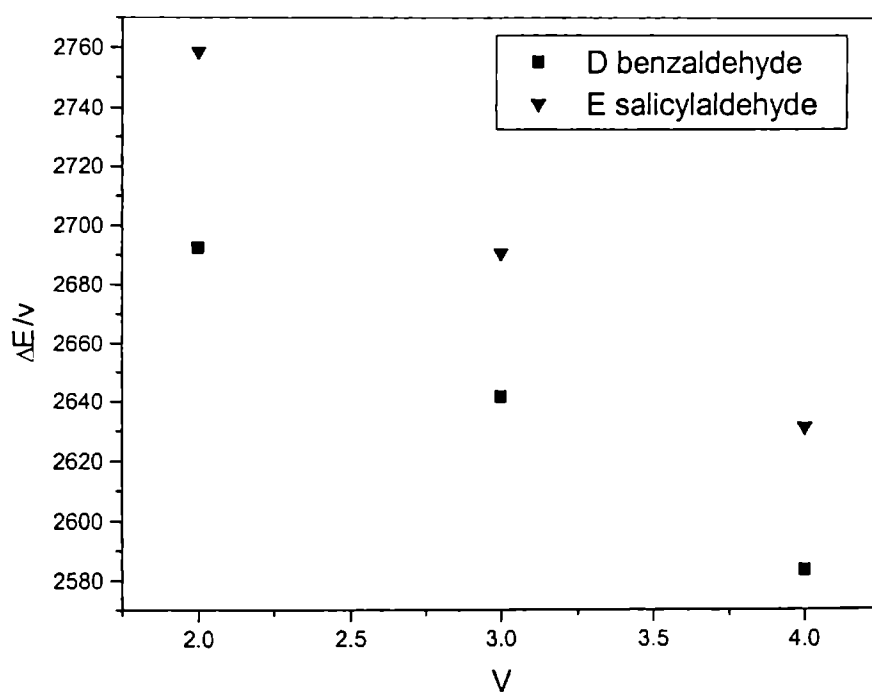


Fig. 2.12 Birge-Sponer plots for aldehydic CH overtones in benzaldehyde and salicylaldehyde

2.3.2 Aldehydic CH overtones

One of the important observations made in earlier fundamental and later overtone studies in acetaldehydes, is the smaller value of aldehydic CH stretching frequency compared to the average alkane value. This observation was explained as due to the lone pair trans effect, i.e., due to the donation of electron density to the antibonding σ orbital of the aldehydic CH bond from the carbonyl oxygen lone pair situated trans to it [7,9,14]. One of the lone pairs of carbonyl oxygen is trans to aldehydic CH bond. Electron donation from this pair to the σ^* orbital of the aldehydic CH bond causes a reduction in its mechanical frequency. A similar lone pair trans effect can be expected to be operative in benzaldehyde also, since the relative orientation of the aldehydic CH bond and a lone pair is the same as in acetaldehyde. The observed values of aldehydic CH mechanical frequency and anharmonicity in acetaldehyde are 2873 cm^{-1} and -64.6 cm^{-1} whereas the corresponding values in benzaldehyde are 2857 cm^{-1} and -54.6 cm^{-1} . The extent of donation of lone pair electron density from the trans lone pair to the aldehydic CH antibonding orbital can be assumed to depend on the C=O bond length [7]. The experimental C=O bond length values in acetaldehyde and benzaldehyde [14,15] are 1.207 \AA and 1.212 \AA respectively. One can expect that the large value of C=O distance in benzaldehyde, which occurs due to the π electron conjugation with the benzene ring can cause reduction in the lone pair trans effect resulting in a reduced value of σ^* electron density in benzaldehyde compared to that in acetaldehyde. This in turn can be expected to result in an increased value of aldehydic CH mechanical frequency in benzaldehyde compared to acetaldehyde. But the observed value of mechanical frequency in benzaldehyde is slightly lower (by $\sim 16\text{ cm}^{-1}$) than in acetaldehyde. This observation is consistent with the slightly larger value of CH bond length in benzaldehyde (1.120 \AA compared to 1.114 \AA in acetaldehyde, difference= 0.006 \AA). Also the observed value of aldehydic CH anharmonicity in benzaldehyde is much smaller (by $\sim 10\text{ cm}^{-1}$) than in acetaldehyde. We propose the following explanation for the reduced value of aldehydic CH mechanical frequency in benzaldehyde. As mentioned earlier, the lone pair trans

effect operative in acetaldehyde (donation of electron density to the σ^* orbital of aldehydic CH bond from the oxygen lone pair trans to the CH bond) results in a decrease in the aldehydic CH mechanical frequency compared to the average alkane value. The other lone pair of the carbonyl oxygen donates electron density to the σ^* orbitals of the out of plane methyl CH bonds which are trans to it. According to McKean [14], the in plane methyl CH bond is affected by an indirect trans effect due to the aldehydic CH bond which is originally influenced by lone pair trans effect. In other words, there is a donation of electron density from the σ^* orbital of the aldehydic CH bond (which is originally populated by the lone pair trans to it) to the σ^* orbital of the in plane methyl CH bond. Now considering benzaldehyde, the methyl group is replaced by the phenyl ring, which results in the absence of the above indirect lone pair trans interaction. It is clear that the aldehydic CH bond will then be subjected to increased lone pair trans effect, tending to decrease its mechanical frequency. This effect will however be opposed by the decrease in lone pair trans effect due to the increased C=O distance in benzaldehyde. The observed decrease in mechanical frequency is thus a net value resulting from the two opposing effects.

The important observation that the aldehydic CH anharmonicity value is appreciably smaller in benzaldehyde than in acetaldehyde indicates that the phenyl ring creates an intramolecular environment in which the aldehydic CH potential curve is made more harmonic. This is evident from the large value of aldehydic CH bond dissociation energy in benzaldehyde. This observation is similar to that was made in methyl substituted alkanes, where the steric crowding due to increased methyl substitution was shown to decrease the CH anharmonicity values. At present we are unable to explain the mechanism of reduction of anharmonicity that is operative in benzaldehyde.

Considering the aldehydic CH local mode parameters in salicylaldehyde, the important observation is that the aldehydic CH mechanical frequency (2947 cm^{-1}) is larger by about 90 cm^{-1} than that in benzaldehyde (larger by 73 cm^{-1} than in acetaldehyde) whereas the anharmonicity value (-63.6 cm^{-1}) is close to that in acetaldehyde. As can be read from the table, the increased mechanical frequency results in an increased value of bond dissociation energy in

salicylaldehyde compared to acetaldehyde. It is well established that strong intramolecular hydrogen bonding between OH and CHO groups occurs in salicylaldehyde. It is established that the hydrogen bonding interaction causes a lengthening of the C=O bond, a shortening of the exocyclic C-C bond and a lengthening of the C-C bond between the substituents [15]. The aldehydic CH bond length reported for salicylaldehyde is 1.110 \AA , which is 0.01 \AA shorter than that in benzaldehyde. The smaller value of bond length is consistent with the large value of mechanical frequency observed in the present experiment. An examination of the bond length data [15] shows that the C=O bond length in salicylaldehyde (1.225 \AA) is larger than the corresponding value in benzaldehyde (1.212 \AA) (difference= 0.013 \AA). The difference in C=O bond lengths between salicylaldehyde and benzaldehyde is about twice the corresponding difference between benzaldehyde and acetaldehyde. The large value of C=O bond length, which occurs due to the intramolecular hydrogen bonding, can lead to a decreased lone pair trans effect causing an increase in the aldehydic CH mechanical frequency. However the very high value of aldehydic CH mechanical frequency in salicylaldehyde (which is almost close to the average alkane value) compared to benzaldehyde cannot be attributed as due to a mere decrease in lone pair trans effect resulting from increased value of C=O distance, but points to an almost complete absence of the lone pair trans effect. We propose the following explanation for the high value of aldehydic CH mechanical frequency in salicylaldehyde. It is clear from the orientation of the hydroxyl and aldehyde groups that the intramolecular hydrogen bonding interaction makes use of the carbonyl oxygen lone pair situated trans to the aldehydic CH bond. Thus the intramolecular hydrogen bonding can be expected to inhibit the donation of electron density from the lone pair to the aldehydic CH antibonding orbital, which in turn causes an increase in aldehydic CH mechanical frequency to a value very close to that of alkanes [7]. The above observation is thus an additional evidence for the originally operative lone pair trans effect involving aldehydic CH bonds. It is observed that the aldehydic CH anharmonicity value in salicylaldehyde is close to that in acetaldehyde. This result shows that the steric effect operative in benzaldehyde, which renders the aldehydic CH vibrations more harmonic, is

absent in salicylaldehyde. Thus, in spite of the increased mechanical frequency value, the bond dissociation energy in salicylaldehyde is smaller than that in benzaldehyde.

2.3.3 Aryl CH overtones

Extensive studies reported in substituted benzenes have shown that an electron withdrawing substituent causes an increase while an electron donating substituent causes a decrease in aryl CH mechanical frequency values [16-21]. The increased value of aryl CH mechanical frequency in benzaldehyde with respect to benzene occurring due to the electron withdrawal from the ring by the CHO group was reported earlier [13,21]. The aryl CH mechanical frequency in salicylaldehyde observed in the present work is intermediate between benzene and benzaldehyde. This can be explained as due to the conjugation of one of the lone pairs of the hydroxyl oxygen atom with the π electrons of the benzene ring [22]. This conjugation effectively donates electron density to the ring causing an opposing effect to the electron withdrawal by the aldehyde group. This causes a decrease in the aryl CH mechanical frequency with respect to benzaldehyde.

In conclusion, we have analyzed the NIR vibrational overtone spectra of liquid phase benzaldehyde and salicylaldehyde. The reduced value of aldehydic CH mechanical frequency in benzaldehyde with respect to acetaldehyde is explained as due to the absence of the indirect trans effect in that compound. The large value of aldehydic CH mechanical frequency observed in salicylaldehyde is explained as due to the inhibition of donation of electron density from oxygen lone pair to the aldehydic CH bond. The observed value of aryl CH mechanical frequency in salicylaldehyde agrees with the nature of substituents on the benzene ring.

Table 2.1. Experimental values of overtone energy (cm^{-1}), mechanical frequency X_1 (cm^{-1}) anharmonicity X_2 (cm^{-1}) and dissociation energy D (cm^{-1}) of aryl and aldehydic CH local modes in benzene [12]], benzaldehyde and salicylaldehyde. The least square correlation coefficients (γ) are also given.

	Molecule	$\Delta V=2$	$\Delta V=3$	$\Delta V=4$	$\Delta V=5$	X_1	X_2	γ	D
Aryl CH	Benzene	5983	8760	11442	14015	3148.1	-57.6		41455
	Benzaldehyde	5986.2	8791.2	11486.3	14060.7	3172.2	-60.2	-0.9999	40218
	Salicylaldehyde	5983.4	8809	11507.5	14118.3	3160.7	-56.4	-0.9997	42716
Aldehydic CH	Benzaldehyde	5384.7	7924.6	10332.7		2857.4	-54.6	-0.9992	35969
	Salicylaldehyde	5517	8071.7	10525.2		2947.7	-63.6	-0.9992	32697

2.3.4 Analysis of the overtone spectrum of phenyl hydrazine

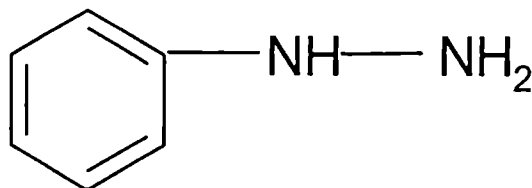


Fig.2.13. The molecular structure of phenyl hydrazine

The observed overtone absorption spectra of phenyl hydrazine for the aryl CH ($\Delta V=2-5$) and NH ($\Delta V=2-4$) local modes are shown in Figs. 2.14-2.16. In these figures, the peaks denoted by 'a' and 'b' represent the NH overtones (NH^1 – high energy and NH^2 – low energy) and 'c' represent the CH overtones. Two well resolved bands are observed at each NH overtone quantum level (except for $\Delta V=2$ region), corresponding to nonequivalent NH bonds (see below). The $\Delta V=2$ region show multiple peaks arising from combination bands and the peak position in this region is assigned as the one giving the best fit in the Birge-Sponer plot with the higher overtone peaks shown in figures 2.17 and 2.18. The transition energies and the local mode parameters obtained from Birge-Sponer plot are given in Table 2.2. The CH and NH local mode parameters reported [23] for aniline and the NH local mode parameters reported for hydrazine [24] are also included in the Table 2.2. The aryl CH mechanical frequency and anharmonicity values in phenyl hydrazine are greater than those in liquid benzene by $\sim 25\text{cm}^{-1}$ and $\sim 7\text{cm}^{-1}$ respectively. The N-H mechanical frequency values in phenyl hydrazine are less by 57cm^{-1} and 77cm^{-1} and anharmonicity values are less by 1.46cm^{-1} and 3.4cm^{-1} than those in hydrazine.

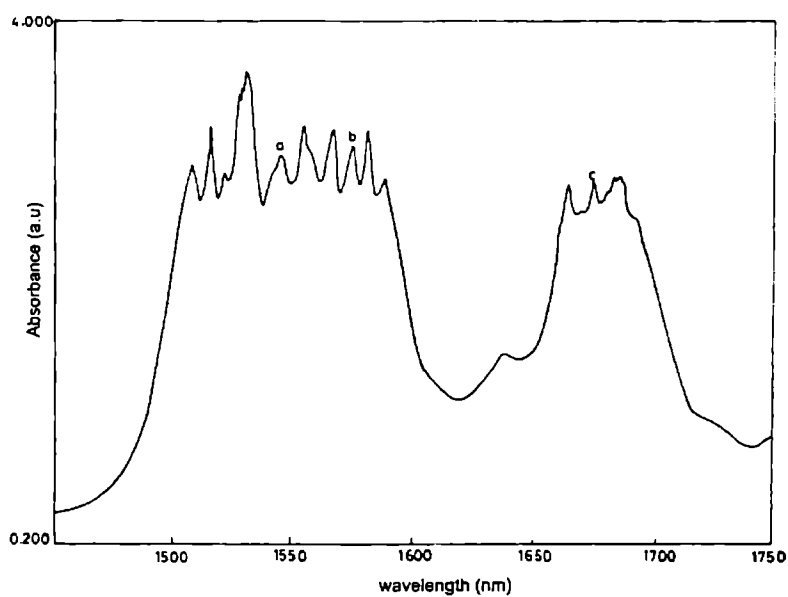


Fig.2.14. The aryl CH and NH overtone peaks of phenyl hydrazine in the $\Delta V=2$ region. The pure overtone peak of CH is marked as 'c' and those of NH are marked as 'a' – high energy NH^1 and 'b' – low energy NH^2

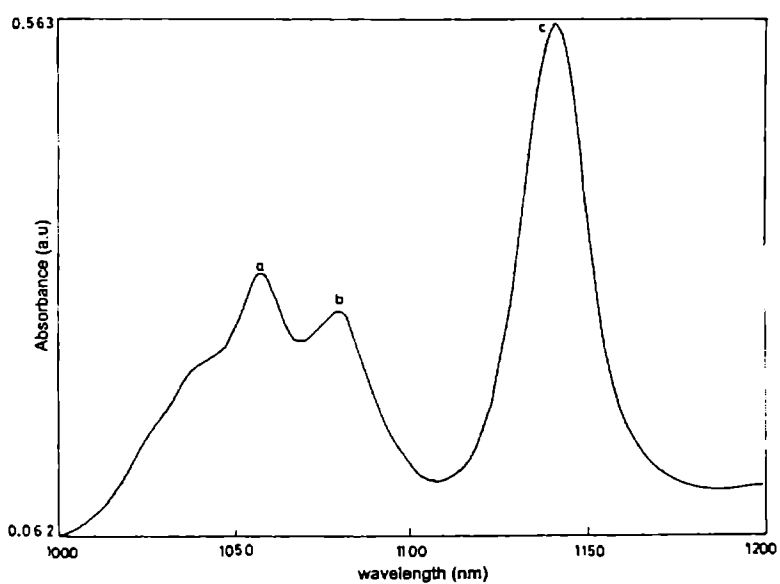


Fig. 2.15. The aryl CH and NH overtone peaks of phenyl hydrazine in the $\Delta V=3$ region.

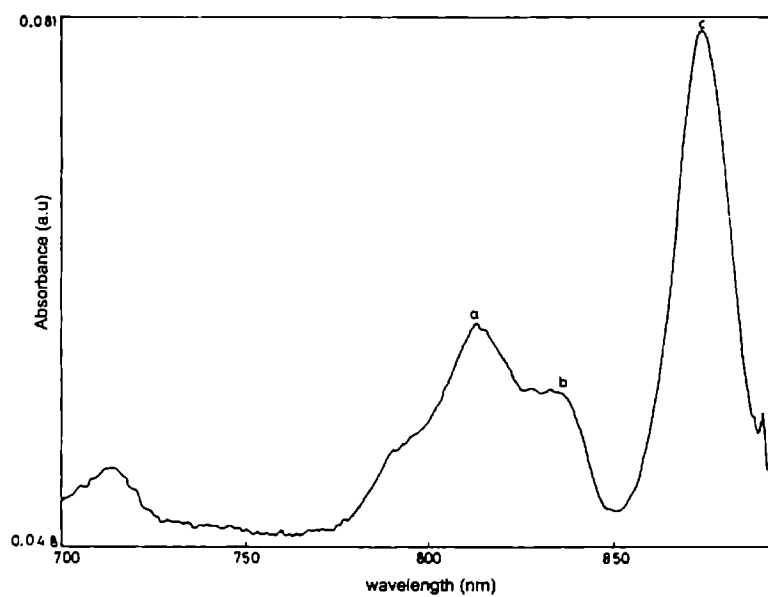


Fig. 2.16. The aryl CH and NH overtone peaks of phenyl hydrazine in the $\Delta V=4$ region.

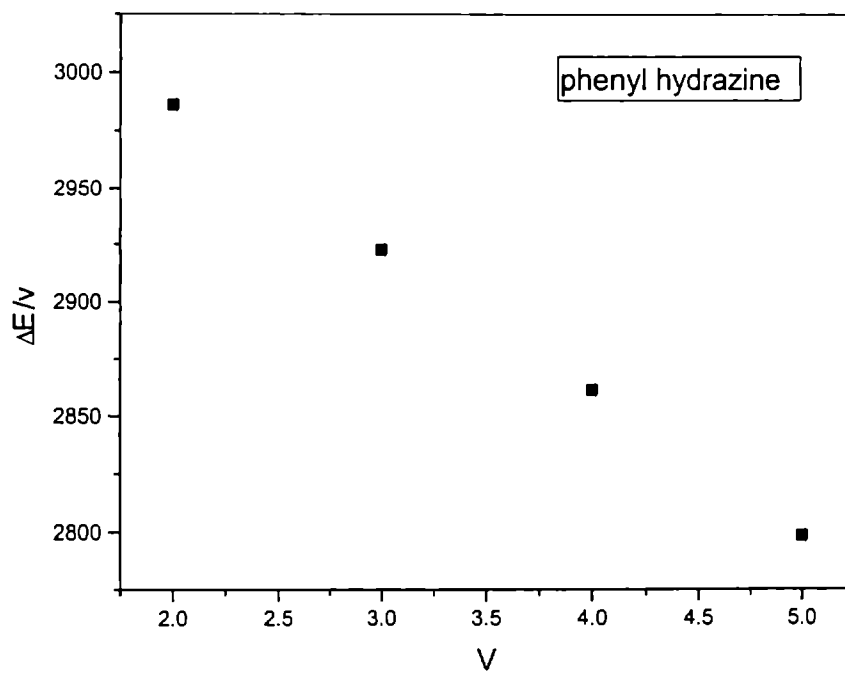


Fig. 2.17 Birge-Sponer plot for ring CH overtones of phenyl hydrazine

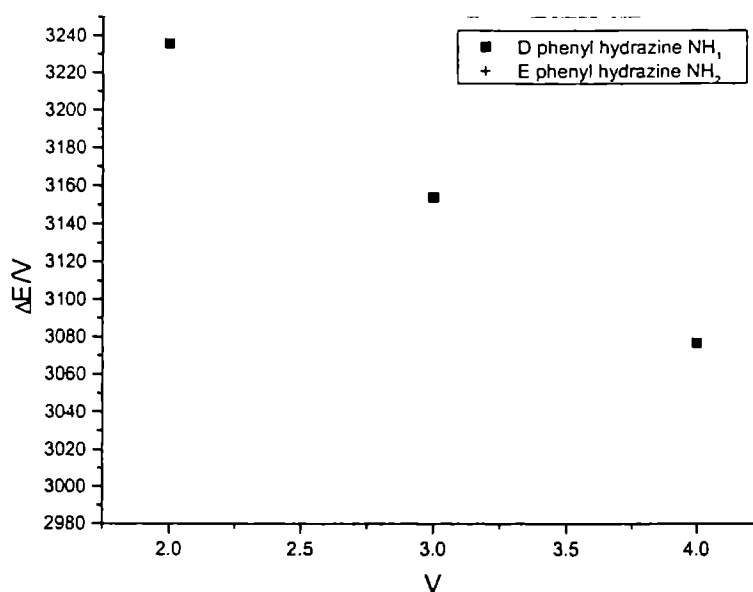


Fig. 2.18. Birge-Sponer plots for NH (NH¹ and NH²) overtones of phenyl hydrazine

Since phenyl hydrazine is a derivative of the compound hydrazine, a comparison of the reported results in hydrazine with the present observations will be useful in analyzing the results. One of the important observation made in the overtone studies in gas phase hydrazine [24], as measured by intracavity photoacoustic and FTIR spectroscopy, is the occurrence of distinct NH overtone bands corresponding to the existence of two types of conformationally nonequivalent NH bonds in this molecule. The low energy band arises from the NH bond trans to the lone pair and the high energy band from the NH bond trans to hydrogen. The intensity of low energy band is considerably greater than that of high energy band.

In an earlier paper, Hadzi et al [25] had reported the occurrence of two abnormally spaced NH stretching bands in the IR spectrum of N, N-dialkyl hydrazine. They explained this observation as due to the interaction of one of the NH bond with the lone pair of the other nitrogen atom. The strength of the interaction between the lone pair and the NH bond depends on the mutual orientation and the electron population of the lone pair orbital. These workers also observed that two different NH stretching bands occur in s-diphenyl hydrazine,

indicating that both the NH group and the NH₂ group respond to lone pair interaction.

Bellamy et al [9], based on their studies on infrared frequencies, reported that the lone pair effect in uns-dimethyl hydrazine (unsubstituted) causes nonequivalence of NH oscillators giving rise to two NH stretching bands. A nitrogen atom in NH₂ or NH groups donates its lone pair in to an antibonding orbital of an adjacent NH₂ or NH bond.

Considering the results of the present investigation, as stated earlier, the aryl CH mechanical frequency observed in phenyl hydrazine is greater than that in benzene by $\sim 25\text{cm}^{-1}$. This result shows that the (-NH-NH₂) substituent causes a net electron withdrawal from the ring [26]. Also, the mechanical frequency values of both types of NH bonds in the hydrazine group are smaller than those in hydrazine- by 57cm^{-1} and 77cm^{-1} respectively for the high energy (trans to hydrogen) and low energy (trans to electron lone pair) NH bonds. We propose the following explanation for these observations. The NH bonds in the (-NH-NH₂) group involve in mutual lone pair interaction (each one of the NH bond and lone pair of the other nitrogen mutually interact). The NH bond trans to lone pair electron and the NH bond trans to hydrogen give rise to non-equivalent oscillators. Due to the mutual lone pair interaction, electrons are not conjugated with the ring and remains in the hydrazine part. The absence of lone pair conjugation with the benzene ring and the inductive effect of (-NH-NH₂) group cause a net withdrawal of electrons from the ring. This situation is in contrast to that occurs in aniline where the effect of NH₂ group is a net donation of electron density to the phenyl ring [23]. The net withdrawal of electron from the phenyl ring causes the increase in aryl CH mechanical frequency with respect to benzene [27]. The same effect causes increase in electron density in the (-NH-NH₂) group causing decrease in mechanical frequency of both the non equivalent NH oscillators in the (-NH-NH₂) group with respect to those in hydrazine. The low values of anharmonicity compared to those in hydrazine indicate the occurrence of more harmonic NH potential is in this case.

In conclusion, we have analyzed the near infrared overtone absorption spectrum of liquid phase phenyl hydrazine. The large value of aryl CH mechanical

frequency in phenyl hydrazine with respect to benzene is explained as due to the inductive electron withdrawal by the NH₂ group. The reduction in the values of NH mechanical frequencies in phenyl hydrazine with respect to hydrazine occurs due to the existence of mutual lone pair interaction (the interaction between each one of the NH bond and the adjacent nitrogen lone pair) in hydrazine group as well as the inductive withdrawal of electrons by (-NH-NH₂) group from the phenyl ring.

Table 2.2. Observed overtone energies (cm⁻¹), mechanical frequencies X₁ (cm⁻¹), and anharmonicities X₂ (cm⁻¹) of aryl CH and NH local modes of phenyl hydrazine. The least square correlation coefficients (γ) are also given. The literature values of the local mode parameters for benzene [12] and aniline [23] are also given for a comparison.

		ΔV=2	ΔV=3	ΔV=4	ΔV=5	X ₁	X ₂	γ
Phenyl hydrazine	Aryl CH	5972.28	8767.32	11444.3	13991.9	3173	-62.46	-0.9999
	NH ¹	6471.24	9461.63	12306.2		3473	-79.54	-0.9999
	NH ²	6327.11	9259.3	11993.3		3413	-82.6	-0.9993
Aniline	Aryl CH					3136.3	-55.83	
	NH					3549.6	-77.2	
Benzene						3148.1	-57.6	
Hydrazine	NH ¹					3530	-81	
	NH ²					3490	-86	

2.3.5 Analysis of the vibrational overtone spectra of phenol, *o*-chlorophenol and *p*-chlorophenol

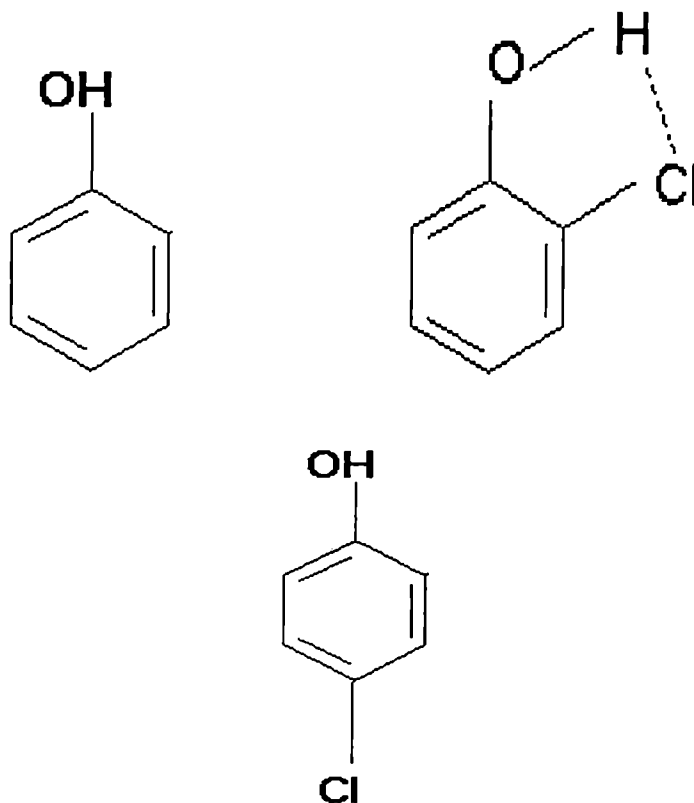


Fig. 2.19. The molecular structures of phenol, *o*-chlorophenol and *p*-chlorophenol.

The absorption of spectra of phenol, *o*-chlorophenol and *p*-chlorophenol in the near infrared region (2000-700 nm) show pure overtone bands at different quantum levels along with many combination bands. In the present analysis, we consider only the pure overtone bands arising from the ring CH and OH oscillators of these molecules. The overtone bands in the $\Delta V=2-4$ regions of phenol, *o*-chlorophenol and *p*-chlorophenol are shown in figures 2.20 – 2.31. In these figures, the peaks denoted by 'a' represent the aryl CH overtones and 'b' represent OH overtones. The peak observed at 1456 nm for *o*-chlorophenol is close to that reported for the cis conformation [29]. The OH overtone bands of *o*-

chlorophenol in these regions at various concentrations are shown in figures 2.32 - 2.34. The band assignments, transition energies and local mode parameters of the ring CH and OH oscillators are given in Table 2.3. The Birge-Sponer plots for ring CH overtones of phenol, *o*-chlorophenol and *p*-chlorophenol are shown in figure 2.35 and that for OH overtones of phenol and *o*-chlorophenol are shown in figure 2.36. The B-S plots for ring CH and OH overtones of *o*-chlorophenol at different concentrations are shown in figures 2.37 and 2.38. The OH local mode parameters of *p*-chlorophenol are not included since we could record only two OH overtone bands of this compound. The OH local mode mechanical frequency in *o*-chlorophenol is much smaller (by $\sim 31 \text{ cm}^{-1}$) than that in phenol while the ring CH mechanical frequency is increased by $\sim 27 \text{ cm}^{-1}$. The ring CH local mode parameters in all the compounds represent the average value over the various non-equivalent ring CH oscillators, since the observed liquid phase spectra do not show a corresponding resolved structure. As can be seen, there is an increase of $\sim 27 \text{ cm}^{-1}$ for the ring CH mechanical frequency in *o*-chlorophenol with respect to phenol whereas the corresponding increase in *p*-chlorophenol is only $\sim 5 \text{ cm}^{-1}$. The increase in the ring CH mechanical frequency in *o*-chlorophenol and *p*-chlorophenol is due to the electron withdrawing nature of the chlorine atom and is in agreement with the reported results in substituted benzenes [28]. The important observation here is the appreciable increase in the ring CH mechanical frequency of *o*-chlorophenol with respect to that in *p*-chlorophenol.

The transition energies and local mode parameters of *o*-chlorophenol dissolved in carbon tetrachloride at different concentrations are given in Table 2.4. Even though the first overtone region of the OH oscillator shows multiple peaks at higher concentrations, we could assign the overtone transitions as the peak that is giving best fit in the Birge-Sponer plot with higher overtones. The OH local mode parameters at lower concentrations are larger than those at higher concentrations whereas the aryl CH local mode parameters are almost insensitive to the variation in concentration. The variation in concentration affects only the –OH group through modification of its bonding environment (see below).

In chlorophenols, the electron withdrawing effect exerted by the chlorine atom attached to the ring, which reduces the electron density at the ring carbon

sites, also causes a reduction in electron density at the oxygen atom. This can cause a net attraction of the electron clouds associated with hydrogen atom in OH group, thus causing an increase in the OH mechanical frequency. But the OH mechanical frequency in *o*-chlorophenol is less than that in phenol ($\sim 31 \text{ cm}^{-1}$). This shows that the above mechanism of increasing the OH force constant is opposed by some interaction present in this molecule. We propose that intramolecular hydrogen bonding between the chlorine atom and hydrogen atom in OH group, which can be most dominant in *o*-chlorophenol, is responsible for the reduced OH mechanical frequency compared to that in phenol. The chlorine atom in *o*-chlorophenol involves in intramolecular hydrogen bonding with OH group, which is attached to the adjacent carbon site in the benzene ring causing a reduction in the force constant of the OH bond. This explains the reduced value of OH oscillator mechanical frequency in *o*-chlorophenol compared to phenol. A comparison with *p*-chlorophenol could not be made since only two OH overtone peaks are observed and the OH overtone in the $\Delta V=4$ region could not be obtained due to the poor signal to noise ratio in this region.

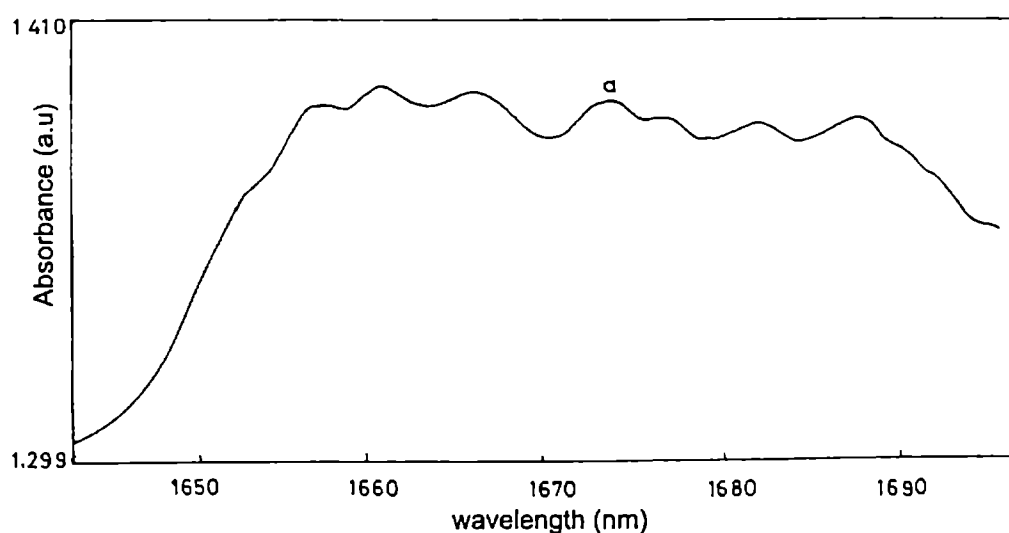


Fig. 2.20 The aryl CH overtone peak of phenol in the $\Delta V=2$ region

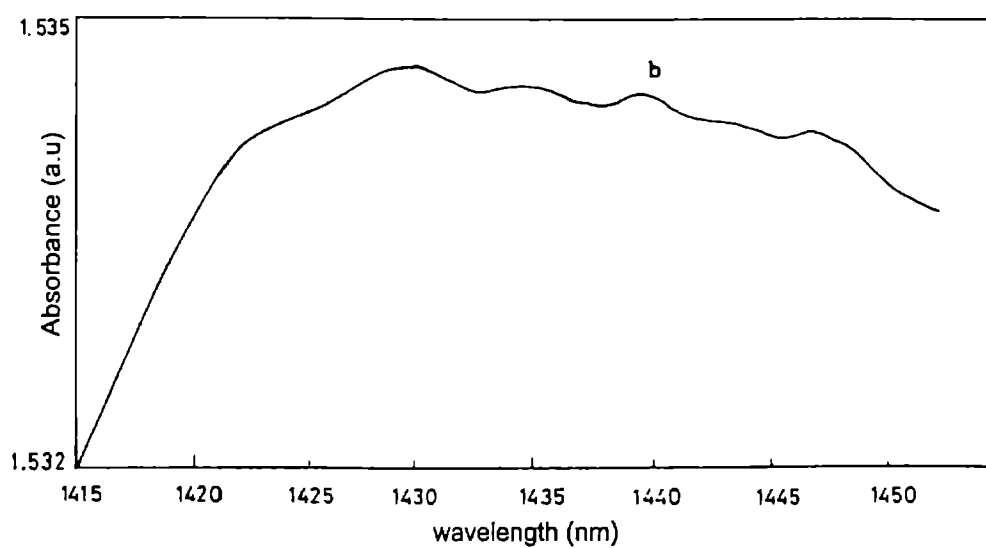


Fig. 2.21 The OH overtone peak of phenol in the $\Delta V=2$ region.

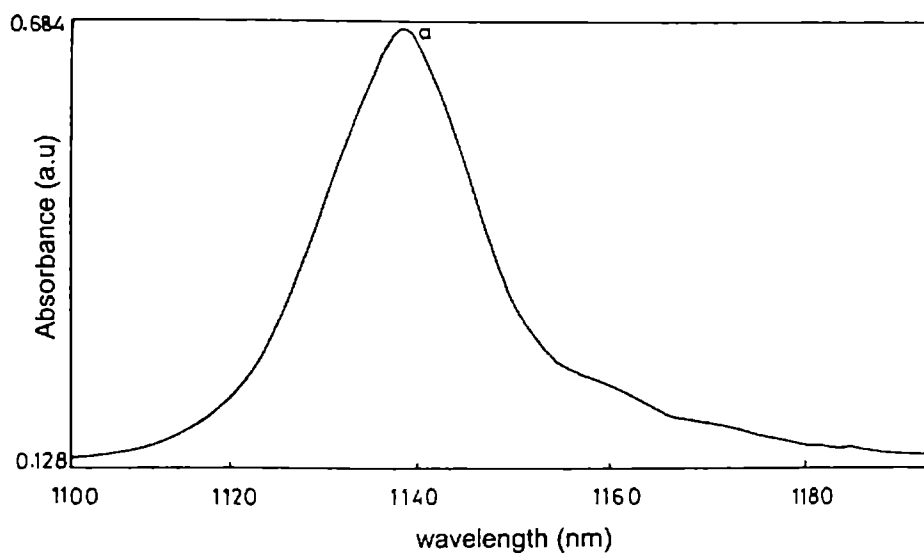


Fig. 2.22 The aryl CH overtone peak of phenol in the $\Delta V=3$ region.

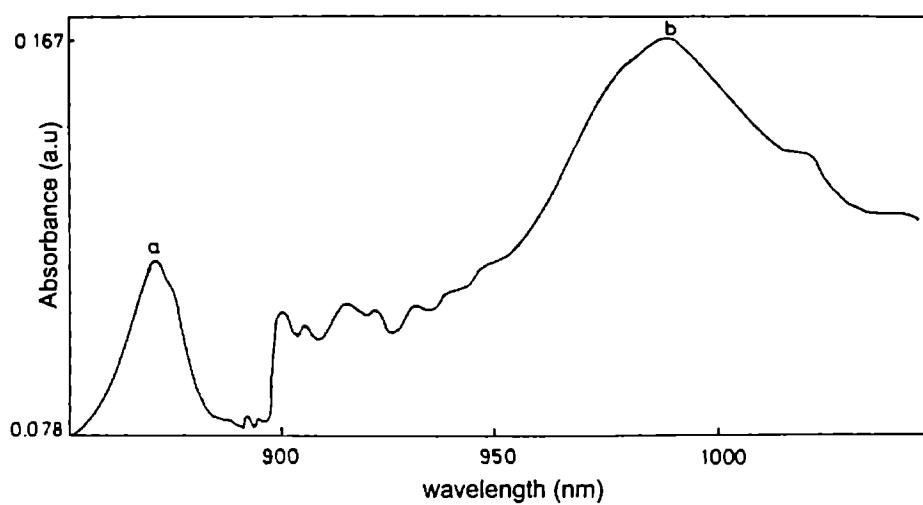


Fig.2.23 The aryl CH overtone peak in the $\Delta V=4$ region ('a') and the OH overtone peak in the $\Delta V=3$ region of phenol ('b').

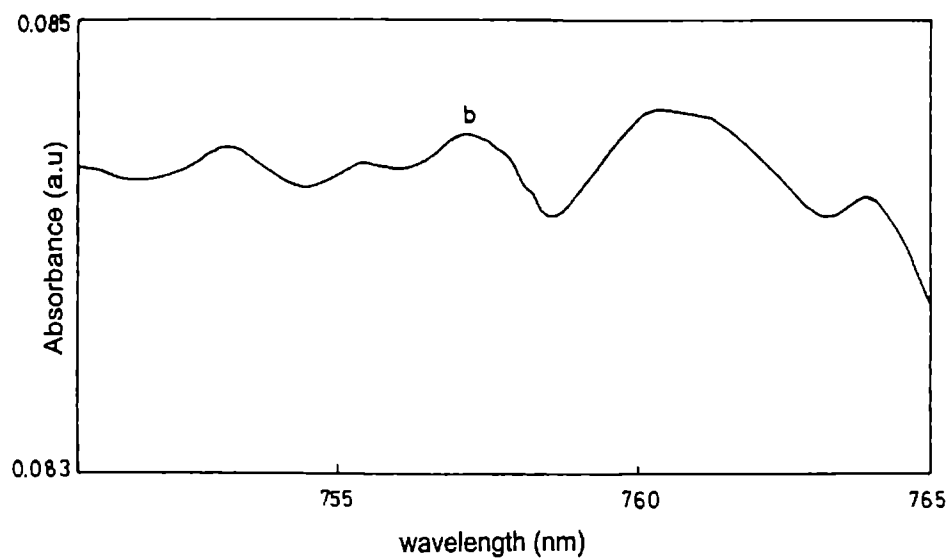


Fig. 2.24 The OH overtone peak of phenol in the $\Delta V=4$ region. The peak position is marked as 'b'

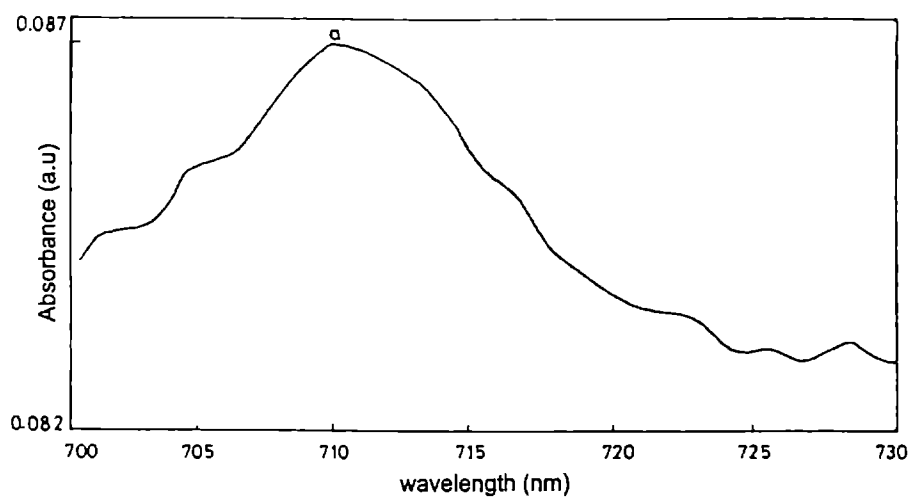


Fig. 2.25 The aryl CH overtone peak of phenol in the $\Delta V=5$ region. The pure overtone peak is marked as 'a'

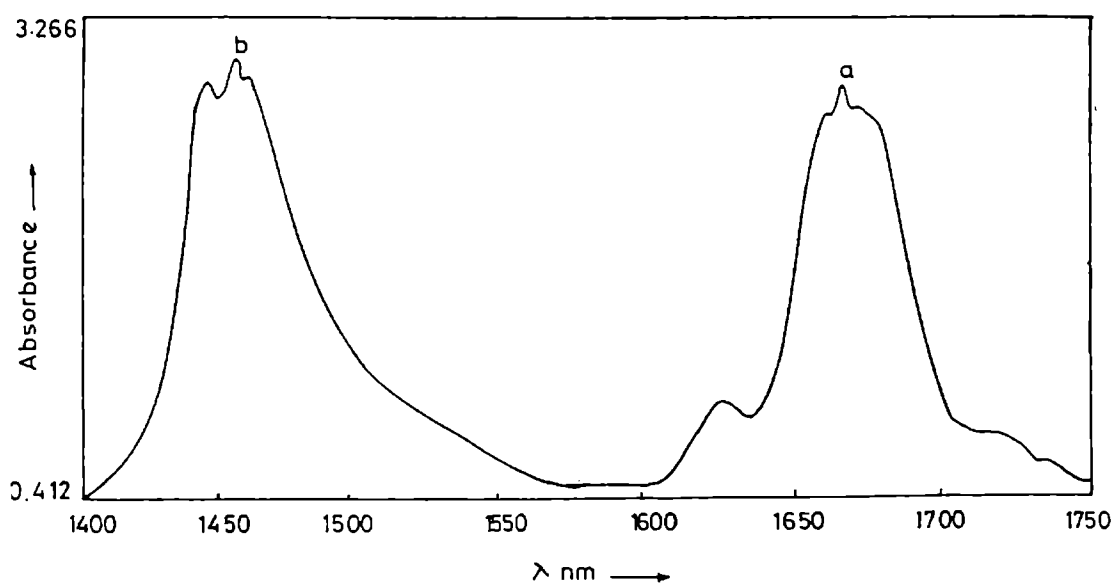


Fig. 2.26 The aryl CH ('a') and OH ('b') overtone peaks in the $\Delta V=2$ region of o-chlorophenol.

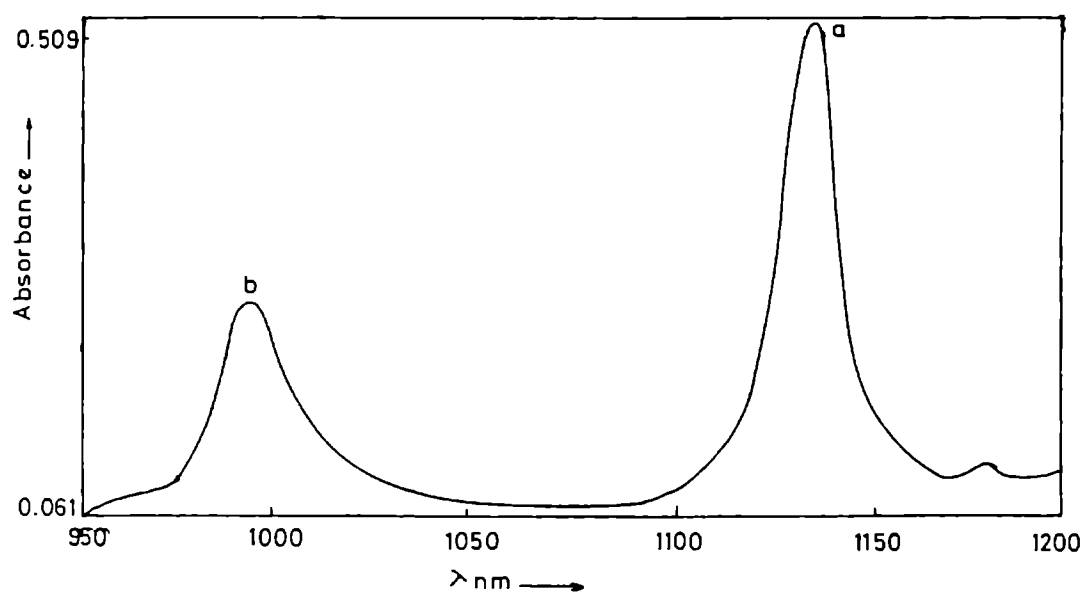


Fig. 2.27 The aryl CH and OH overtone peaks in the $\Delta V=3$ region of o-chlorophenol.

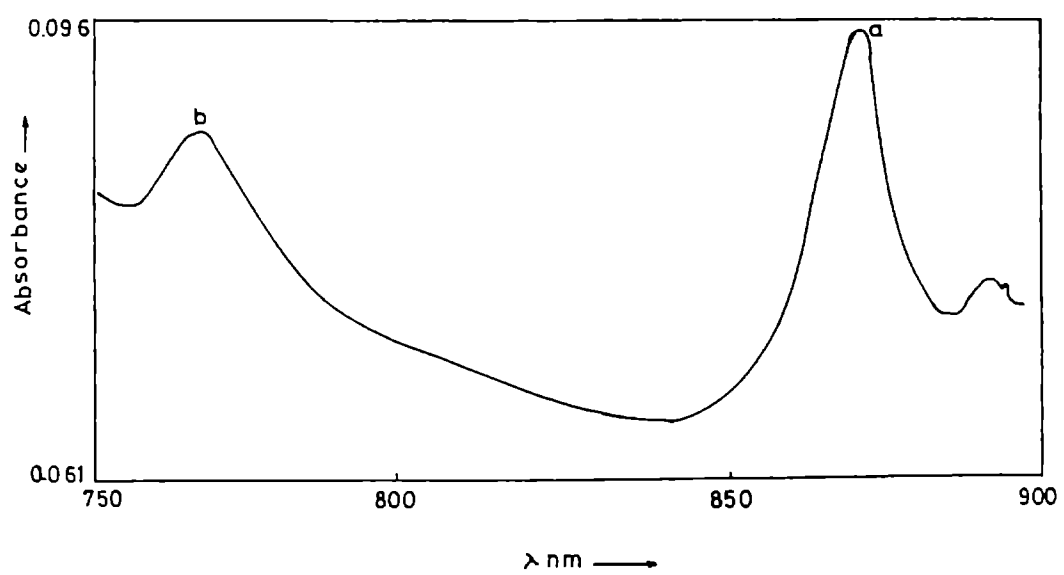


Fig. 2.28 The aryl CH and OH overtone peaks in the $\Delta V=4$ region of o-chlorophenol.

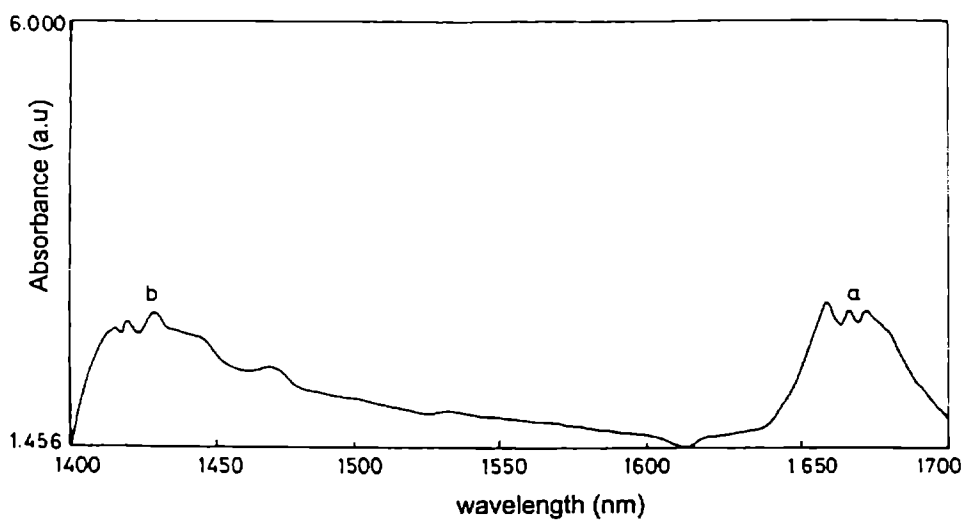


Fig. 2.29 The aryl CH and the OH overtone peaks in the $\Delta V=2$ region of p-chlorophenol

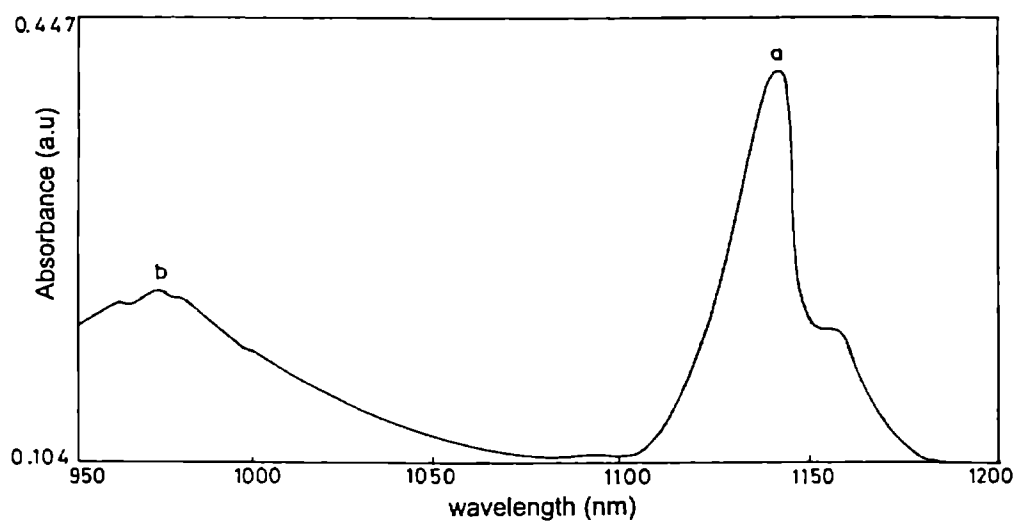


Fig. 2.30 The aryl CH and the OH overtone peaks in the $\Delta V=3$ region of p-chlorophenol.

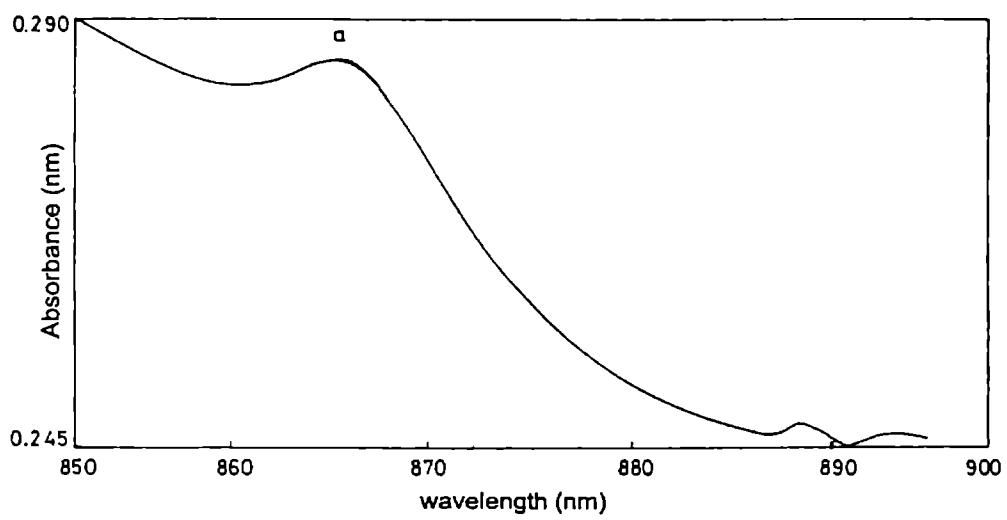


Fig. 2.31 The aryl CH overtone peak in the $\Delta V=4$ region of p-chlorophenol.

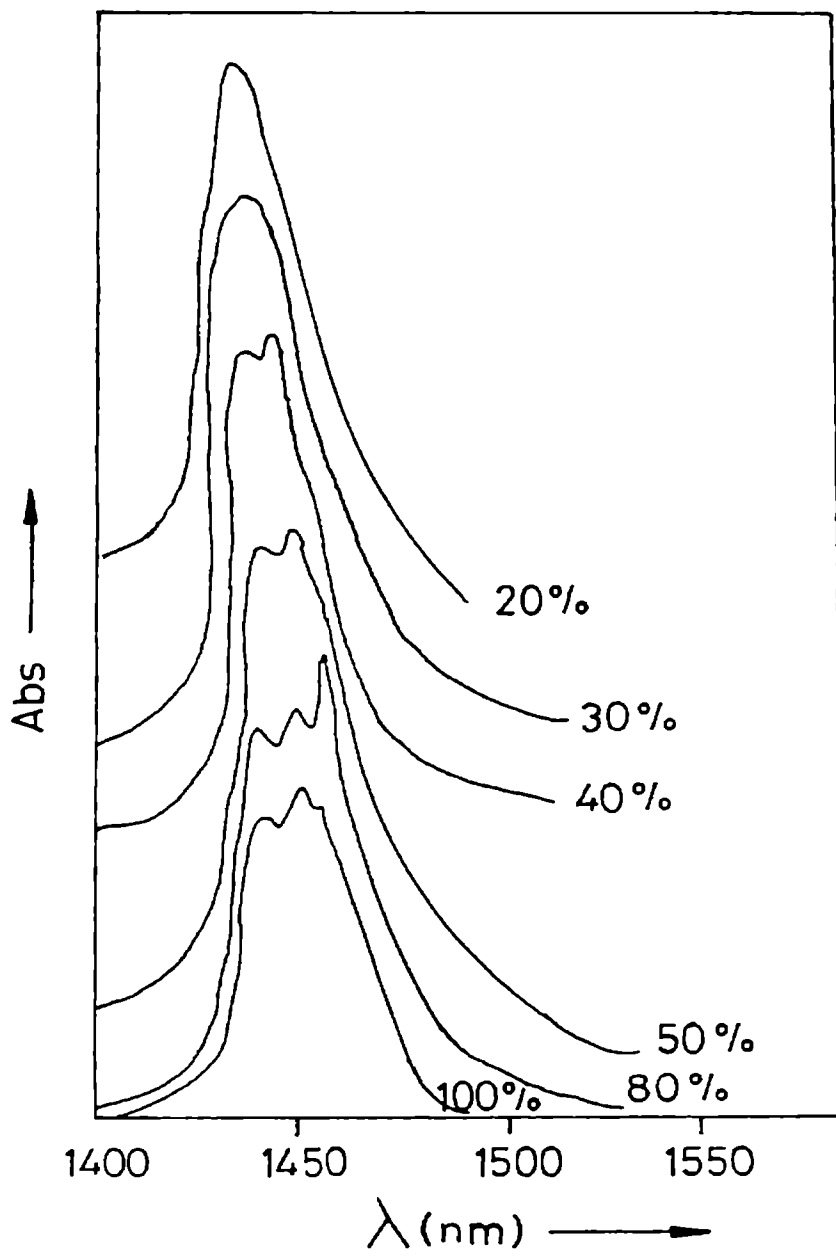


Fig. 2.32 The OH overtone peaks of o-chlorophenol at different concentrations in the $\Delta V=2$ region.

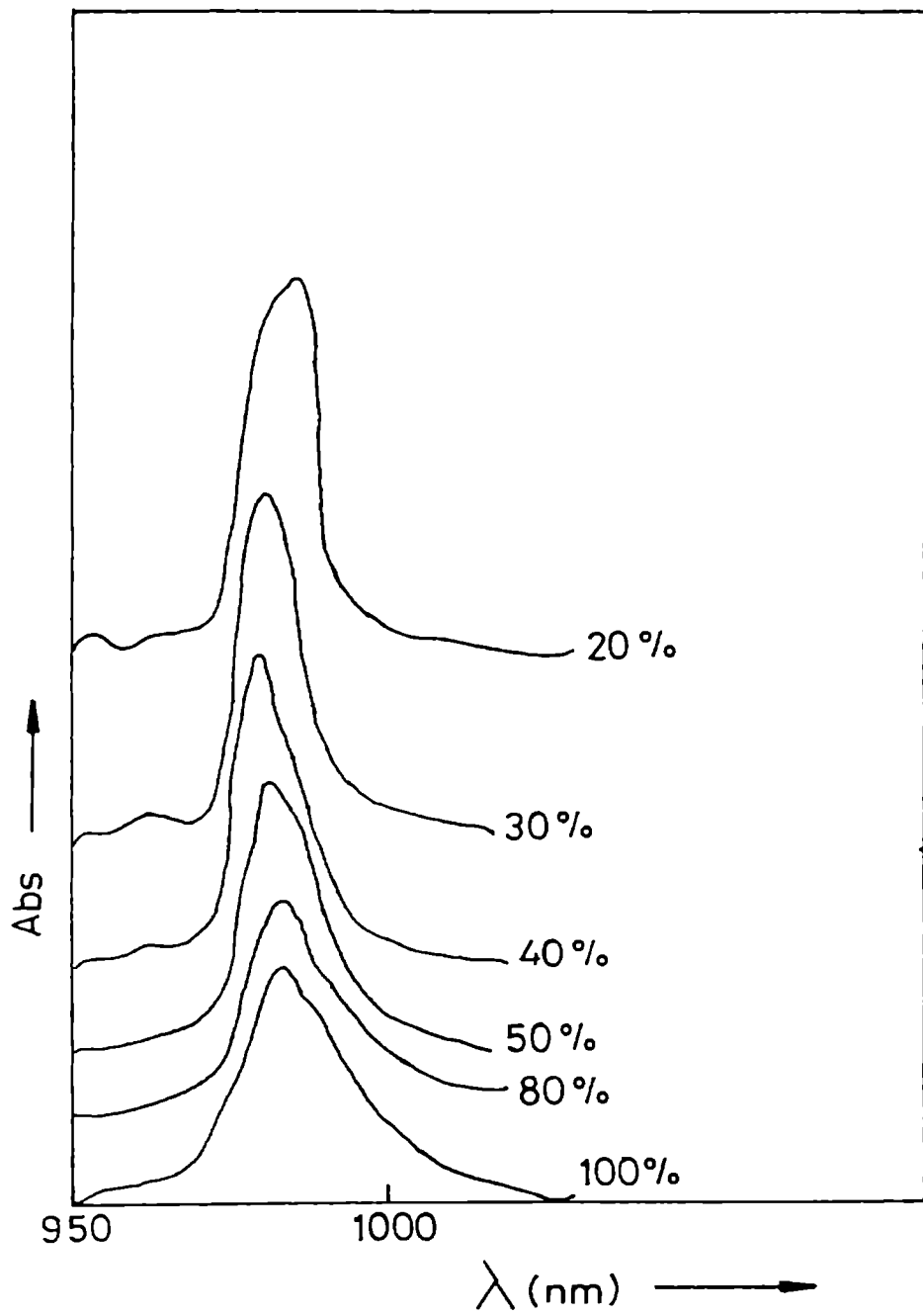


Fig. 2.33 The OH overtone peaks of o-chlorophenol at different concentrations in the $\Delta V=3$ region.

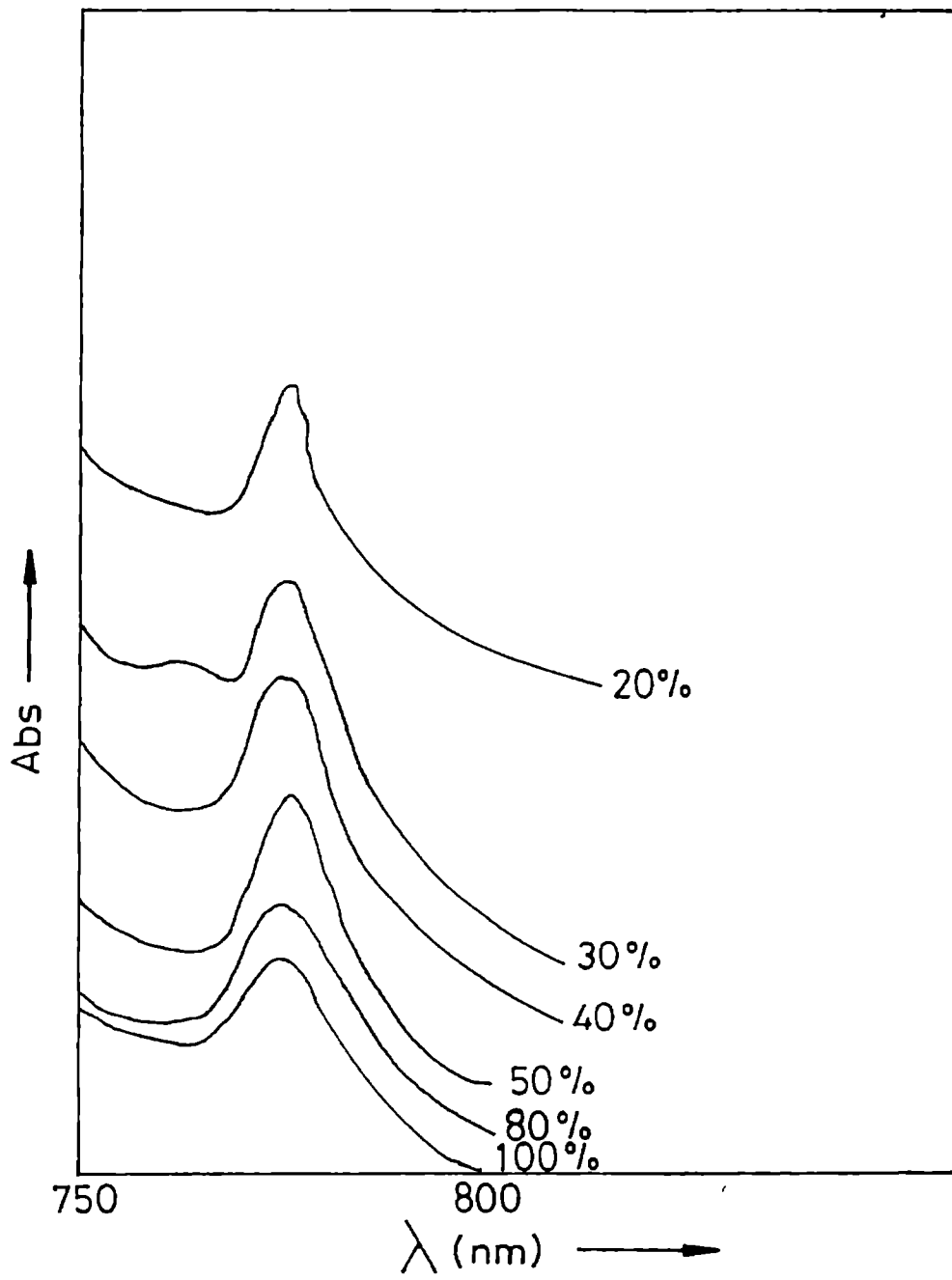


Fig. 2.34 The OH overtone peaks of o-chlorophenol at different concentrations in the $\Delta V=4$ region.

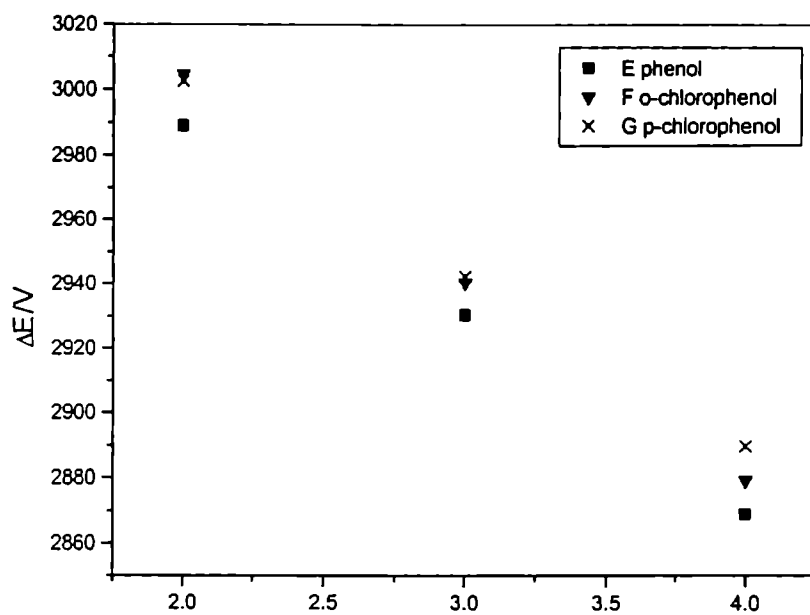


Fig. 2.35. Birge-Sponer plots for ring CH overtones of phenol, o-chlorophenol and p- chlorophenol.

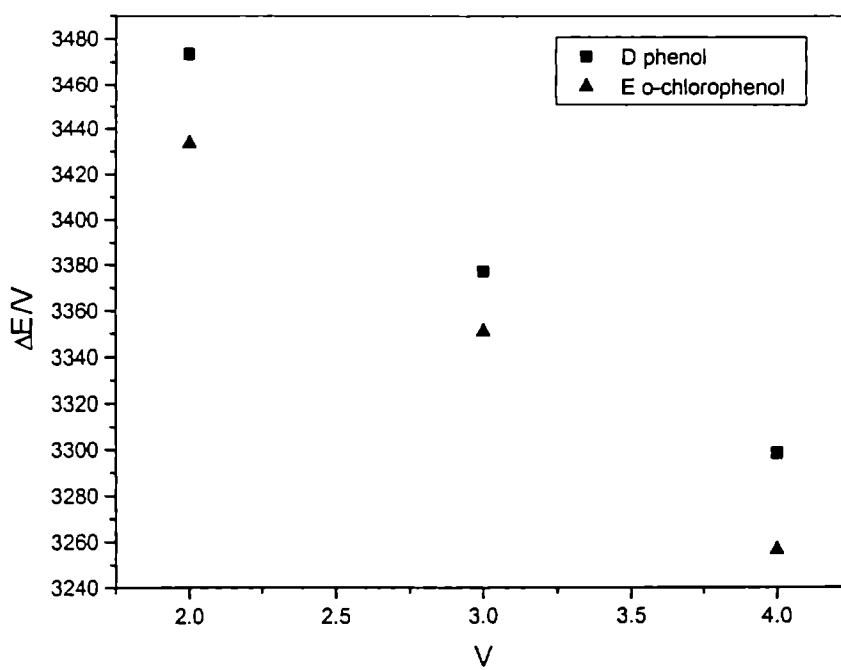


Fig. 2.36 Birge-Sponer plots for OH overtones of phenol and o-chlorophenol.

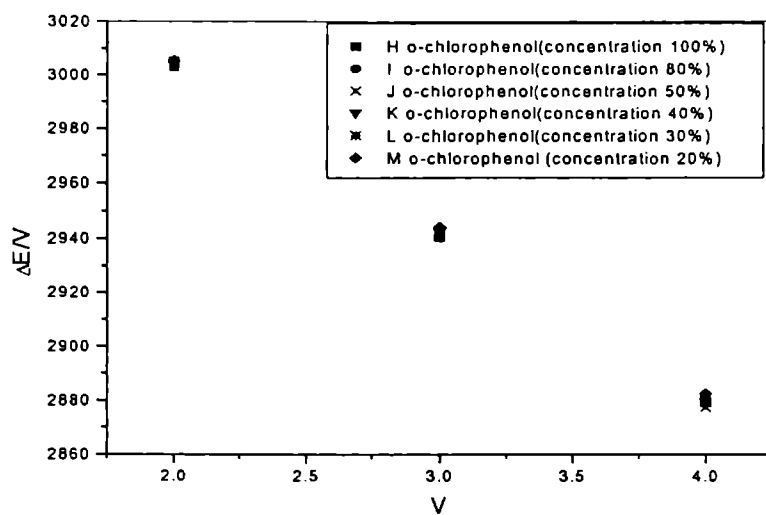


Fig. 2.37 Birge-Sponer plots for ring CH overtones of o-chlorophenol at different concentrations.

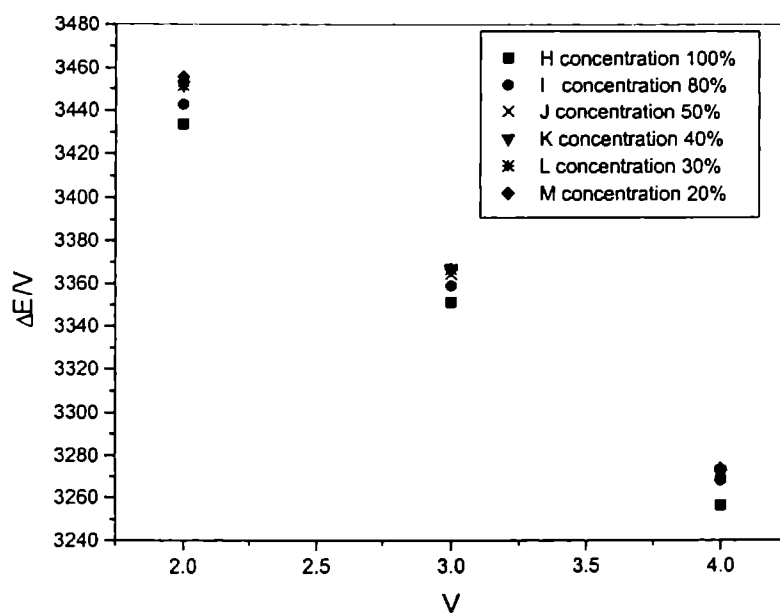


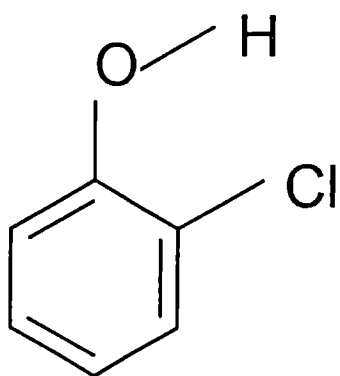
Fig. 2.38 Birge-Sponer plots for OH overtones of o-chlorophenol at different concentrations.

Yamamoto et al [9] studied the emissive properties of the S_1 state of the rotational isomers of *o*-chlorophenol by electronic spectroscopy in a supersonic jet. Their studies show that intramolecular hydrogen bonding between the chlorine atom and the H atom of the OH group has a large effect on the rate of the nonradiative process from the S_1 state.

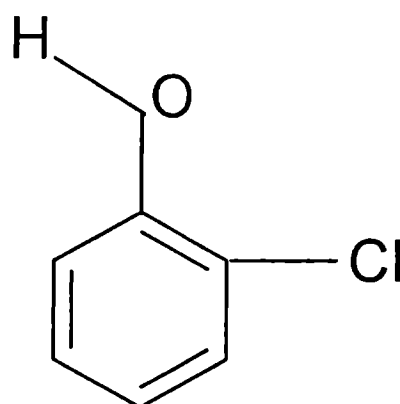
The difference in aryl CH mechanical frequency values between chlorobenzene [27] and *o*-chloroaniline [23] is very small. This shows that chlorine plays a major role in these compounds and that the NH_2 group has no effective role in determining the aryl CH mechanical frequency in *o*-chloroaniline due to the presence of intramolecular hydrogen bonding [23]. A similar effect can be expected for *o*-chlorophenol also. In *o*-chlorophenol, the chlorine plays the important role in increasing the mechanical frequency by withdrawing electrons from the ring, while the OH group does not make any considerable change in the ring mechanical frequency due to the presence of hydrogen bonding and. In substituted phenols, σ_{ortho} value of chlorine is 0.68, a value much higher than that of *p*-chlorophenol ($\sigma = 0.23$). In *p*-chlorophenol, the OH group acts as a donating group ($\sigma = -0.37$) and the chlorine atom ($\sigma = 0.23$) withdraws electrons from the ring [28]. The net withdrawing effect increases the aryl CH mechanical frequency of *p*-chlorophenol compared to that of benzene [12]. But due to high σ_{ortho} value of chlorine in ortho substituted phenols and due to the presence of intramolecular hydrogen bonding, the net withdrawal of electrons increases the aryl CH mechanical frequency in *o*-chlorophenol compared to that of *p*-chlorophenol. This is also evident from the pK_a values of these molecules. The pK_a value for *o*-chlorophenol is 8.6 and *p*-chlorophenol is 9.4. It is well known that electron-withdrawing groups enhance the acidity while electron-donating groups decrease the acidity and compounds having less pK_a values will be more acidic. Hence it is obvious that in *o*-chlorophenol, the net electron-withdrawing effect from the ring is more dominant compared to *p*-chlorophenol and hence the mechanical frequency of the ring CH in *o*-chlorophenol is higher than that in *p*-chlorophenol.

It is observed that the OH mechanical frequency values in *o*-chlorophenol at higher concentrations are smaller than that in lower concentrations while the aryl CH mechanical frequency value is almost unaffected by change in

concentration. We propose the following explanation for the variation of the OH mechanical frequency with respect to change in concentration. At high concentrations, due to the presence of intramolecular hydrogen bonding in *o*-chlorophenol, most of the molecules are in the *cis* form [9]. This intramolecular bonding makes use of the oxygen lone pair thereby increasing the electron density of the OH bond. This increase in the electron density causes a decrease the OH mechanical frequency value. It is known that there is increased population of the *trans* form of *o*-chlorophenol at low concentrations; this *trans* form of the molecule has a free-OH capable of forming intermolecular hydrogen bond. In general for any concentration, both the hydrogen bonded (*cis*) and open (*trans*) forms exist in conformational equilibrium [11]. It is also concluded that at any finite concentration, dimers are formed between *cis* and *trans* molecules joined by an intermolecular OH...O hydrogen bond, thus weakening the intramolecular bond [29,10]. This causes a decrease in electron density of the OH bond and hence an increase in the mechanical frequency of the OH oscillator. As the concentration is decreased from high values, the population of the *trans* conformer increases, thus increasing the number of dimers formed by intermolecular hydrogen bonds. This explains the occurrence of high values of OH mechanical frequency at lower concentrations. Akai et al [30] studied the photoreaction mechanisms of *o*-chlorophenol and its multiple chloro-substituted derivatives. These studies and the DFT calculations of *o*-chlorophenol also support the presence of the two conformers of *o*-chlorophenol and the existence of intramolecular hydrogen bonding in the *cis* conformer. The *cis*, *trans* and *cis-trans* forms of *o*-chlorophenol are shown in fig. 2.39.



o-chlorophenol - cis



o-chlorophenol - trans

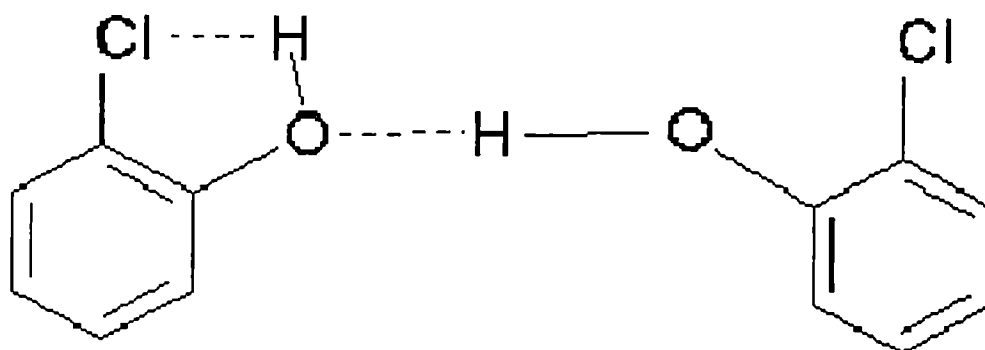


Fig.2.39 The structure of *o*-chlorophenol dimer (cis-trans)

In conclusion, the near infrared overtone absorption spectra of liquid phase phenol, *o*-chlorophenol, *p*-chlorophenol and carbon tetrachloride solution *o*-chlorophenol at different concentrations are analyzed. The analysis of the mechanical frequency values of the aryl CH and OH oscillators in pure compounds reveals the existence of intramolecular hydrogen bonding in *o*-chlorophenol. In *o*-chlorophenol solution, as the concentration is decreased from high (saturated) values, the population of the *trans* form of the molecule increases,

thus causing the formation of *cis-trans* dimer (due to intermolecular hydrogen bonding) to become dominant. This causes a decrease in the strength of the intramolecular hydrogen bonding originally present in the *cis* form. The weakening of intramolecular bonding causes a decrease the electron density of the OH bond and hence an increases the mechanical frequency value of the OH oscillator. This explains the increased values of OH mechanical frequency for lower concentrations. The present study shows that vibrational overtone spectroscopy can be used as a good diagnostic tool for probing even weak hydrogen bonding interactions existing in molecules.

Table.2.3 The observed overtone transition energies (cm^{-1}), mechanical frequencies X_1 (cm^{-1}), and anharmonicities X_2 (cm^{-1}) of the aryl CH and OH oscillators in phenol, *o*-chlorophenol and *p*-chlorophenol. The least square correlation coefficients (γ) are also given. The literature values of the aryl CH local mode parameters of chlorobenzene [27] and *o*-chloroaniline [23] are given for a comparison.

Molecule	$\Delta V=2$ (cm^{-1})	$\Delta V=3$ (cm^{-1})	$\Delta V=4$ (cm^{-1})	$\Delta V=5$ (cm^{-1})	X_1 (cm^{-1})	X_2 (cm^{-1})	γ
Phenol Aryl CH OH	5978 6947	8791 10132	11475 13194	14067	3165±4 3733±20	-58.8±0.8 -87.5±5	-0.999 -0.998
<i>o</i> -chloro phenol Aryl CH OH	6009 6867	8821 10053	11517 13024		3192±4 3702±15	-62.6±0.9 -88.8±3.6	-0.9999 -0.999
<i>p</i> -chloro phenol Aryl CH	6005	8827	11559		3170±9	-56.4±2.1	-0.999
chlorobenzene Aryl CH					3161	-56.7	
<i>o</i> -chloro aniline Aryl CH					3166	-58.7	

Table 2.4 The observed overtone transition energies, mechanical frequencies and anharmonicities of CH and OH local modes of *o*-chlorophenol (all in cm^{-1}). The least square correlation coefficient (γ) is also given.

Concentration of <i>o</i> -chloro phenol %	Overtone	$\Delta V=2$ (cm^{-1})	$\Delta V=3$ (cm^{-1})	$\Delta V=4$ (cm^{-1})	X_1 (cm^{-1})	X_2 (cm^{-1})	γ
100	Aryl CH	6010	8821	11517	3193±4	-62.9±1	-0.9999
	OH	6867	10053	13024	3702±15	-88.8±3.6	-0.999
80	Aryl CH	6006	8821	11521	3187±3	-61.4±0.8	-0.9999
	OH	6885	10077	13072	3706±9	-87.3±2.2	-0.999
50	Aryl CH	6006	8827	11510	3192±5	-62.8±1.2	-0.9999
	OH	6903	10093	13079	3725±9	-90.9±2.2	-0.999
40	Aryl CH	6008	8827	11517	3191±2	-62.4±0.4	-0.9999
	OH	6903	10100	13084	3724±13	-90.3±3.1	-0.999
30	Aryl CH	6010	8827	11517	3194±1	-62.9±0.1	-1
	OH	6907	10100	13089	3727±9	-90.6±2.2	-0.999
20	Aryl CH	6011	8832	11529	3190±0.3	-61.6±0.1	-1
	OH	6911	10100	13094	3729±5	-91±1.3	-0.9999

References

- 1 B.R.Henry, *Vibrational spectra and structure*, ed. Durig J.R. (Elsevier, Amsterdam.), 10 (1981) 269.
- 2 M.S.Child and L.Halonen, *Adv. Chem. Phys*, 57 (1984) 1.
- 3 B.R.Henry, *Acc. Chem. Res.*, 20 (1987) 429.
- 4 M.Quack, *Ann. Rev. Phys. Chem.*, 41 (1990) 398.
- 5 H.L.Fang and R.L.Swofford, *Appl. Opt.*, 21 (1982) 55.
- 6 H.L.Fang, D.M.Miester and R.L.Swofford, *J. Phys. Chem.*, 88 (1984) 405.
- 7 H.L.Fang, D.M.Miester and R.L.Swofford, *J. Phys. Chem.*, 88 (1984) 410.
- 8 H.L.Fang, R.L.Swofford, M.McDevitt and A.B.Anders, *J. Phys. Chem.*, 89 (1985) 225.
- 9 L.J.Bellamy and D.W. Mayo, *J. Phys. Chem.*, 80 (1976) 1217.
- 10 S.Yamamoto, T.Ebata, Mitsuo Ito, *J. Phys. Chem.*, 93 (1989) 6340.
- 11 G.Buemi, *Chem. Phys.*, 277 (2002) 241.
- 12 C. K. N. Patel, A. C. Tam and R. J. Kerl, *J. Chem. Phys.*, 71 (1979) 1470.
- 13 P. K. Srivastava, G. Ullas and S. B. Rai, *Pramana*, 43 (1994) 231.
- 14 D. C. McKean, *Chem. Soc. Rev.*, 7 (1978) 399.
- 15 K. B.Borisenko, C. W. Bock and I. Hargittai, *J. Phys. Chem.*, 100 (1996) 7426.
- 16 Y. Mizugai and M. Katayama, *J. Am. Chem. Soc.*, 102 (1980) 6424.
- 17 Ff Y. Mizugai, M. Katayama and N. Nakagawa, *J. Am. Chem. Soc.*, 103 (1981), 5061.
- 18 K. M. Gough and B. R. Henry, *J. Phys. Chem.*, 87 (1983) 3433.
- 19 R. Nakagaki and I. Hanazaki, *Spectrochim. Acta A*, 40 (1984) 57.
- 20 M. K. Ahmed, D. J. Swanton and B. R. Henry, *J. Phys. Chem.*, 91 (1987) 293.
- 21 T. M. A. Rasheed, K. P. B. Moosad, V.P.N. Nampoori and K. Sathianandan, *J. Phys. Chem.*, 91 (1987) 4228.
- 22 V. M. Potapov, *Stereochemistry*, Mir publishers (Moscow), p.478 (1978).
- 23 S. Shaji, T. M. A Rasheed, *Spectrochim. Acta*, part A 57 (2001) 337-347.

- 24 H.L.Fang, R.L.Swofford and D.A.C.Compton, *Chem. Phys Lett.*,108,6(1984) 539.
- 25 D.Hadzi, J.Jan and (in part) A.Ocvirk, *Spectrochim.Acta*, 25A(1969) 97
- 26 R.Nakagaki and I. Hanasaki, *Spectrochim.Acta*, 40 A (1984) 57.
- 27 K..M.Gough, B.R.Henry, *J. Phys. Chem.*, 87 (1983) 3433.
- 28 Bentley, Kirby, *Elucidation of organic structures by physical and chemical methods Part 1*, 2nd edition, John Wiley and sons, Inc. (USA) 1963 p.638.
- 29 E.A.Allan, L.W.Reeves, *J. Phys. Chem.*, 67 (1963) 591.
- 30 N.Akai, S.Kudoh, M.Takayanagi, M.Nakata, *J.Photochem. And Photobiology A:Chemistry*, 146 (2001) 49.

CHAPTER 3

NIR ANALYSIS OF SOME ALIPHATIC MOLECULES

3.1. Introduction

As described in chapter 1, overtone absorption spectroscopy and the local mode model provide a valuable probe of molecular structure, inter and intra molecular interactions, conformational aspects and substituent effects in aliphatic and aromatic compounds [1-4]. The local mode parameters X_1 (mechanical frequency) and X_2 (anharmonicity) distinguish between both chemically nonequivalent X-H oscillators as well as conformationally nonequivalent X-H oscillators [5-8].

This chapter describes the analysis of the NIR vibrational overtone spectra of liquid phase formamide, allyl alcohol, allyl chloride and nitromethane. Formamide is the simplest molecule which may be linked by hydrogen bonds between C=O and N-H groups. The analysis of overtone spectrum of formamide shows that the CH mechanical frequency value is much larger than the aldehydic CH mechanical frequency value in acetaldehyde. We have explained this observation as due to the inhibition of lone pair trans effect due to intermolecular hydrogen bonding and due to lone pair interaction between carbonyl oxygen and NH_2 . Allyl alcohol is used as a starting material in the syntheses of various polymers, pharmaceuticals, pesticides and other allyl compounds. Allyl chloride is a chemical intermediate used in many applications. It is a highly versatile product due to the presence of dual reactive sites - at the double bond and at the chlorine atom. The observed decrease in the mechanical frequency value of methylene CH in the vinyl group of allyl alcohol compared to that of chloro methyl CH in benzyl chloride is explained as due to the occurrence of lone pair trans effect originating from the oxygen atom. The mechanical frequency value of methylene CH in allyl chloride is close to that reported for chloro methyl CH in benzyl chloride. The lowering of the mechanical frequency value of vinyl CH in allyl alcohol with respect to ethylene points to the donation of electrons by the CH_2OH group. A

reverse effect is shown to occur in allyl chloride due to the withdrawal of electrons. Nitromethane (CH_3NO_2) is an asymmetric top molecule consisting of a heavy frame (NO_2) and a lighter top (CH_3), the local symmetries of which are C_{2v} and C_{3v} respectively. The relative rotation of the groups is quasi free with a very low 6-fold torsional barrier in the ground vibrational state. Taking into account the local symmetry of the CH_3 group, the overtone spectrum of nitromethane requires a treatment under the local mode picture. The spectrum could be assigned through the diagonalization of a coupled anharmonic oscillator Hamiltonian symmetrized under C_{3v} point group. The observed transition energies of the local mode overtones and local-local combinations are found to agree with those predicted by the calculations.

3.2 Experimental

High purity (>99%) formamide, allyl alcohol and allyl chloride from Sisco Research Lab. Pvt. Ltd., Bombay, (India), and nitromethane from CDH Ltd, India are used for the present experiments. The near infrared absorption spectra in the range 2000-700nm are recorded using a Hitachi model U3410 UV-VIS-NIR spectrophotometer, which uses a tungsten lamp as the near infrared source. All spectra are recorded at room temperature ($26 \pm 1^\circ\text{C}$) from pure liquids of 1 cm path length with air as reference.

3.3 Results and Discussion

3.3.1 Analysis of the overtone spectra of formamide

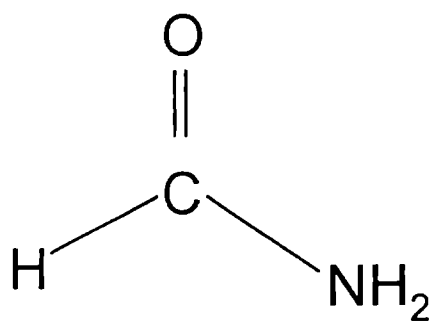


Fig. 3.1 The molecular structure of formamide

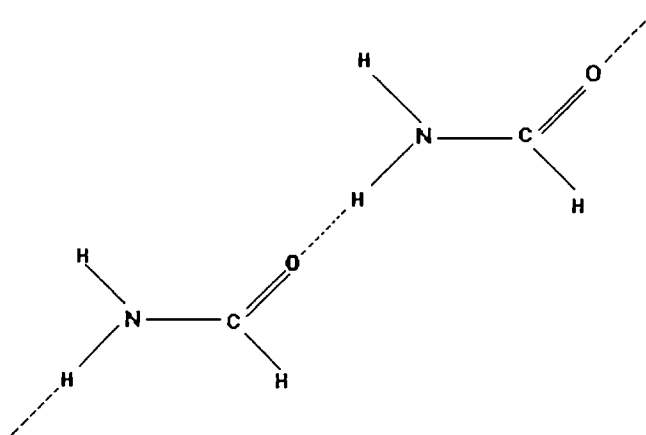


Fig. 3.2 Hydrogen- bonded model of formamide

The observed overtone absorption spectra of formamide in the $\Delta V = 2-4$ regions corresponding to the CH and NH local modes are shown in figs.3.3-3.6. In these figures, the peaks denoted by 'b' represent alkyl CH overtones and those denoted by 'a' represent NH overtones. The band assignments, transition energies and the local mode parameters are given in Table 3.1. The NH local mode parameters reported for aniline [9] are also given for a comparison. The alkyl CH mechanical frequency in formamide is found to be much greater than the aldehydic CH mechanical frequency in salicylaldehyde [10] (by $\sim 96 \text{ cm}^{-1}$), whereas the NH mechanical frequency is observed to be close to that in aniline.

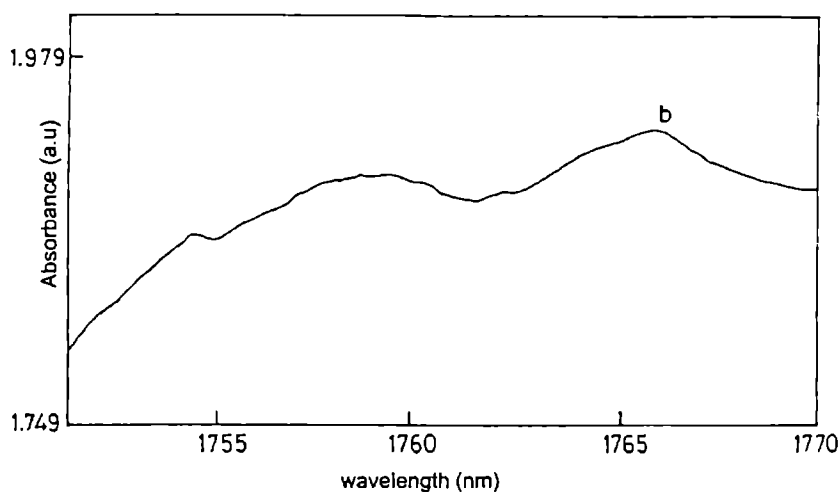


Fig. 3.3 alkyl CH overtone peak in the $\Delta V=2$ region

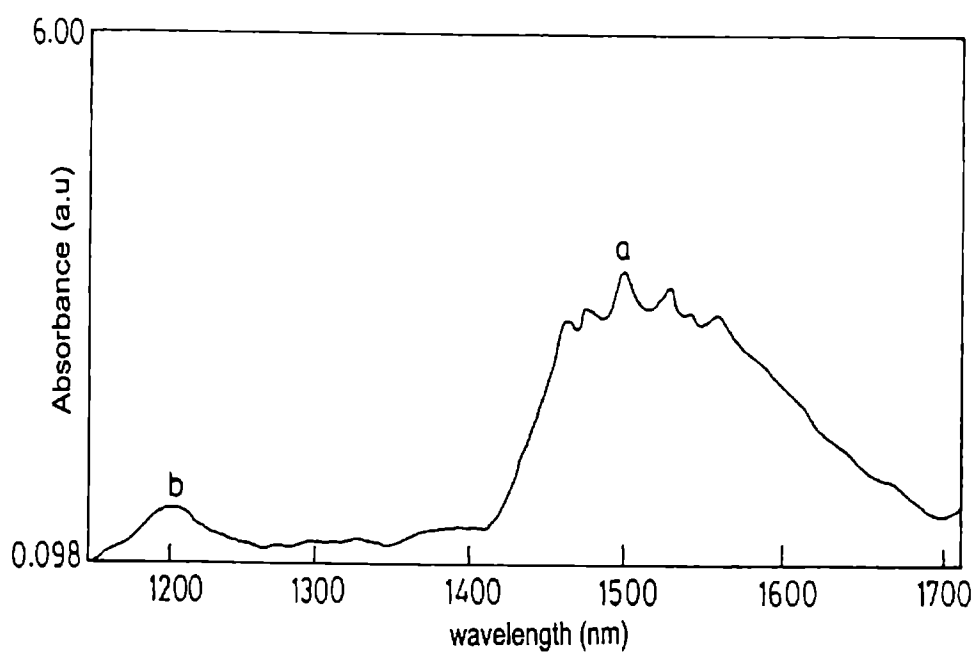


Fig. 3.4 NH overtone peak in the $\Delta V=2$ region (marked as 'a') and alkyl CH overtone peak in the $\Delta V=3$ region (marked as 'b').

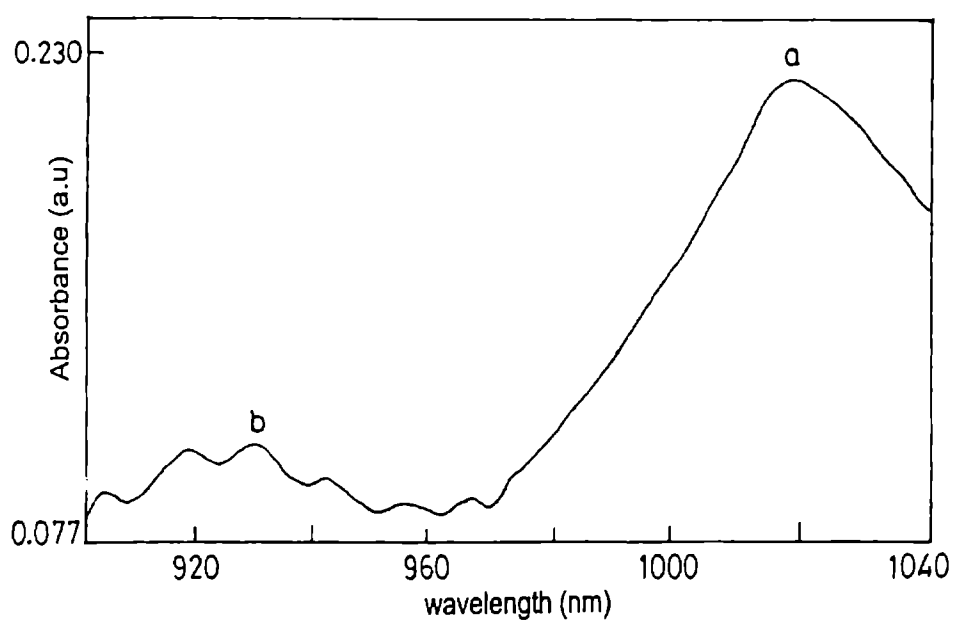


Fig. 3.5 NH overtone peak in the $\Delta V=3$ region (marked as 'a') and alkyl CH overtone peak in the $\Delta V=4$ region (marked as 'b').

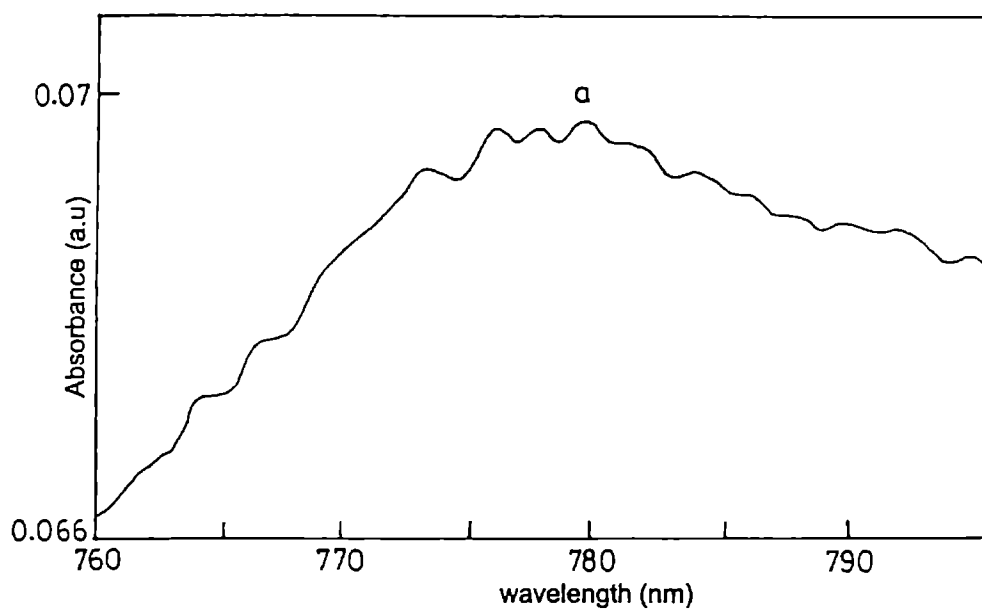


Fig. 3.6 NH overtone peak in the $\Delta V=4$ region.

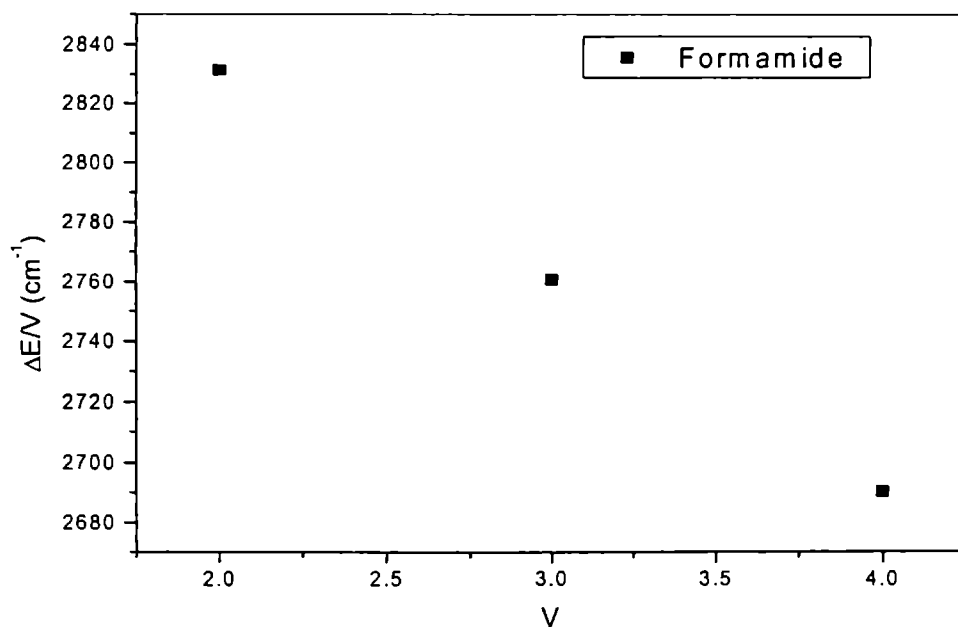


Fig. 3.7 Birge- Sponer plot for alkyl CH overtone in formamide.

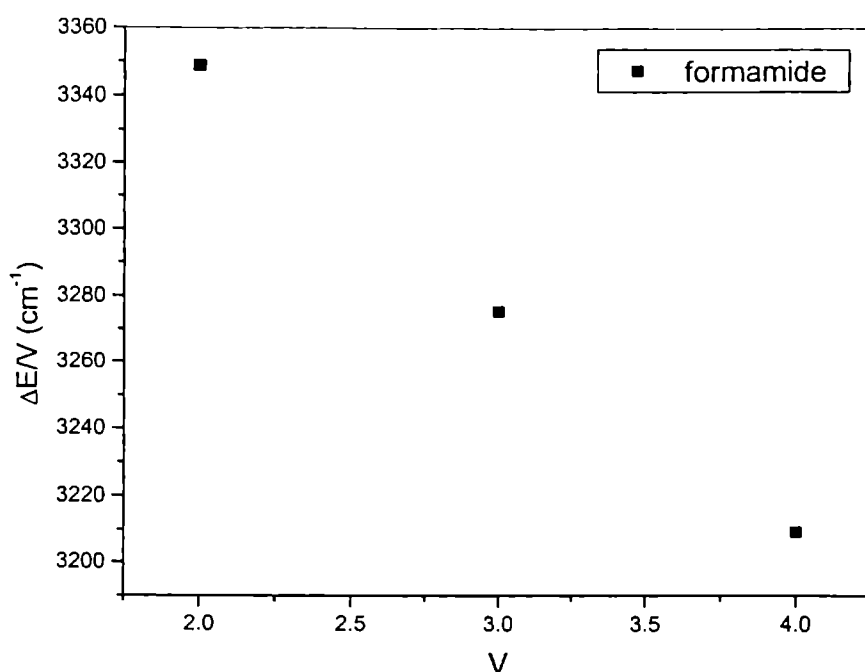


Fig. 3.8 Birge- Sponer plot for NH overtone in formamide

An examination of the previous results on different aldehydes will be useful in interpreting the observations on formamide. These details are already given in chapter 2 where our work on benzaldehyde and salicylaldehyde is presented. Here we recall some of the points that are relevant for the analysis of the spectral results of formamide. It is well known from the overtone studies in acetaldehyde that the aldehydic stretching frequency is smaller compared to the average alkane value. This is explained as due to the lone pair trans effect [7, 11]. The extent of donation of electron density from the trans lone pair to the aldehydic CH antibonding orbital can be assumed to depend on the C=O bond length [7]. The experimental C=O bond length values in benzaldehyde and salicylaldehyde are 1.212 Å and 1.225 Å respectively. The large value of C=O bond length can lead to a decreased lone pair trans effect, causing an increase in CH mechanical frequency. Accordingly, the aldehydic CH mechanical frequency in salicylaldehyde becomes greater than that in benzaldehyde. However, as concluded in chapter 2, in salicylaldehyde the lone pair trans effect is not only decreased, but completely inhibited, due to the presence of intramolecular hydrogen bonding [10]. The C=O bond length in formamide is 1.243 Å which

is even greater than that in salicylaldehyde [12]. The large value of C=O bond distance can cause appreciable reduction in the lone pair trans effect.

The aldehydic CH bond length reported for salicylaldehyde is 1.110 \AA , which is 0.01 \AA shorter than that in benzaldehyde. The smaller value of bond length is consistent with the large value of mechanical frequency in salicylaldehyde. The alkyl CH mechanical frequency in formamide is 3044 cm^{-1} , which is much higher than that in salicylaldehyde. This large value of alkyl CH mechanical frequency is consistent with the smaller value of CH bond length in formamide (1.105 \AA) [13]. These observations point to the complete absence of lone pair trans effect in formamide. We propose the following explanation for the high value of alkyl CH mechanical frequency in formamide. The large value of C=O bond length occurs due to the interaction of the lone pair electrons of carbonyl oxygen and NH_2 group as well as due to the occurrence of intermolecular hydrogen bonding. The adjacent strongly electronegative carbonyl group tends to bind the unshared pair to the nitrogen via an inductive effect [14]. This interaction and the intermolecular hydrogen bonding can be expected to inhibit the donation of electron density from the lone pair to alkyl CH antibonding orbital, which in turn causes an increase in alkyl CH mechanical frequency. The interaction of lone pair electrons of carbonyl oxygen and NH_2 group “uses” the electron lone pair density associated with the NH_2 group. This situation can be compared to the situation in aniline where conjugation of the lone pair electrons of the NH_2 group with the phenyl ring occurs. Consequently, the NH mechanical frequency value in formamide becomes close to that in aniline.

In conclusion, the NIR overtone absorption spectrum of liquid phase formamide is analyzed using local mode model. The analysis of the mechanical frequency values of CH and NH oscillators reveals the inhibition of lone pair trans effect in formamide due to the binding of the lone pair of the NH_2 group by the carbonyl group and due to the presence of intermolecular hydrogen bonding.

Table 3.1: Observed overtone transition energies (cm^{-1}), mechanical frequencies X_1 (cm^{-1}), and anharmonicities X_2 of alkyl CH and NH local modes in formamide. The least square correlation coefficients (γ) are also given. The mechanical frequencies and anharmonicities of salicylaldehyde and aniline are also given for a comparison.

Molecule	$\Delta V=2$	$\Delta V=3$	$\Delta V=4$	X_1	X_2	γ
Formamide						
Alkyl CH	5663.16	8282.26	10759.63	3044	-70.84	-1
NH	6697.48	9826.07	12836.97	3557.52	-69.75	-0.9999
Salicylaldehyde						
Aldehyde CH				2947.7	-63.6	
Aniline						
NH				3549.56	-77.16	

3.3.2 Analysis of overtone spectra of allyl alcohol and allyl chloride

The molecular structures of allyl alcohol and allyl chloride are shown in figures 3.9 and 3.10



Fig. 3.9

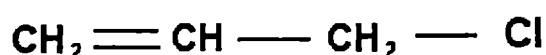


Fig. 3.10

The observed absorption spectra of the compounds, allyl chloride and allyl alcohol in the near infrared region are shown in figures 3.11-3.17. The major peaks in the overtone spectra are due to CH bonds of vinyl group. The peak positions and the local mode parameters obtained from Birge-Sponer plots are given in Table 3.2. In the figures, 'a' denotes vinyl CH pure overtone peaks, 'b' denotes the pure overtone peaks due to side group CH, 'c' denotes the peaks due to OH second overtone and the other peaks are due to combinations. The vinyl CH mechanical frequency and anharmonicity values in allyl chloride are greater than those in ethylene by $\sim 6 \text{ cm}^{-1}$ and $\sim 7 \text{ cm}^{-1}$ whereas in allyl alcohol the mechanical frequency is less by $\sim 25 \text{ cm}^{-1}$ and the anharmonicity almost unchanged with respect to ethylene.

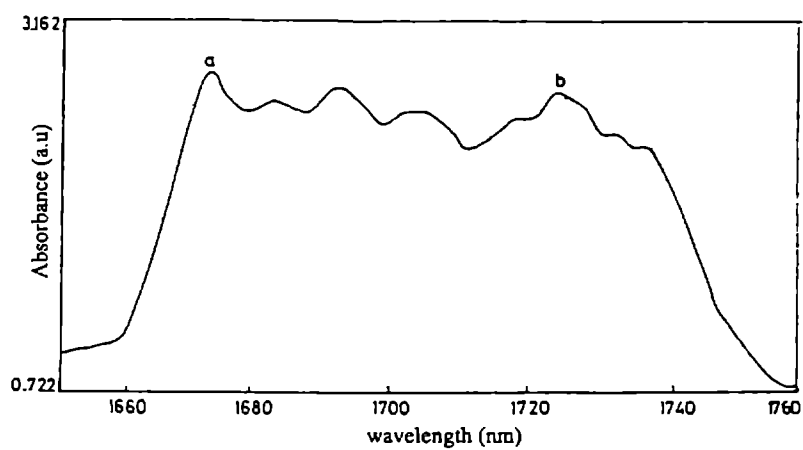


Fig. 3.11 Vinyl and methylene CH overtone peaks in the $\Delta V=2$ region of allyl chloride.

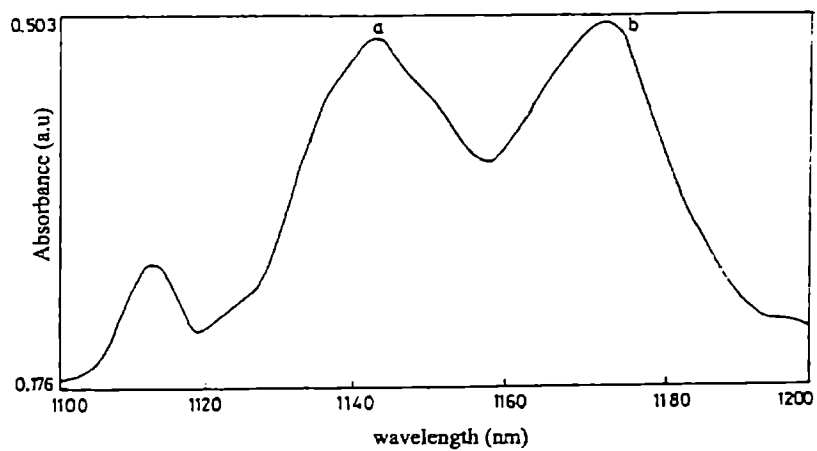


Fig. 3.12 Vinyl and methylene CH overtone peaks in the $\Delta V=3$ region of allyl chloride.

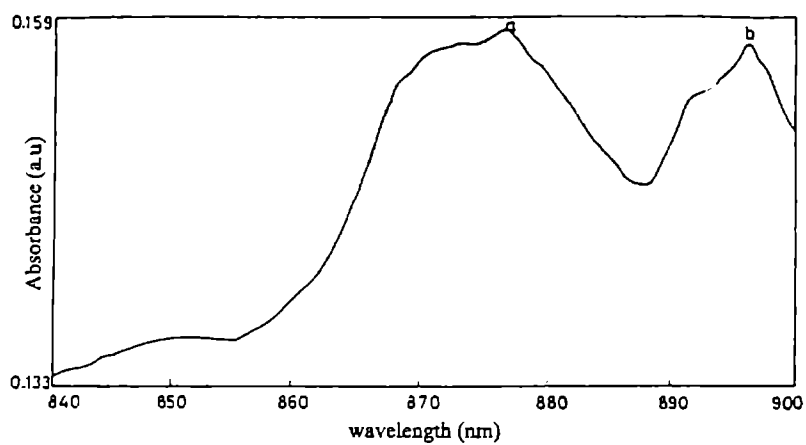


Fig. 3.13 Vinyl and methylene CH overtone peaks in the $\Delta V=4$ region of allyl chloride.

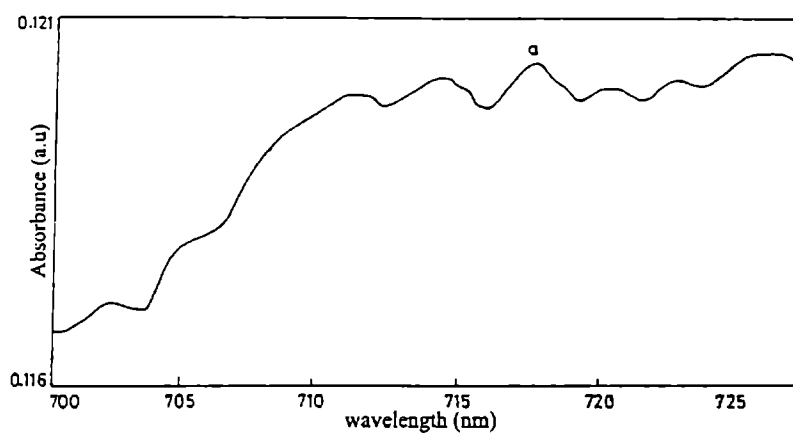


Fig. 3.14 Vinyl CH overtone peak in the $\Delta V=5$ region of allyl chloride.

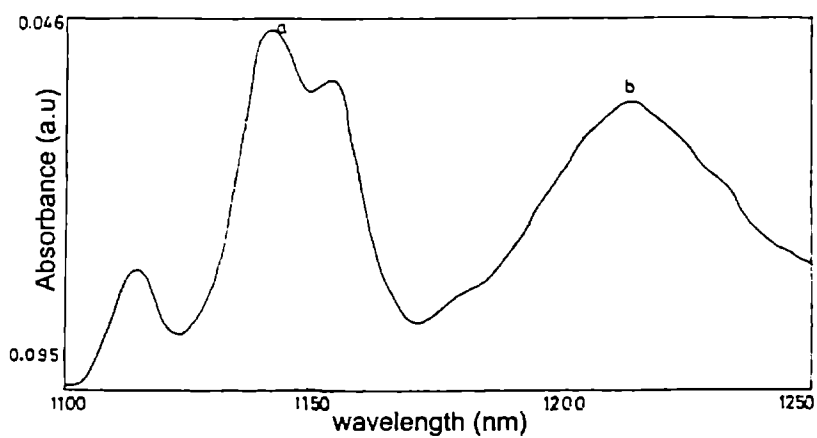


Fig.3.15 Vinyl and methylene CH overtone peaks in the $\Delta V=3$ region of allyl alcohol.

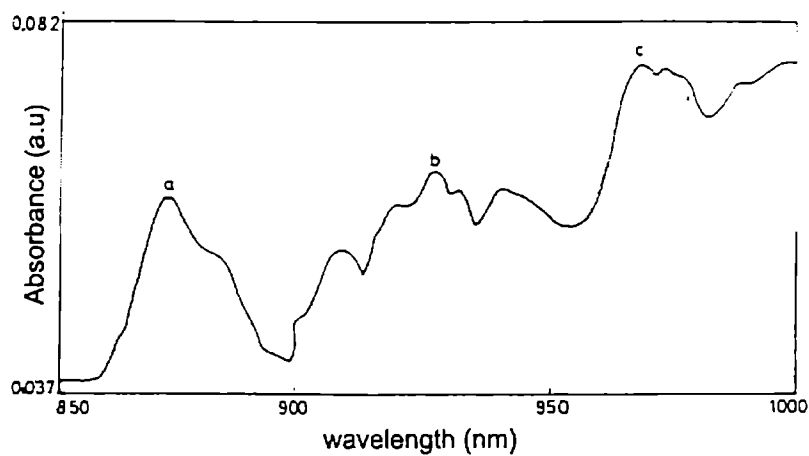


Fig.3.16 Vinyl and methylene CH overtone peaks in the $\Delta V=4$ region and OH overtone peak ('c') in the $\Delta V=3$ region of allyl alcohol.

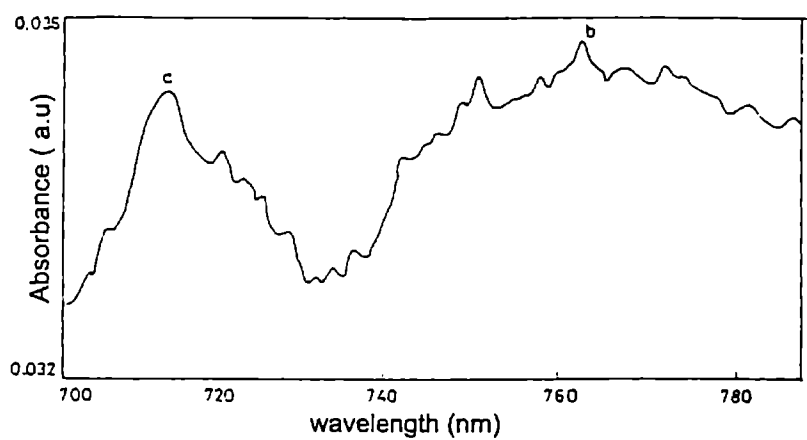


Fig.3.17 Vinyl and methylene CH overtone peaks in the $\Delta V=5$ region of allyl alcohol.

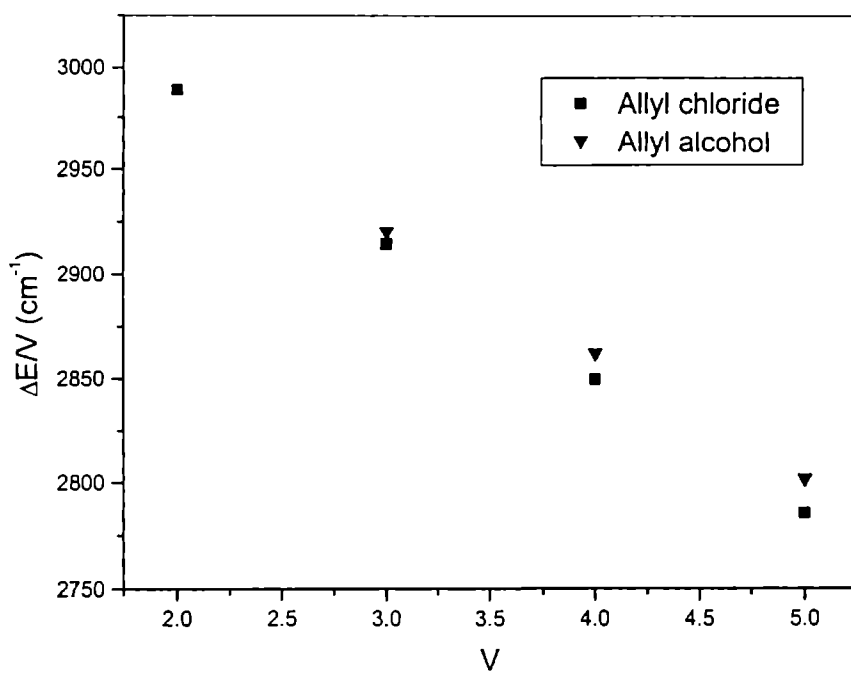


Fig.3.18 Birge-Sponer plots for vinyl CH overtones of allyl chloride and allyl alcohol.

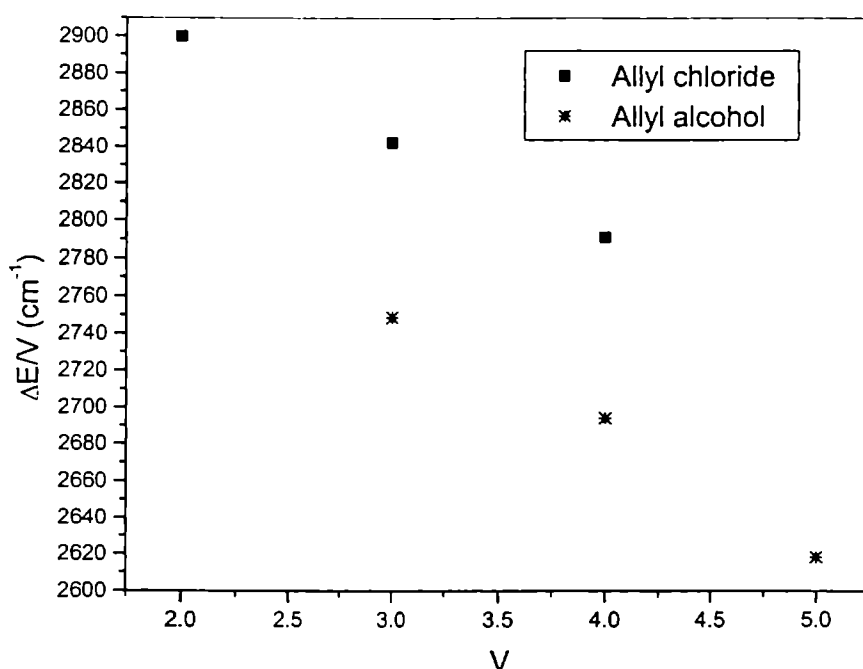


Fig.3.19 Birge-Sponer plots for chloromethyl CH overtones of allyl chloride and allyl alcohol.

Since allyl chloride and allyl alcohol are the derivatives of ethylene, a comparison of the present observations with the reported results for ethylene will be useful in analyzing the results. The reported values of the mechanical frequency and anharmonicity of ethylene are 3182 cm^{-1} and 60.6 cm^{-1} [15]. As stated earlier, the mechanical frequency value of vinyl CH in allyl chloride is greater by $\sim 6 \text{ cm}^{-1}$ and that in allyl alcohol is less by $\sim 25 \text{ cm}^{-1}$ with respect to ethylene. It is well established from overtone studies of substituted benzenes that an electron-withdrawing group causes a decrease in bond length and hence increases the force constant, which in turn will give an increase in mechanical frequency whereas an electron-donating group causes a decrease in mechanical frequency [16-18]. The present observations can be explained on similar lines; CH_2Cl acts as electron withdrawing group as in benzyl chloride [19] resulting in an increased value of the vinyl CH mechanical frequency in allyl chloride. In allyl alcohol, CH_2OH donates electrons and consequently the CH mechanical

frequency of the vinyl group decreases. The large value of anharmonicity constant in vinyl group of allyl chloride shows that the potential energy curve becomes more anharmonic with respect to that of ethylene. This is evident from the dissociation energy values given in table 3.2

In the overtone spectra of allyl chloride and allyl alcohol, the methylene CH overtone peaks occur on the low energy side of the vinyl CH overtone peaks. The mechanical frequency value of chloromethyl CH in allyl chloride is very close to the reported value for benzyl chloride [19]. In allyl alcohol, the mechanical frequency of methylene CH is found to be less than that of the chloromethyl CH in allyl chloride. According to the results of conformation studies [20], in allyl alcohol, one of the lone pair electrons of the oxygen atom is trans to the CH bond of the CH₂OH group thereby causing an interaction of electron with CH bond. This results in an increase in the electron density at methylene CH, resulting in the decrease in CH mechanical frequency compared to that of chloro methyl CH in allyl chloride.

In conclusion, the near infrared overtone absorption spectra of liquid phase allyl chloride and allyl alcohol are analyzed using local mode model. The analysis shows that the large value of CH mechanical frequency in vinyl group of allyl chloride with respect to ethylene is due to electron withdrawal by CH₂Cl and smaller value of mechanical frequency in vinyl group of allyl alcohol is due to the electron donation by CH₂OH. Moreover, the mechanical frequency value of chloromethyl CH in allyl chloride is close to that for benzyl chloride. In the CH₂OH group of allyl alcohol, one of the lone pair electrons trans to CH bond interacts with CH bond, donating electron density to its antibonding orbital, which in turn reduces the mechanical frequency value of the methylene CH oscillator.

Table 3.2: Observed overtone transition energies (cm^{-1}), mechanical frequencies X_1 (cm^{-1}), anharmonicities X_2 and dissociation energies (cm^{-1}) of vinyl and methylene CH in allyl chloride and allyl alcohol. The least square correlation coefficients (γ) are also given. The mechanical frequencies and anharmonicities of benzyl chloride, and ethylene are also given for a comparison.

Molecule	$\Delta V=2$	$\Delta V=3$	$\Delta V=4$	$\Delta V=5$	X_1	X_2	γ	D
Allyl Chloride								
Vinyl CH	5978	8743.6	11398.6	13929.5	3188.14	-67.4	-0.9993	36113
Methylene CH	5799.5	8526.6	11163.2		3062.09	-54.5	-0.9995	41525
Ethylene								
					3182	-60.6		
Allyl alcohol								
Vinyl CH		8761.2	11449.5	14009.5	3157.76	-59.2	-0.9999	40517
Methylene CH		8245.4	10777	13094.2	3006.8	-64.8	-0.9997	33382
Benzyl Chloride								
Methylene CH					3062.7	-53		

3.3.3 Analysis of CH overtone absorption spectrum of nitromethane using local mode picture

The molecular structure of nitromethane is shown in figure 3.20

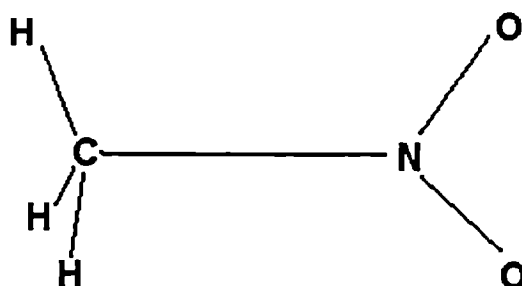
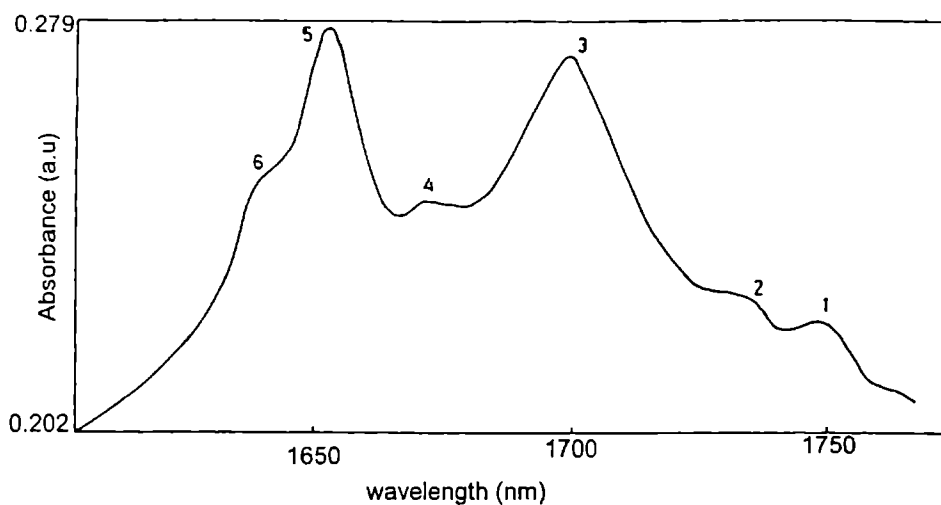


Fig. 3.20

The near infrared absorption spectrum of nitromethane in the region 2000-700 nm is shown in Figures.3.21-3.24. The first overtone region shows two main bands with high and low energy shoulders. In the second overtone region, the spectrum is relatively simpler with a strong band peaked at 8732 cm^{-1} and two weaker ones peaked at 8887 and 9130 cm^{-1} . The third and fourth overtone regions show doublet structure. The assignments of the spectral peaks are given in table 3.4.

Nitromethane (CH_3NO_2) is an asymmetric top molecule consisting of a heavy frame (NO_2) and a lighter top (CH_3), the local symmetries of which are C_{2v} and C_{3v} respectively [21]. The CH overtone spectrum is to be analyzed under C_{3v} local mode picture, which takes in to account the kinetic, and potential energy coupling between the CH oscillators. The effective Hamiltonian for the problem is obtained by assuming harmonic coupling between local mode oscillator states of a given manifold of constant total quantum number, while neglecting the coupling between states belonging to different manifolds. The analysis of the overtone spectra of neopentanes [22, 23], deuterated methanes [24, 25] and methyl cyanide [26] were carried out using this approach.



z

Fig. 3.21 CH overtone spectrum of nitromethane in the $\Delta V=2$ region. The positions marked are (1) local-normal combination (2) local-normal combination (3) A_1 component of $|200\rangle$ (4) E component of $|200\rangle$ (5) A_1 component of $|110\rangle$ (6) E component of $|110\rangle$

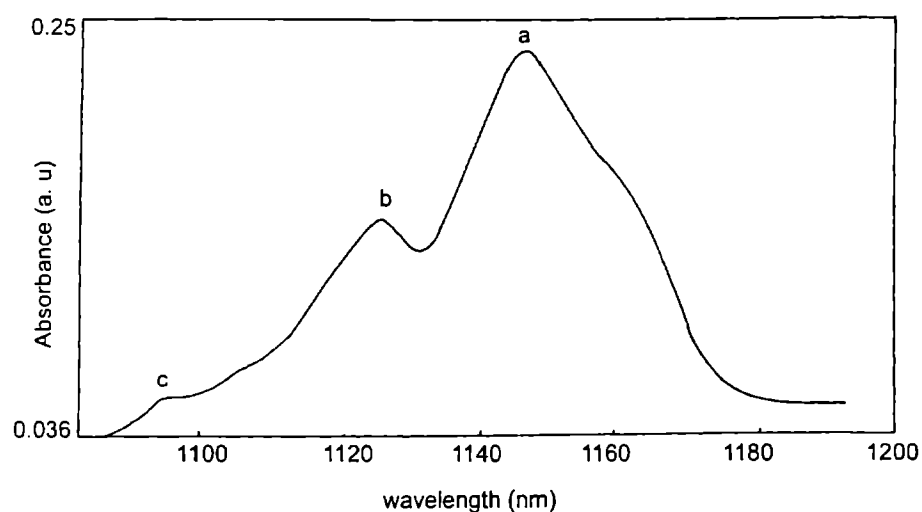


Fig.3.22 CH overtone spectrum of nitromethane in the $\Delta V=3$ region. The positions marked (a) A, E component of $|300\rangle$ (b) A, E component of $|210\rangle$ (c) A_1 component of $|111\rangle$.

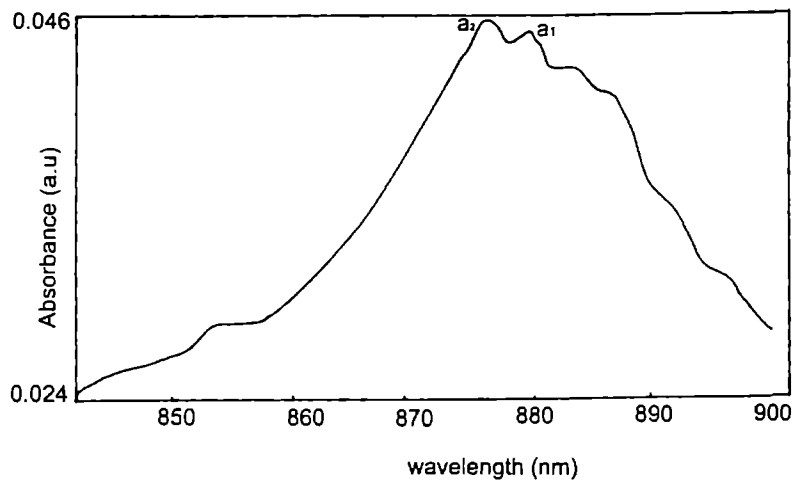


Fig.3.23 CH overtone spectrum of nitromethane in the $\Delta V=4$ region; a_1 represents local-normal combination and a_2 represents pure overtone.

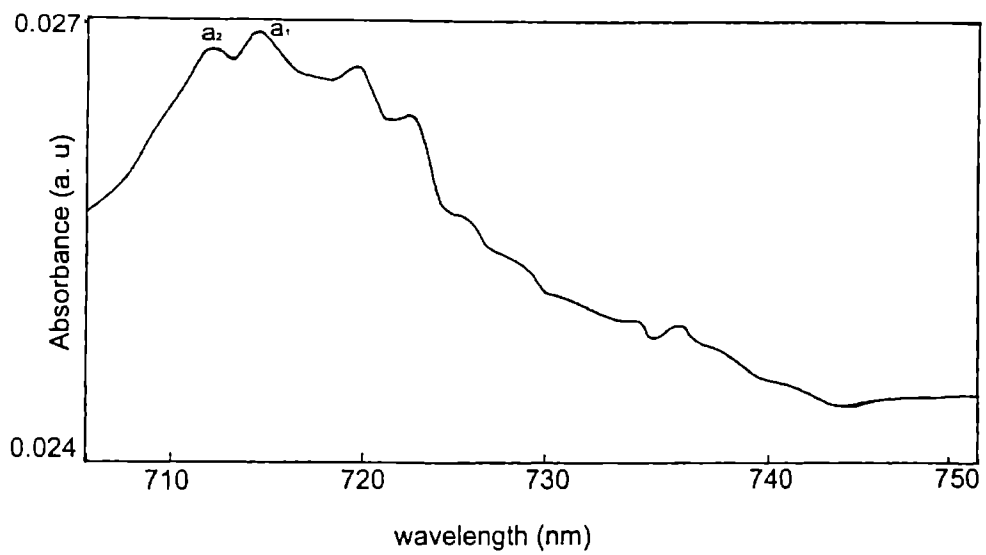


Fig.3.24 CH overtone spectrum of nitromethane in the $\Delta V=5$ region; a_1 represents local-normal combination and a_2 represents pure overtone.

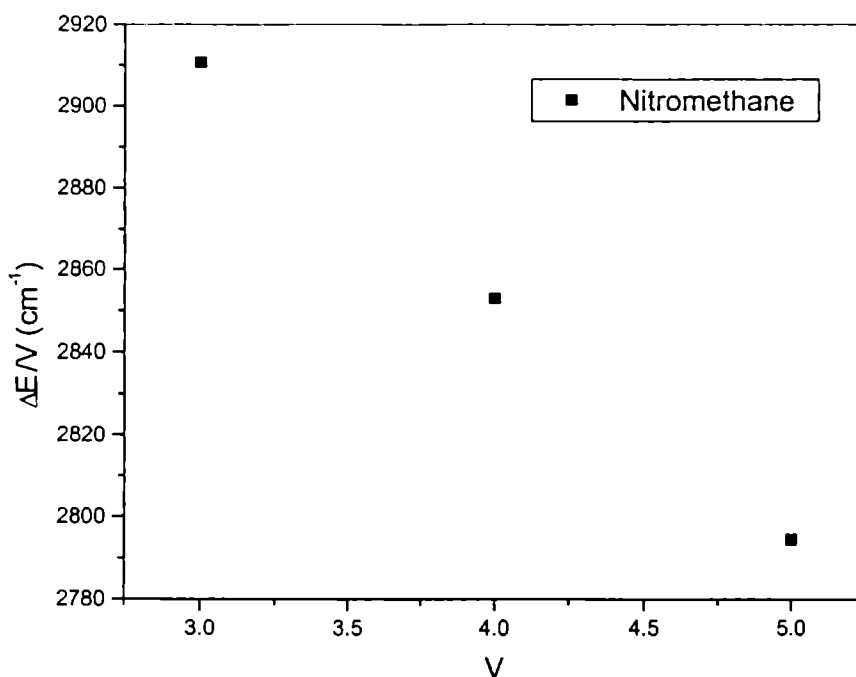


Fig.3.25 Birge-Sponer plot for CH overtones in nitromethane.

The general form of the C_{3v} coupled oscillator Hamiltonian is

$$(H-E_0)\omega^{-1} = (V_1+V_2+V_3) - (V_1^2+V_2^2+V_3^2 + V_1+V_2+V_3) x + \gamma(p_1p_2 + p_1p_3 + p_2p_3) + \phi(q_1q_2 + q_1q_3 + q_2q_3) \quad (1)$$

Here ω and ωx are frequency and anharmonicity, respectively, of the local CH oscillator, E_0 is the energy of the ground state and V_1 , V_2 and V_3 are the quantum numbers of the three oscillators. The parameter γ characterizes the kinetic energy coupling between different CH oscillators and ϕ , the corresponding potential energy coupling. p_i and q_i of equation (1) are normalized momentum and coordinate variables, respectively and are conveniently expressed in terms of creation a^\dagger and annihilation a operators.

$$p = a^\dagger - a \quad (2)$$

$$q = a^\dagger + a \quad (3)$$

The Hamiltonian is diagonalised within a symmetrized local mode basis. For constructing the C_{3v} local mode Hamiltonian we require harmonic frequency ω , anharmonicity ωx and effective coupling parameter $\omega\gamma' = \omega(\gamma-\phi)$ for inter oscillator kinetic and potential coupling. Using the observed pure local mode transition

energies, the parameter ω and ω_X for CH bonds are obtained from the Birge-Sponer relation

$$\Delta E_{v \leftarrow 0} = \omega V - \omega_X (V^2 + V) \quad (4)$$

The parameter $(\gamma - \phi)$ is related to the energy difference between the fundamental symmetric and antisymmetric CH stretching transitions through the relation, $3\omega(\gamma - \phi) = E(|100\rangle_E) - E(|100\rangle_{A1})$. The matrix forms of the Hamiltonian were already given in chapter 1. With the observed fundamental CH stretching transitions 3050 and 2968 cm^{-1} [27], we get $3\omega(\gamma - \phi) = 82 \text{ cm}^{-1}$. The local mode frequency of the fundamental CH stretching transition is $2/3E(|100\rangle_E) + 1/3E(|100\rangle_{A1}) = 3023 \text{ cm}^{-1}$. The values of the fundamental CH stretching transitions can be predicted from the relation, $E(|100\rangle_{A1}) = \omega - 2\omega_X - 2(\gamma - \phi)\omega$ and $E(|100\rangle_E) = \omega - 2\omega_X + (\gamma - \phi)\omega$. The local mode parameters obtained by fitting the peak positions of the second, third, and fourth overtone bands (Table 3.3) in a Birge-Sponer plot are $\omega = 3143.28 \text{ cm}^{-1}$, $\omega_X = -58.12 \text{ cm}^{-1}$ with least square relation = -0.99999. These local mode parameters predict the local mode frequency of the fundamental CH stretching transition as 3027 cm^{-1} and the frequency of the fundamental CH stretching transition as $E(|100\rangle_E) = 3054 \text{ cm}^{-1}$ and $E(|100\rangle_{A1}) = 2972 \text{ cm}^{-1}$. These values agree well with the values cited earlier.

All the parameters governing the matrix elements of the effective Hamiltonian for the different manifolds are now available, the diagonalization of which predicts the values of the pure overtone and local-local combination positions. The calculated and observed peak positions are given in Table 3.4. The values of peak positions of the observed bands in the region $\Delta V = 2$ agree with those reported in ref. [28].

As can be seen from the results, the peak observed in the first overtone region at 5881 cm^{-1} correspond to the transition to $|200\rangle_{A1}$ state which agrees with the calculated of 5885 cm^{-1} . The peak at 5964 cm^{-1} corresponds to the transition to $|200\rangle_E$ state has the calculated value of 5928 cm^{-1} . The isolated peak observed at 6050 cm^{-1} correspond to transition $|110\rangle_{A1}$ state and its high energy shoulder at 6098 cm^{-1} correspond to transition to $|110\rangle_E$ state. They have the calculated values of 6052 cm^{-1} and 6091 cm^{-1} respectively. The peaks observed in the second

overtone region at 8732 cm^{-1} correspond to pure overtone where calculated A_1 and E components are expected to merge to common values. The corresponding calculated values are 8704 cm^{-1} and 8714 cm^{-1} . Out of the various symmetry components of the $|210\rangle$ local-local combination state, only one component $|210\rangle_{A_1}$ is experimentally observed, which has transition energy of 8887 cm^{-1} . The calculated transition energy value for this component is 8872 cm^{-1} . The observed and calculated transition energy values of corresponding to $|111\rangle_{A_1}$ state are 9130 cm^{-1} and 9118 cm^{-1} respectively. The overall agreement in the present work between observed and calculated peak positions are similar to that reported for liquid phase neopentane [22].

As explained earlier, a doublet structure is observed for the bands in the 3rd and 4th overtone regions. We propose that the peaks appearing along with the pure overtone peaks as due to the excitation of stretch-bend local-normal combination states. Such combination states, when becomes accidentally degenerate (Fermi resonance) with pure overtone states, can play important role in the relaxation of local mode states [29].

Extensive studies reported in substituted benzenes have shown that an electron withdrawing substituent causes an increase while an electron donating substituent causes a decrease in aryl CH mechanical frequency value [16,17,30]. Similar effect can be seen in alkyl CH local modes also. The mechanical frequency of alkyl CH of nitromethane is greater than ($\sim 112\text{ cm}^{-1}$) that of neopentane [22]. Since nitro group is a strong electron withdrawing substituent, it causes a decrease in the electron density of alkyl CH that results in an increase in the alkyl CH mechanical frequency value.

In conclusion, the near infrared CH vibrational overtone spectrum of liquid phase nitromethane is analyzed using the local mode picture. This approach uses a C_{3v} coupled oscillator Hamiltonian to predict the transition energies of pure CH local mode and local-local combination states of the methyl group. It is found that the observed transition energies generally agree with the calculated values.

Table 3.3: Observed overtone transition energies (cm^{-1}), mechanical frequency X_1 (cm^{-1}), and anharmonicity X_2 of alkyl CH in nitromethane. The least square correlation coefficient (γ) is also given.

Nitromethane	$\Delta V=3$	$\Delta V=4$	$\Delta V=5$	X_1	X_2	γ
Alkyl CH	8732.1	11412	13972	3143.3	-58.1	-.99999

Table 3.4: Calculated and observed transition energies (cm^{-1}) of pure local mode overtone and local-local combinations in nitromethane. All figures are rounded to nearest integers.

Upper state	Calculated	Observed
$ 100\rangle_{A1}$	2972	2968
$ 100\rangle_E$	3054	3050
$ 200\rangle_{A1}$	5885	5881
$ 200\rangle_E$	5928	5964
$ 110\rangle_{A1}$	6052	6050
$ 110\rangle_E$	6091	6098
$ 300\rangle_{A1}$	8704	8732
$ 300\rangle_E$	8714	
$ 210\rangle_{A1}$	8872	8887
$ 210\rangle_E$	8928	
$ 210\rangle_E$	9021	
$ 210\rangle_{A2}$	9047	
$ 111\rangle_{A1}$	9118	9130
$ 400\rangle_{A1}$	11391	11412
$ 400\rangle_E$	11393	
$ 310\rangle_E$	11740	11723
$ 500\rangle_{A1,E}$	13972	13972

The energy of $|500\rangle$ state is calculated using B-S relation

References

1. B R Henry; *Vibrational spectra and structure*, ed. J.R Durig (Elsevier Amsterdam.), 10 (1981) 269.
2. B.R.Henry; *Acc. Chem. Res.*, 20(1987) 429.
3. M S Child and L. Halonen; *Adv. Chem. Phys.*,57 (1984) 1.
4. M.Quack; *Ann. Rev. Phys. Chem.*, 41 (1990) 839.
5. H. L. Fang and R .L. Swofford; *Appl. Opt.* ,21(1982) 55.
6. H. L. Fang, D. M. Miester and R.L.Swofford; *J. Phys.Chem.*,88(1984) 405.
7. H. L. Fang, D.M. Miester and R.L. Swofford; *J. Phys.Chem.*,88,(1984) 410.
8. H. L. Fang, R.L. Swofford, M.Mc Devitt and A.B.Anders; *J. Phys.Chem.*,89(1985) 225.
9. L. J. Bellami and D.W.Mayo; *J. Phys. Chem.* 80 (1976) 1217.
10. Sunny Kuriakose, K. K. Vijayan and T.M.A. Rasheed; *Asian J. Spect.* 1(2001) 17.
11. D.C.Mc Kean; *Chem. Soc. Rev.*, 7 (1978) 399.
12. Linus Pauling; *The nature of the chemical bond*, 3rd edition, Oxford and I B H Publishing Company, Calcutta, India. (1960) 281.
13. D. C. Mc Kean, J. N. Duncan and L. Batt , *Spectrochim Acta A*, 29 (1973) 1037.
14. David A. Shirley; *Organic chemistry*, Holt, Rinehart and Winston, Inc, USA (1964) p 443.
15. J..M.Jasinski; *Chem.Phy.Lett*,123(1986) 121.
16. Y .Mizugai and M.Kattayama; *J.Am.Chem.Soc*,102 (1980) 6424.
17. Y.Mizugai, M.Kattayama and N.Nakagawa; *J.Am.Chem.Soc*,103 (1981) 5061.
18. R.Nakagaki and I.Hanasaki; *Spectrochim.Acta*, 40 A (1984) 57.
19. T.M.A. Rasheed and V.P.N. Nampoori; *Pramana*, 42,No 3(1994) 245.
20. V.M.Potapov; *Stereochemistry*, Mir Publishers (Moscow), (1978) P 252.

21. M.Halonen, L.Halonen, A.Callegiri and K.K.Lehmann; *J. Phys. Chem. A* 102 (1998) 9124.
22. B.R.Henry, A.W.Tarr, O.S.Mortensen, W.F.Murphy, D.A.C.Compton; *J. Chem. Phys.* 79 (1983) 2583.
23. A.W.Tarr, B.R.Henry; *J. Chem. Phys.* 84 (1986) 1355.
24. L.Halonen, M.S.Child; *J. Chem. Phys.* 79 (1983) 4355.
25. G.A.Voth, R.A.Marcus, A.H.Zewail; *J. Chem. Phys.* 81 (1984) 5494.
26. T.M.A.Rasheed, S.Shaji; *Asian J. Phys.* 8 (1999) 199.
27. J.R.B.Gomes, F.Illas, *Int. J. Mol. Sci.* 2 (2001) 211.
28. D.Cavagnat, L.Lespade; *J. Chem. Phys.* 106 (1997) 7946.
29. D.Cavagnat, L.Lespade and C.Lapouge; *J. Chem. Phys.* 103 (1995) 10502 and references therein.
30. T.M.A.Rasheed, K.P.B.Moosad, V.P.N.Nampoori, K.Sathianandan; *J. Phys. Chem.* 91(1987) 4228.

CHAPTER IV
PULSED LIF AND RAMAN STUDIES OF SOME ORGANIC
MOLECULES

4.1 Introduction

For studying details of molecular energy levels and structural aspects, both fluorescence and Raman spectroscopy have become effective spectroscopic tools. Fluorescence results when an atomic/molecular system is excited into an upper state by absorption of energy quantum and then decaying back to a lower state in a time less than 10^{-5} s. Raman scattering results when light from a monochromatic source is allowed to scatter from a solid or collection of molecules. The technological advances in lasers provided all the areas of spectroscopy with ideal light sources satisfying the requirements for each in terms of monochromaticity, tunability, directionality, coherence properties, irradiance and spectral coverage. In the laser era, both laser induced fluorescence (LIF) and Raman spectroscopy have become standard tools for studying molecules and also found widespread diagnostic and analytical applications [1-8]. Both the above areas are provided with more advantages by the use of pulsed lasers. With small values of temporal pulsed duration (microseconds to femtoseconds) pulsed laser output generally possesses high peak powers (ratio of pulse energy to pulse duration). While the short duration laser pulses find important applications in time resolved studies of different molecular processes [8], the high peak powers govern the intensities of single shot fluorescence and Raman spectra [9-11]

This chapter gives the details of experimental arrangement for recording the pulsed LIF and Raman spectra of some organic compounds, the spectral assignments of the observed LIF spectra of liquid phase N,N diethyl aniline and thin film of polymerized *o*-chloroaniline and the spectral assignments of the observed Raman spectra of liquid phase nitromethane, *o*-chlorophenol, *p*-chlorotoluene and *m*-toluidine.

4.2 Fluorescence

Fluorescence results from a quantum mechanical interaction between electromagnetic radiation and bound atomic/molecular electrons. A photon colliding with a molecule (atom) will either be absorbed or scattered. The probability of absorption is greatest when the quantum energy of this photon matches with one of the atom's excitation energy gaps, provided the transition is spectroscopically allowed. If the photon is absorbed, the molecule is electronically excited where it is unstable. If the molecule is relatively isolated, as in a low-pressure gas, this additional energy is dissipated by the emission of another photon of the same frequency in a random direction. In denser gases, liquids and solids, however, the energy is dissipated by intermolecular collisions, resulting in the emission of a band of photon frequencies. If these photons have frequencies within the visible spectrum, the material will appear to glow. If this energy decay occurs rapidly (within around 10^{-7} s), the process is termed fluorescence; otherwise, for slower decay, the transition is called phosphorescence [4,12,13]

The special characteristics of laser output high power density, monochromaticity, directionality and the possibility of selecting suitable sources as per wavelength and /or power requirements make them ideal excitation sources for fluorescence emission. In laser-induced fluorescence (LIF), a sample absorbs electromagnetic radiation from a laser and some of its molecules are excited to higher energy levels. Fluorescence is emitted at wavelengths longer than the exciting radiation. Both the absorbed and emitted wavelengths are characteristic of a given molecule. Because the emitted wavelength is different from the exciting wavelength, fluorescence detection is possible under very low-level optical background and hence is very sensitive compared to absorption measurements. In some cases LIF sensitivities approach the level of detection of a single atom or molecule [8]. LIF is established to be a useful technique to study the electronic structure of molecules and to make quantitative measurements of analyte concentrations. Analytical applications include monitoring gas-phase

concentrations in the atmosphere, flames, and plasmas; and remote sensing using light detection and ranging (LIDAR).

4.2.1 Fluorescence properties of aliphatic compounds

Very few aliphatic and saturated cyclic organic compounds fluoresce or phosphoresce. All electrons in aliphatic compounds are either very tightly bound or are involved in sigma bonding. Thus, absorption of ultraviolet energy by a saturated molecule usually results, directly or indirectly, in bond disassociation, because of both the high energies ($> 50,000 \text{ cm}^{-1}$) required for excitation and the fact that the electron, which is to be excited, is usually strongly involved in bonding. Clearly, excitation energy dissipated via scission of chemical bonds cannot reappear as fluorescence, with the result that fluorescence quantum yields of saturated organic compounds are usually zero. The only important exceptions to that statement are aliphatic aldehydes and ketones, in which the non-bonding electrons on the carbonyl oxygen can be excited to antibonding $\text{-C=O } \pi$ orbitals without severe disruption of molecular binding [8].

4.2.2 Fluorescence properties of aromatic compounds

Analytically useful photoluminescence is restricted to compounds possessing large conjugated systems, in which π electrons, which are less strongly bound within the molecule than sigma electrons, can be promoted to π^* antibonding orbitals by the absorption of electromagnetic radiation of fairly low energy without extensive disruption of bonding. In liquid solution, most unsubstituted aromatic hydrocarbons exhibit rather intense fluorescence in the ultraviolet or visible, with fluorescence energies decreasing, often with increasing fluorescence yield, as the length of the conjugated system is increased.

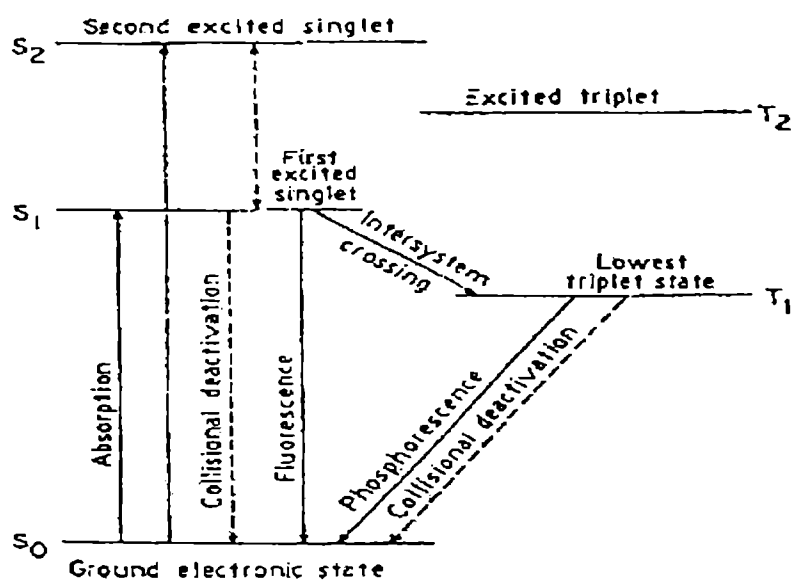


Fig. 4.1 Energy level diagram for fluorescence

From most aromatic hydrocarbons fluorescence is observed usually with comparable yields, signifying that $S_1^* \rightarrow T_1^*$ intersystem crossing proceeds with a rate constant not greatly different from that for fluorescence. For particular aromatic hydrocarbons in which $S_0 \rightarrow S_1^*$ absorption is forbidden, for symmetry (eg. benzene) or other reasons, with a correspondingly long fluorescence lifetime, phosphorescence yields are likely to be appreciably larger than those for fluorescence. It has been demonstrated that direct coupling between singlet and triplet (π, π^*) states in aromatic hydrocarbons is relatively weak, hence the actual spin-orbit coupling mechanism responsible for phosphorescence of aromatic hydrocarbons most probably involves mixing of (π, π^*) singlets with (π, σ^*) triplets, and vice versa [13]. It is generally found that the most intensely fluorescent aromatic molecules are characterized by rigid, planar structures. The principal effect of increasing molecular rigidity is to decrease vibrational amplitudes, which in turn usually reduces the efficiency of intersystem crossing and internal conversion that compete with fluorescence [14]. Molecules consisting of more than one aromatic ring system separated by alkyl chains or carbon-carbon single bonds frequently exhibit unusual fluorescence spectra [13]. In simple cases,

however, the fluorescence spectrum may resemble that of two or more essentially non interacting aromatic compounds [15,16]. A number of aromatic compounds, which consist of two aryl groups separated by alkene chains, can exhibit cis-trans isomerism. The cis isomers are generally non-fluorescent, while the trans species exhibit rather intense fluorescence, as in the particular case of stilbene. Presumably cis-stilbene is rendered nonplanar by steric interference of the ortho-hydrogens of the two aromatic rings. Occasionally, both cis- and trans-isomers may fluoresce, but with different energy distributions and efficiencies, as in the case of 2-vinylanthracene [17].

Fluorescence yields and energies of aromatic hydrocarbons are usually altered by ring substitution. Substituent effects upon the chemical and physical properties of organic molecules in their ground electronic states remain a lively area of investigation, and very much less are known about the influence of substituents upon the behavior of excited states. In order to predict the effect of substituents upon fluorescence spectra, some information concerning substituent effects on the chemical behavior of excited states is required. One useful approach to this problem has been the measurement of Lewis or Bronsted acidities of electronically excited molecules [18, 19]. A number of investigations of excited state protolytic dissociation of substituted phenols have been reported [20-22]; the results demonstrate that conjugation between substituents and aromatic π -clouds is very significantly enhanced by electronic excitation. Significant conjugation involving unoccupied orbitals in substituents appears to be a rather general phenomenon in excited states of substituted benzenes. For example, excited-state protolyses of phenols with a number of sulfur-containing substituents have been examined [22]. Fluorescence energies are much more sensitive to substituent effects than are those for phosphorescence.

A number of fairly reliable generalizations can be stated concerning substituent effects upon luminescence intensities of aromatics. Substituents that act as conjugative electron donors often increase the total luminescence yield of an aromatic system, with the larger effect being noted in the fluorescence spectrum. The conjugation between substituents and aromatic π -clouds is

enhanced to a greater extent in the first excited singlet than in the lowest triplet. It is likely that the principal effect of a conjugative electron-donating substituent is simply to increase radiative transition probabilities, in either direction, between S_0 and S_1^* so that the emission competes more effectively with radiationless deactivation. Strongly electron-donating substituents frequently diminish overall emission yields, and it is likely that at least part of that substituent effect also results from a change in the probability of $S_0 \leftrightarrow S_1^*$ radiative transitions [13]. Most strongly electron-accepting substituents, however, produce much larger decreases in fluorescence yields than one would predict on that basis. For example, one of the most powerful electron-withdrawing substituents is $-\text{NO}_2$, which, when present in an aromatic system, commonly produces complete quenching of fluorescence unless the lowest excited singlet can be populated by absorption of relatively low-energy radiation [13].

Various structural and other factors affect the fluorescence and phosphorescence emission in organic molecules. They are well documented in literature [4,12].

4.3 LIF in molecular structural studies – some recent works

Laser Induced fluorescence is an important technique that is applied in radical detection. LIF was used for the detection of SiH_2 radicals in an a-Si:H deposition plasma [23]. The fluorescence emission from NO_3 was excited by different laser wavelengths. The LIF spectrum exhibits vibrational coarse structure involving fundamentals, overtones and combinations of five vibrational modes of the radical [24]. Hertl et al [25] have reported the LIF detection and kinetics of SiH_2 radical in Ar/ H_2 / SiH_4 radio frequency discharges and Misra et al [26] have reported LIF spectroscopy of the jet-cooled methyl thio radical (CH_3S)

LIF technique using excitation in the A-X and D-X electronic systems have proven to be a reliable technique for two dimensional imaging of nitric oxide (NO) concentrations in practical combustion systems [27]. The principles of LIF using tunable lasers, the calibration of optical systems and the application of LIF

in diagnosing high temperature plasmas were reviewed by Muraoka et al [4]. Harrington et al [28] have reported LIF measurements of formaldehyde in a methane/air diffusion flame. This is an important optical measurement in flames of naturally occurring formaldehyde as an important intermediate in the oxidation of hydrocarbons. Klein-Douwel et al. [29] carried out LIF studies of formaldehyde hot bands in flames. The detection of formaldehyde in flames by use of excitation at one of the higher K sub band heads of the A-X4₁⁰ band was shown to provide an efficient method of imaging this important intermediate while reducing temperature bias in the measurement over a wide range.

Santos et al [30] reported the molecular structures and vibrations of m-methyl aniline in the S₀ and S₁ states studied by laser induced fluorescence spectroscopy and *ab initio* calculations. They studied the UV fluorescence excitation and dispersed fluorescence spectra of jet cooled m-methyl aniline for the S₁-S₀ transition, leading to the observation of some new bands. The main spectral bands were assigned by comparison with those of other relevant substituted benzenes. This study established the spectral evidence for the internal rotation of the methyl group in the electronic ground and excited states of the molecule. Lee et al. [31] reported the LIF excitation spectra of jet-cooled 4-(9-anthryl) aniline where two weakly coupled electronic states were shown to exist.

Kirby et al [32] reported the planar laser induced fluorescence (PLIF) imaging of CO using vibrational (IR) transitions. They demonstrated a new imaging diagnostic method suitable for measurements of infrared active molecules, namely infrared planar laser induced fluorescence (IRPLIF), in which a tunable infrared source is used to excite vibrational transitions in molecules and vibrational fluorescence is collected by an infrared camera. These workers also reported the application of vibrational (Infrared) planar laser induced fluorescence (PLIF) imaging technique for imaging CO₂ molecules where a simple, inexpensive, high pulse energy transversely excited atmospheric CO₂ laser was used to saturate the CO₂ absorption transition at 10.6 μm.

Saarinen et al used LIF method to investigate collision-induced processes in the hydrogen stretching vibrational overtone region of the ground electronic state of acetylene. They studied the collision induced vibration – rotation

fluorescence spectra and rovibrational symmetry changes in acetylene, leading to the deduction of spectroscopic information about symmetric states, which are not reachable by one photon absorption from the ground vibrational state. LIF method has been used to study the highly excited vibrational overtones in acetylene. Jungner et al. [33] reported the laser-induced vibration – rotation fluorescence due to infrared forbidden transitions from overtone levels in acetylene. The laser induced dispersed fluorescence experiment offers new possibilities when applied to vibration – rotation states within ground electronic states; this helps in probing new states in symmetrical molecules that are not accessible by one photon absorption spectroscopy [34].

Hayashi et al. [35] used LIF spectroscopy as an *in situ* diagnostic for phenol and intermediate products in an aqueous solution degraded by corona discharges. They established the applicability of LIF spectroscopy for monitoring phenol concentration during degradation. Pepper et al. [36] reported the *in situ* measurements of subsurface contaminants with a multi-channel LIF system. Chen et al. [37] reported the temporal, spectral and intensity dependant properties of the two photon induced fluorescence emission from phycoerythrin excited by a 1.06 μm laser beam.

4.4 Raman spectroscopy

Raman spectroscopy is established to be a useful technique for molecular structural studies and for the identification of a wide range of substances – solids, liquids and gases. It is a straightforward, non-destructive technique requiring no sample preparation. Basically Raman spectroscopy involves illuminating a sample with monochromatic light and using a spectrometer to examine light scattered by the sample.

At the molecular level, photons can interact with matter by absorption or scattering processes. Scattering may occur either elastically or inelastically. The elastic process is called Rayleigh scattering, whilst the inelastic process is termed Raman scattering. The electric field component of the scattering photon perturbs the electron cloud of the molecule and may be regarded as exciting the system to a

virtual state. Raman scattering occurs when the system exchanges energy with the photon and the system subsequently decays to vibrational energy levels above or below that of the initial state. A simplified energy diagram (Fig 4.2) that illustrates these concepts is shown below. A mode of vibration of a molecule is Raman active if a change in polarizability occurs during that mode of vibration. The frequency shift corresponding to the energy difference between the incident and scattered photon is equal to the frequency of the corresponding mode of vibration, and is termed as the Raman shift. Depending on whether the system has lost or gained vibrational energy, the Raman shift occurs either as an up or down shift for the frequency of the scattered photon relative to that of the incident photon. The energy of the scattered radiation is less than the incident radiation for the Stokes lines and the energy of the scattered radiation is more than the incident radiation for the anti-Stokes lines. A plot of detected number of photons versus Raman shift from the incident laser energy represents a Raman spectrum. As stated earlier, the wave number values of the Stokes and anti-Stokes lines give a direct measure of the vibrational energies of the molecule. The ratio of the intensity of the Raman anti-Stokes and Stokes lines is predicted to be

$$\frac{I_A}{I_S} = \left(\frac{\nu_i + \nu_{vib}}{\nu_i - \nu_{vib}} \right)^4 e^{\left(\frac{-h\nu_{vib}}{kT} \right)} \quad (1)$$

The Boltzmann exponential factor is the dominant term in equation (1), which makes the anti-Stokes features of the spectra much weaker than the corresponding Stokes lines. Infrared spectroscopy and Raman spectroscopy are complementary techniques, because the selection rules are different. For example, homonuclear diatomic molecules do not show an infrared absorption spectrum, since they have no dipole moment, but do show a Raman spectrum, since the stretching and contraction of the bond changes the interactions between electrons and nuclei, thereby changing the molecular polarizability. For polyatomic

molecules possessing a center of inversion symmetry (like benzene, carbon dioxide etc.), it is observed that the modes that are active in the IR spectrum are not active in the Raman spectrum and vice-versa. This is called the rule of mutual exclusion. In molecules with little or no symmetry, modes are likely to be active in both infrared and Raman spectroscopy. Different materials have different vibrational modes, and hence exhibit their characteristic Raman spectra. This makes Raman spectroscopy a useful tool for material identification.

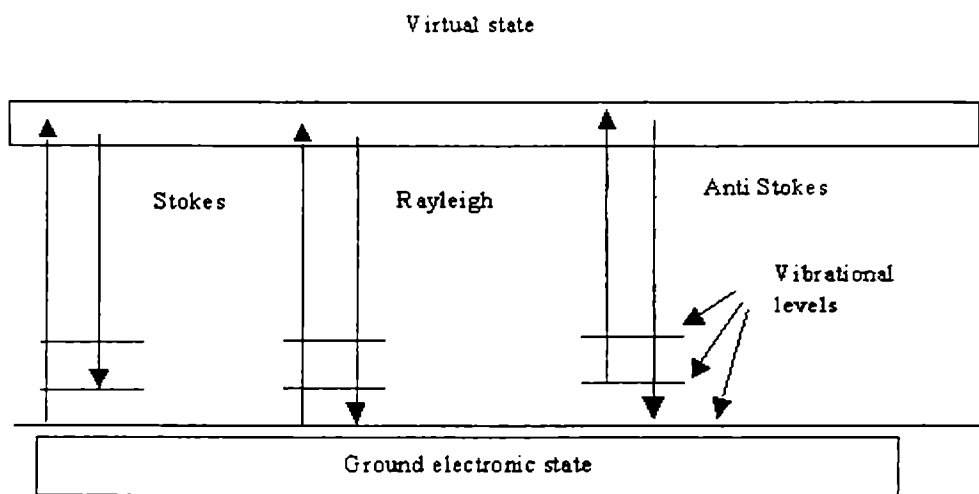


Fig. 4.2 Schematic representation of the quantum transitions in Raman effect.

Both infrared (IR) and Raman spectroscopy deal with the measurement of the vibrational energies of molecules, but the mechanisms of the activities are different. For a vibrational motion to be IR active, the dipole moment of the molecule must change. For a vibration to be Raman active, the polarizability of the molecule must change with the vibrational motion. Thus, Raman spectroscopy complements IR spectroscopy. Experimentally, one measures the Stokes lines, rather than the antiStokes lines, in a Raman spectrum. Unlike infrared absorption, Raman scattering is a low probability process; typically the Stokes lines are $\sim 10^5$ times weaker than the Rayleigh scattered component. Hence an excitation source with high irradiance is always preferable. Also, for measuring even the very small wavenumber (a few cm^{-1}) difference between the excitation and the Stokes lines,

the excitation source should also be highly monochromatic. In modern Raman spectrometers, lasers are used as the excitation source due to their high monochromaticity and high irradiances.

4.5 Laser Raman Spectroscopy in molecular structural studies – some recent works

Raman spectroscopy is a companion technique to infrared spectroscopy, is capable of giving detailed information about molecular structure and quantitative analysis. Brame Jr. et al [38] and Nakanishi et al [39] reported the laser Raman spectra and their assignments of a large number of organic and inorganic molecules and. Philips et al [40] reported high overtone resonance Raman spectra of photodissociating nitromethane vapour and solutions in cyclohexane, acetonitrile and water solvents at energies up to 15000 cm^{-1} (which is the lowest dissociation limit) under excitation by laser wavelengths 218 and 200 nm. The Raman spectrum of vapor phase pyridine was reported by Klots [41]. He proposed assignment modifications for the pyridine fundamentals, based on the first time Raman vapor spectral measurements and a more complete set of infrared and Raman spectra for the gas and liquid phases. Raman polarization measurements were newly given for some 70 lines between 1600 and 3000 cm^{-1} . Bermejo et al [42] recorded the Raman spectra of the Q branches of the hot bands associated with the ν_2 stretching fundamental of $^{13}\text{C}_2\text{D}_2$ using inverse Raman spectroscopy with an instrumental resolution of about $3 \times 10^{-3}\text{ cm}^{-1}$. Anand et al [43] used a fiber optic Raman spectrometer for in-situ measurement of percentage of methanol by volume in methanol-gasoline mixture.

Town et al [44] carried out the theoretical vibrational studies and reported the Raman spectrum of 4-fluoroaniline. Nair et al. [45] reported the microwave and laser Raman spectra of *o*-chlorotoluene. The Raman spectra exhibited some new lines corresponding to the low lying vibrational modes and a torsional state of methyl group in this molecule. Kolev et al [46] studied the vibrational spectra and structure of benzophenone and its ^{18}O and d_{10} labeled derivatives. They carried

out the vibrational analysis using *ab initio* molecular orbital (MO) calculations and experimental study on the infrared and Raman spectra. The Raman spectrum of gaseous $^{13}\text{C}_2\text{H}_2$ recorded with CCD camera detection was reported by Becucci et al. [47]. They obtained the vibration – rotation bands of fundamentals, overtones and combinations in acetylene. Some lines of the Q branch of $^{12}\text{C}^{13}\text{CH}_2$ were also detected. Edwards et al. [48] carried out a vibrational Raman spectroscopic study of scytonemin. The high resolution Raman study of phonon and vibron bandwidths in isotopically pure and natural benzene crystal was reported by Pinan et al. [49]

Raman spectroscopy has become a preferred technique for online monitoring of dispersion polymerization. McCaffery et al [50] reported a low cost low resolution Raman spectrometer for online monitoring of mini emulsion polymerization. The Raman spectra of polypyrrole and polyaniline were reported by Beleze et al [51] who used the spectra for material characterization. The structural analysis of poly (*o*-toluidine) using Raman spectra was reported by A.Buzarovska et al [52]. Da Silva et al [53] studied the redox behavior of cross-linked polyaniline films by in-situ Raman spectra.

4.6 The present experimental setup

This section described the details of the experimental setup used for recording the fluorescence emission spectra and Raman spectra of the organic compounds. This outlines the experimental configuration, components of the apparatus and the various experimental considerations that are to taken into account.

In the present experiment, we used the most common geometry of the perpendicular configuration. In this configuration, the sample is excited with the laser beam and the emissions are collected using a monochromator – detector assembly at a 90° angle. High purity samples (Extra pure AR grade, 99.9 % from Sisco Research Laboratories, India) are used for the present experiments. The second harmonic emission of a Q-switched Nd:YAG laser at 532 nm (6ns) is used as the laser source. An average output power of 500 mW was found to be suitable

for significant fluorescence emission in the region 550 nm - 700 nm from many of the organic compounds. The Q-switched output from the Nd:YAG laser (Spectra Physics, DCR 150) is allowed to fall on the liquid samples taken in a quartz cuvette. The quartz cuvette containing the liquid samples is kept in a sample compartment to isolate it from ambient light. The sample compartment can be attached to the entrance slit of the monochromator – detector assembly. A cutoff filter at 532 nm is used to prevent the scattered laser beam from the sample cell. The emitted radiations are allowed to fall on a grating monochromator (TRIAx 320) through an entrance slit and the wavelength of emissions separated are allowed to fall on CCD (Spectrum-One from ISA Jobin Yuon-Spex Instruments Inc.) through an exit slit. The Monochromator – CCD system is interfaced to a PC using GPIB DAQ from NI and the program used is Spectra Max for Windows version 3.0. The block diagram and the photographs of the experimental arrangement are shown in fig 4.3

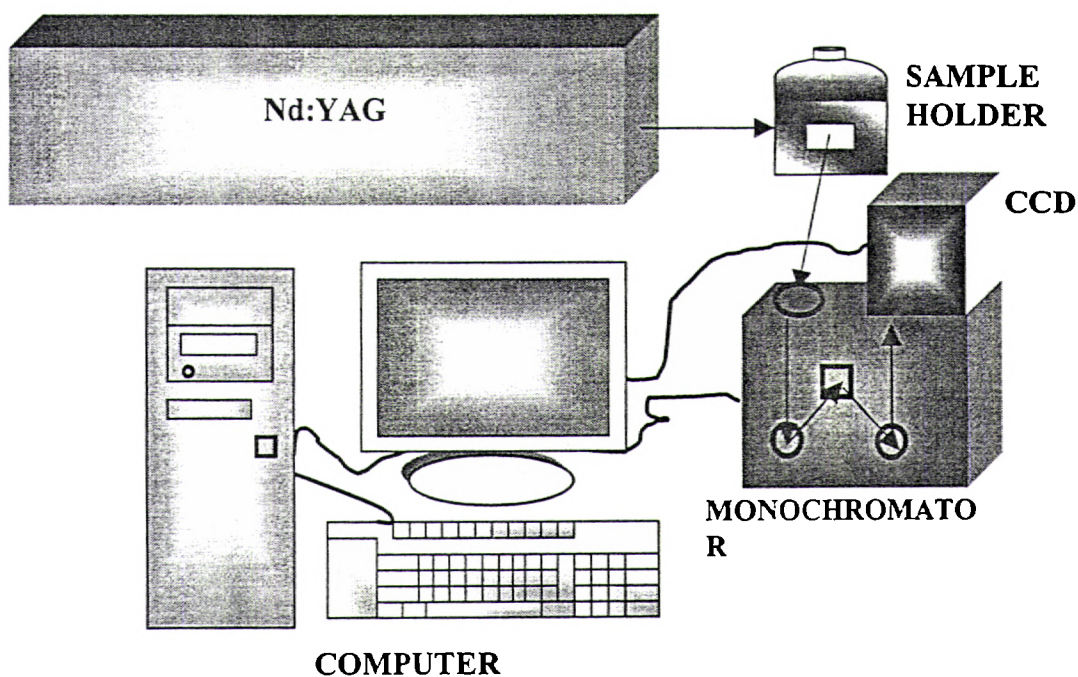
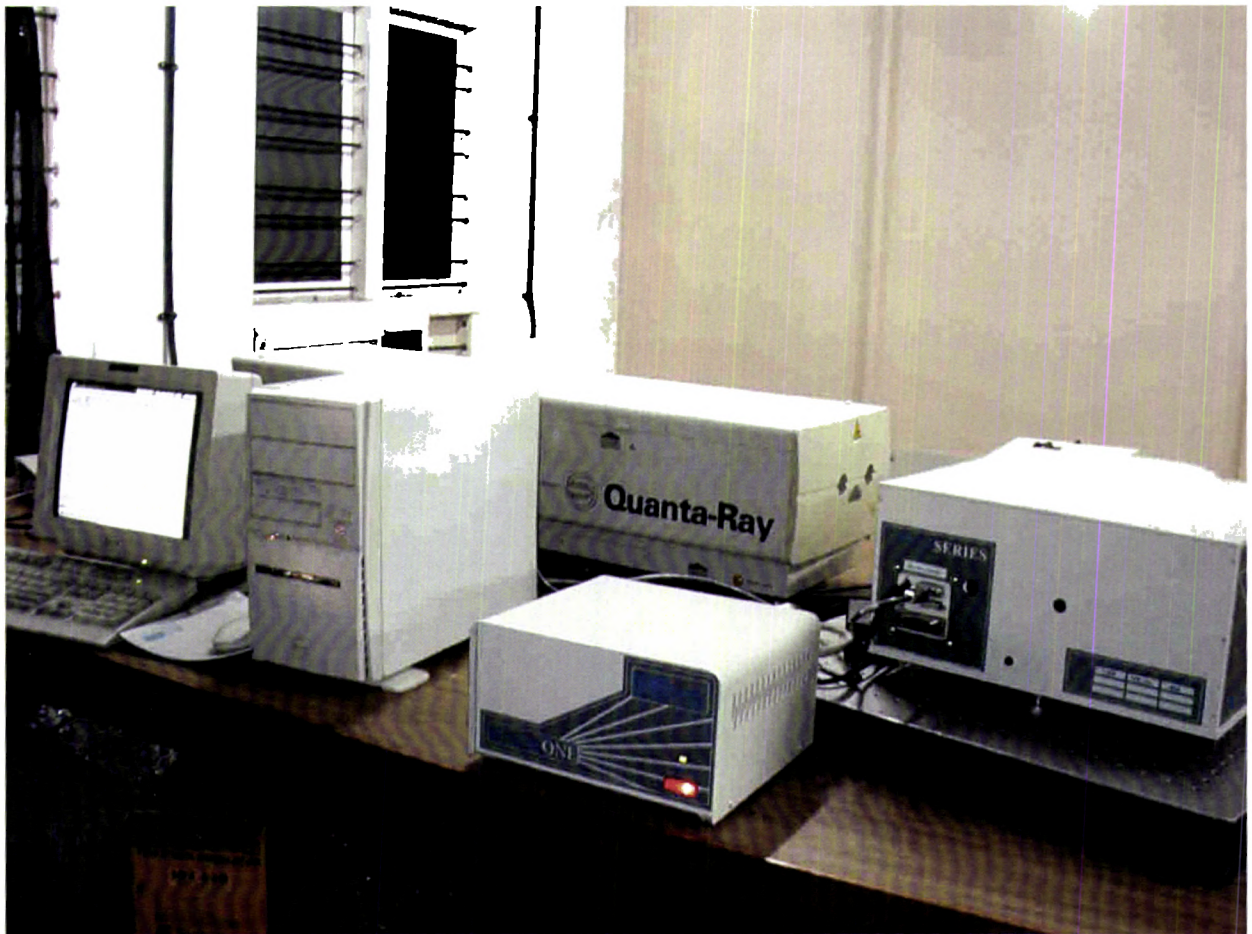


Fig.4.3 The block diagram of the experimental setup used for LIF and laser Raman studies.



(a)



(b)

(Experimental setup for LIF & Laser Raman Spectral Studies)

4.7 Experimental considerations

The LIF spectra are obtained by exciting the sample by second harmonic out of the Q-switched Nd:YAG laser at 532 nm and the emissions from the samples are recorded using the monochromator – detector assembly. There are several experimental factors to be taken care of before recording the spectra. First of all, the output of the laser is to be kept stable. For that as a first step the flash lamp alone is switched on and the lasing rod is pumped for 15 – 20 minutes for thermal stability and then the laser is allowed to operate in the microsecond pulse mode (non-Q-switched mode) for another 15 minutes for the beam and the laser power to become stable. Then after making the flashing rate a minimum energy, the laser is switched over to the Q-switched mode in which we get nanosecond pulses with very high peak power. The laser beam is allowed to fall on the sample quartz cuvette kept in the sample compartment. Special care is taken to avoid back reflection of the laser beam to the laser cavity. The position of the quartz cuvette is slightly adjusted to ensure that the reflected beam from the cell or direct scattering beam does not fall on the entrance slit of the monochromator. A reference spectrum recorded to check the presence of any stray light emissions or flash lamp lines. The calibration is done by recording the laser line and by recording the known emission lines of a neon lamp or mercury lamp. Once the calibrations are done and the setup is aligned properly, it is ready for the spectral measurements.

The power of the laser beam exciting the sample is kept at the required level and the emission spectra are recorded at a longer wavelength region with respect to the excitation wavelength. The region containing the excitation line is excluded to avoid saturation of the detector in which case the weak emission peaks cannot be detected. Then the higher wavelength region is scanned for a wavelength range of 60 nm with a central wavelength by keeping entrance slit width of the order of 0.05 mm and the exit slit width the minimum of 0.001mm. Once the emission peak is obtained, the laser power is varied to check the variation of the peak emission strength of the peak with change in the exciting power. Then the integration time is adjusted to a moderate value and the width of

the exit slit is adjusted to a minimum value possible such that the fluorescence peak is very prominent with maximum spectral resolution. The laser power, entrance slit width, exit slit width and integration time are kept constant then and the emission spectrum is recorded in other regions of higher wavelength also. The software used have all the options to set the central wavelength, number of accumulations, integration time, cosmic removal, integration time, entrance and exit slit width, data file name etc. The data file can be exported as Microsoft excel data and the spectra can be plotted using the software Microcal Origin 5.

4.8 Preparation of the polymer thin film of *o*-chloroaniline

A polymer is a large molecule build up by the repetition of small simple chemical units. The individual molecule that repeats to constitute a polymer is called a monomer and the process by which the monomer units are linked to form the molecule is called polymerization. There are different methods for the preparation of polymer films. We have used the plasma polymerization method for preparing polymer films of *o*-chloroaniline. This method is considered to be much superior to other methods due to its simplicity, industrial importance, high efficiency, pinhole free nature of the films etc.

Plasma polymerization refers to the formation of polymeric materials under the influence of plasma (partially ionized gas). The basic principle involved in all plasma polymerization process is that the free radicals are formed in the system; they then recombine among themselves to form polymeric chain. Here the polymerization takes place under the influence of discharge. The creation and maintenance of plasma necessitate an electric discharge under moderate vacuum conditions. The main source for fragmentation of monomer in plasma is the action of electrons. Therefore, the energy level of electrons may be closely related to the polymer forming process in plasma polymerization. In this method, the polymerization occurs with the help of plasma energy, which involves activated electrons, ions and radicals. The details of our plasma polymerization setup and the method of preparation of polymer films are described elsewhere [54]

4.9 Laser induced fluorescence spectrum of N,N diethylaniline and polymerized o-chloroaniline.

The LIF spectra obtained for liquid phase N,N diethylaniline and polymerized o-chloroaniline are given in figures 4.4 and 4.5. Almost all fluorescent systems that are useful for analysis are complex organic compounds containing one or more aromatic functional groups. The absorption process that leads to the most intense fluorescence in these compounds generally involves a $\pi \rightarrow \pi^*$ transition, although $n \rightarrow \pi^*$ and $\pi \rightarrow \sigma^*$ transitions may also occur [12]. The $n \rightarrow \pi^*$ transition is always less intense because the electrons in the n-orbital are situated perpendicular to the plane of π bond (and hence to the plane of the π^* orbital) and consequently the probability of the jump of an electron from n to π^* orbital is very low and in fact zero according to symmetry selection rules. However vibrations of atoms bring about an overlap between the perpendicular planes and so $n \rightarrow \pi^*$ transition does occur, but only to a limited extent.

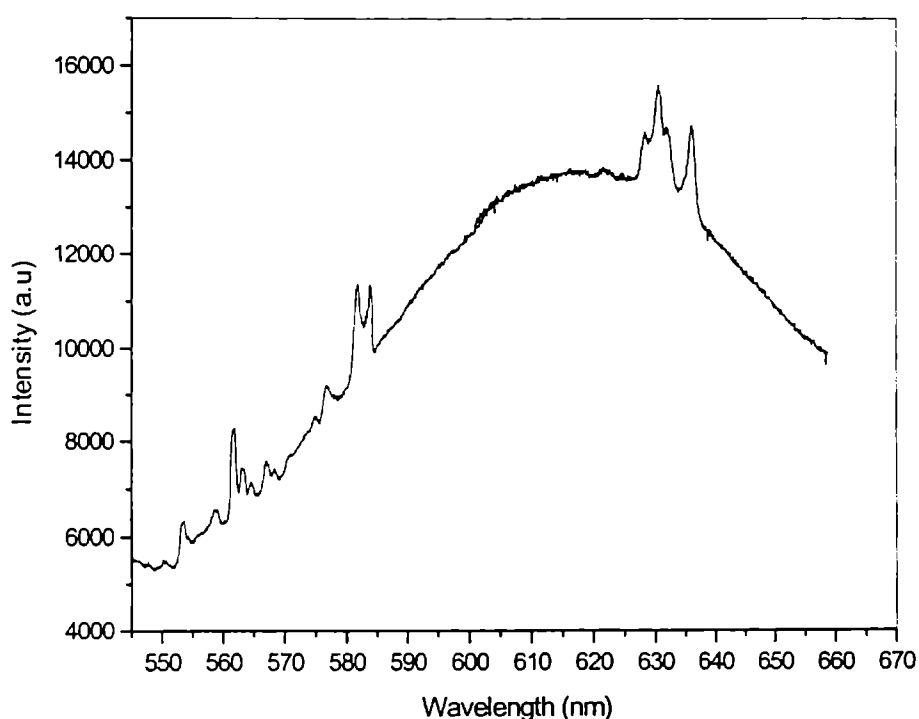


Fig. 4.4 Laser induced fluorescence emission spectrum of N, N diethylaniline excited by 532 nm

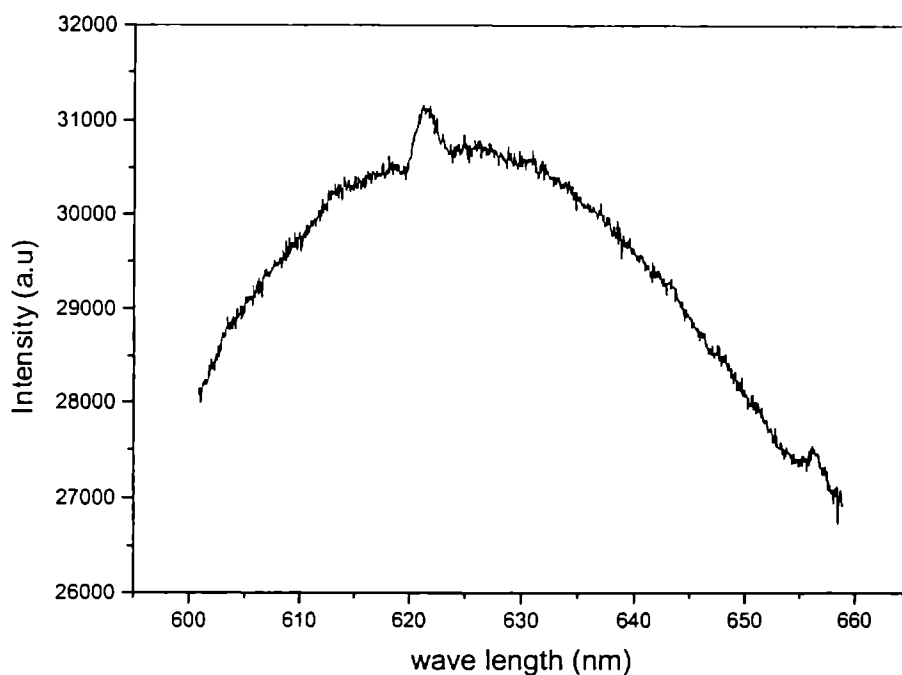


Fig.4.5 Laser induced fluorescence emission spectrum of polymerized o-chloroaniline excited by 532 nm.

As already stated earlier, the fluorescence in organic compounds generally occurs in visible region due to π , π^* or n , π^* excitation transitions. A broad fluorescent band with some sharp peaks are observed in N,N diethylaniline and the fluorescence emission in this compound is centred at 618 nm. The sharp peaks are vibrational Raman lines [55]. Since the fluorescent band is intense, the emission is assigned as due to π , π^* excitation transition. The fluorescence emission in o-chloroaniline polymer is intense and centred at 625 nm. This emission also is assigned as due to π , π^* transition.

4.10 Pulsed laser Raman spectrum of *p*-chlorotoluene, nitromethane, *o*-chlorophenol and *m*-toluidine

The pulsed laser Raman spectra of extra pure liquid phase *p*-chlorotoluene, nitromethane, *o*-chlorophenol and *m*-toluidine are recorded using the same Nd:YAG laser, monochromator and CCD set up used for LIF studies. High purity sample in liquid phase is used for the experiments. The perpendicular

configuration is used for the experiment such that the laser beam falls normally on the sample and the monochromator and CCD is kept perpendicular to the beam direction. The Rayleigh scattered line is also recorded. The Stoke's lines of the spectra are recorded in higher wavelength region of the Rayleigh line. The data can be obtained in ASCII or Microsoft excel (*.xls) format. The Raman shift from the Rayleigh line is plotted. The experimental set up is calibrated by recording the laser Raman spectra of CCl_4 and CS_2 . The reported Raman peaks are obtained for both the compounds.

4.10.1 Pulsed laser Raman spectrum of p-chlorotoluene

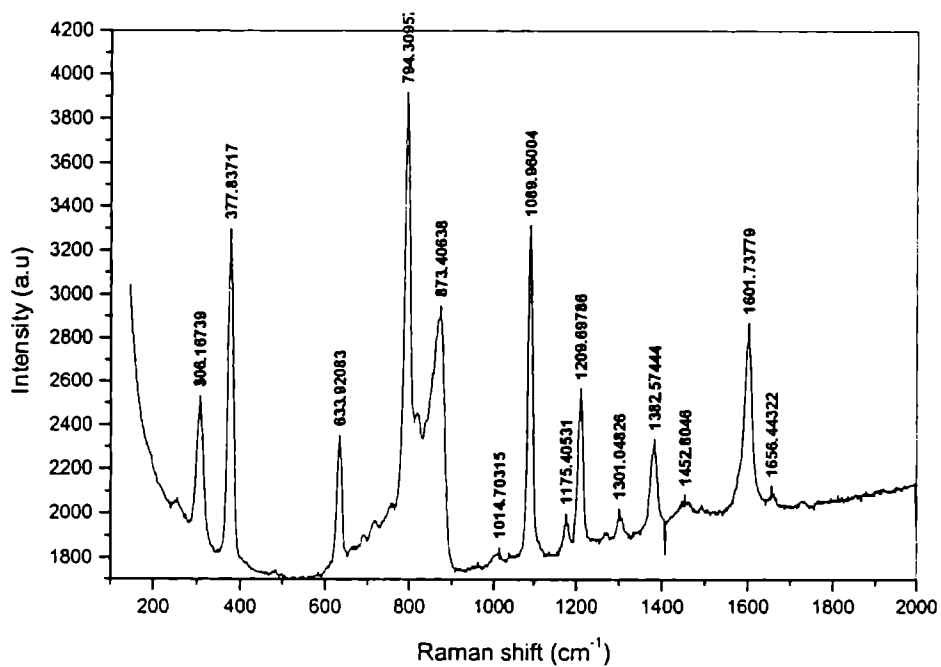


Fig.4.6 pulsed Raman spectrum of p-chlorotoluene in the range 200 - 2000 cm⁻¹

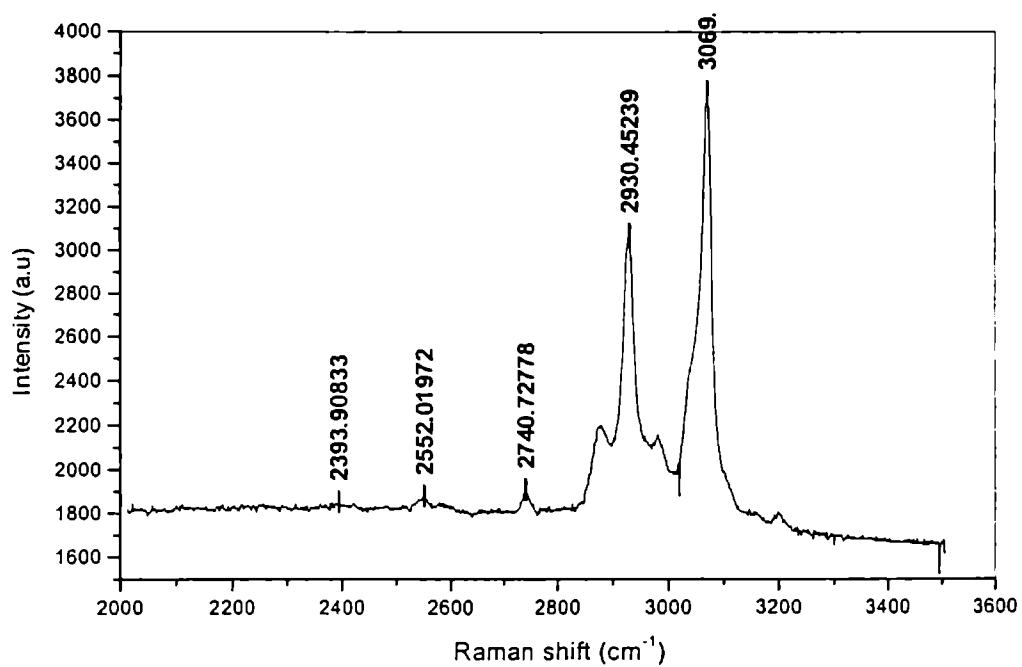


Fig.4.7 pulsed Raman spectrum of p-chlorotoluene in the range 2000 - 3600 cm⁻¹

Observed Raman shifts for *p*-chlorotoluene and their assignments

Raman shift in cm^{-1}	Assignments
306	overtone of ring torsion
378	C-Cl i.p bending
634	C-Cl stretching
794	ring deformation
873	o.p δCH
1015	trigonal ring breathing
1090	i.p δCH
1175	i.p δCH ; characteristic of <i>p</i> -substitution
1210	i.p δCH
1383	$\delta_s(\text{CH}_3)$
1453	$\delta_{as}(\text{CH}_3)$
1602	Aromatic ring
1658	Aromatic ring
2552	combination
2740	$\nu_s(\text{CH}_3)$
2930	$\nu_{as}(\text{CH}_3)$
3069	$\nu(\text{CH})$ Aromatic

In *p*-chlorotoluene, the aromatic CH stretch (3069 cm^{-1}) and aliphatic CH stretch (2930 and 2740 cm^{-1}) are observed. The aromatic ring characteristic peaks appeared 1602 cm^{-1} and 1658 cm^{-1} , are characteristic of phenyl ring and the peak at 1015 cm^{-1} represents the trigonal ring breathing mode. The aromatic ring peaks of in plane CH bending frequencies are observed at 1090 cm^{-1} , 1175 cm^{-1} and 1210 cm^{-1} [39]. This includes the characteristic orthosubstituted aromatic peak also. The symmetric bending mode of methyl group occurs at 1383 cm^{-1} . Ring deformation is observed at 794 cm^{-1} and out of plane CH bending is observed at 873 cm^{-1} . The peak appearing at 634 cm^{-1} is due to C-Cl stretching. The C-Cl in plane bending is observed at 378 cm^{-1} [45]. The peak at 306 cm^{-1} is the overtone of ring torsion. Hence the

Raman peaks for the ring peaks due to the substituents are observed. The observed peaks are well assigned.

4.10.2 Pulsed Raman spectrum of nitromethane

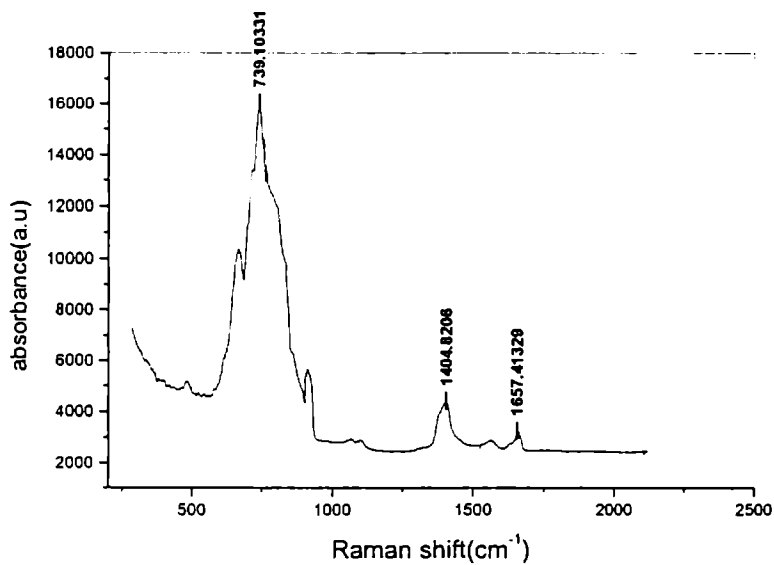


Fig.4.8 pulsed Raman spectrum of nitromethane in the range 200 - 2500 cm⁻¹

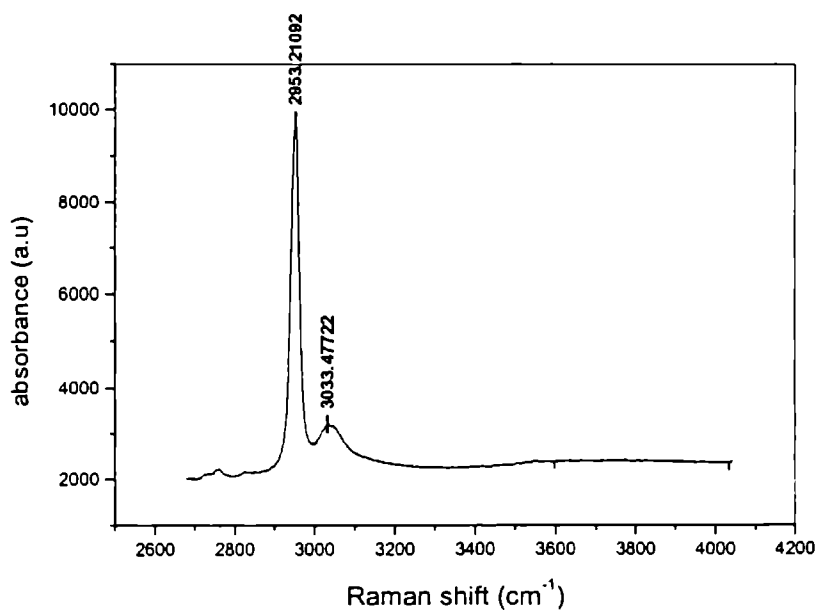


Fig.4.9 pulsed Raman spectrum of nitromethane in the range 2500 - 4000 cm⁻¹

Observed Raman shifts for Nitromethane and their assignments

Raman shift in cm^{-1}	Assignments
487	ρ (NO_2)
660	δ_s (NO_2)
743	
919	ν_s (CN)
1096	ρ (CH_3)
1405	δ_s (CH_3)
1556	ν (NO_2)
1657	ν (NO_2)
2953	ν (CH_3)
3043	ν (CH_3)

In pulsed Raman spectrum of nitromethane, the symmetric stretch of (CH_3) at 2953 cm^{-1} and 3033 cm^{-1} are observed. The peaks appearing at 1405 cm^{-1} and 1096 cm^{-1} are the symmetric bending and rocking of (CH_3) respectively. The peak at 660 cm^{-1} is the (NO_2) symmetric bending and the peak at 487 cm^{-1} is the (NO_2) rocking. The stretching vibrations of NO_2 are observed at 1657 cm^{-1} and 1556 cm^{-1} . The peak observed at 919 cm^{-1} is the CN symmetric stretching vibration [56]. Thus the characteristic Raman peaks are observed and the observed peaks are well assigned.

4.10.3 Pulsed laser Raman spectrum of *o*-chlorophenol

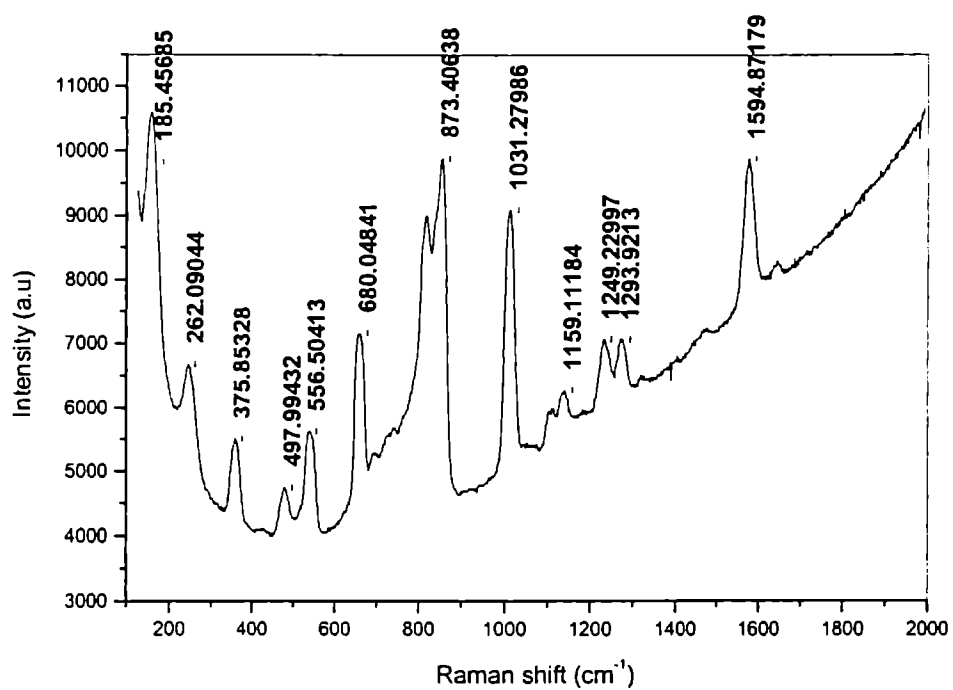


Fig.4.10 laser Raman spectrum of *o*-chlorophenol in the range 200-2000 cm^{-1}

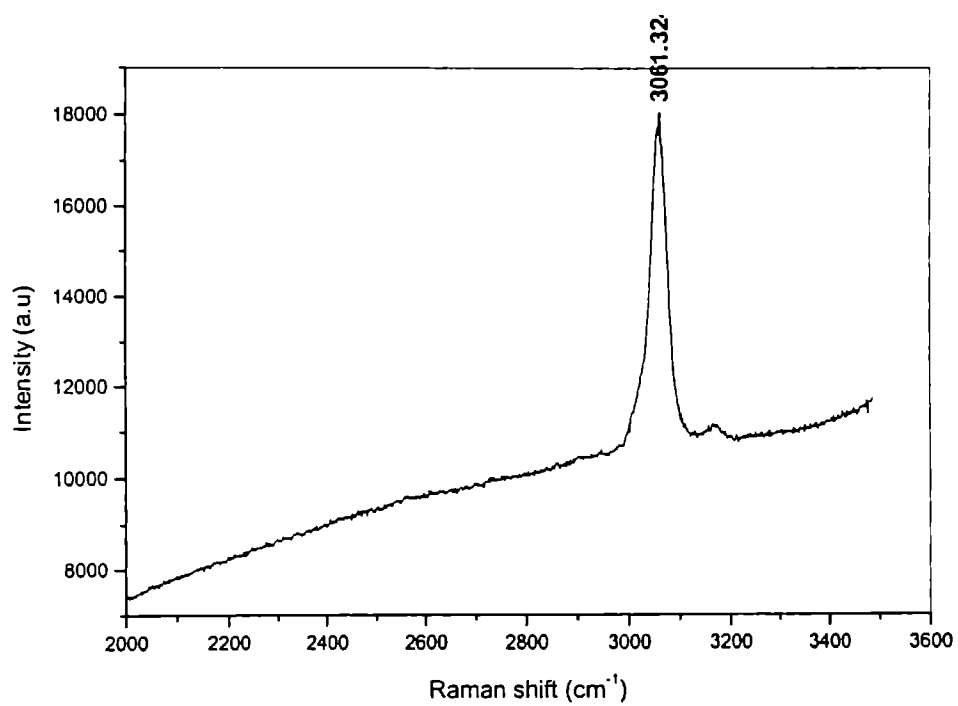


Fig.4.11 Pulsed laser Raman spectrum of *o*-chlorophenol in the range 2000-3600 cm^{-1}

Observed Raman shifts for *o*-chlorophenol and their assignments

Raman shift in cm^{-1}	Assignments
185	
262	C-C o.p bending
376	C-Cl i.p bending
498	C-C-C i.p bending
557	characteristic of <i>o</i> -substituted aromatic ring
680	C-Cl stretch
873	ring CH deformation
1031	i.p δCH ; characteristic of <i>o</i> -substitution.
1159	i.p δCH
1249	i.p δCH
1294	combination
1595	Aromatic ring
3061	Aromatic $\nu_{\text{as}}\text{CH}$

In pulsed laser Raman spectrum of *o*-chlorophenol, the aromatic CH stretch (3061 cm^{-1}) is observed. The aromatic ring characteristic peak appeared at 1595 cm^{-1} is the characteristic of phenyl ring and 1031 cm^{-1} which is the characteristic of *o*-substitution [37]. Aromatic ring characteristic peaks with in plane CH bending frequencies are observed at 1159 and 1249 cm^{-1} [39]. Ring CH deformation mode is observed at 873 cm^{-1} and C-Cl stretch is observed at 680 cm^{-1} . The peak at 557 cm^{-1} is the characteristic of orthosubstituted ring compounds and the peak at 498 cm^{-1} is the C-C-C in plane bending. The C-Cl in plane bending is observed at 367 cm^{-1} and C-C out of plane bending is at 262 cm^{-1} [45]. Raman peaks and peaks due to the substituents are also observed. The observed peaks, including the low-lying vibrational modes are well assigned.

4.10.4 Pulsed laser Raman spectrum of *m*-toluidine

Pulsed laser Raman spectrum of *m*-toluidine

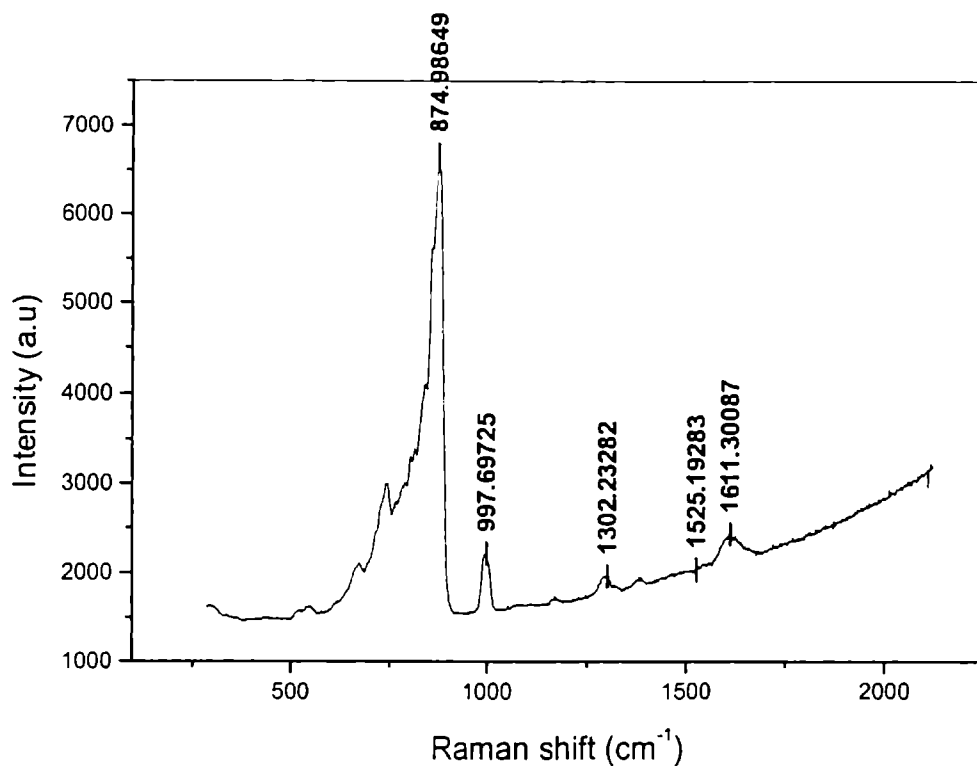


Fig.4.12 Pulsed laser Raman spectrum of *m*-toluidine in the range 100-2000 cm^{-1}

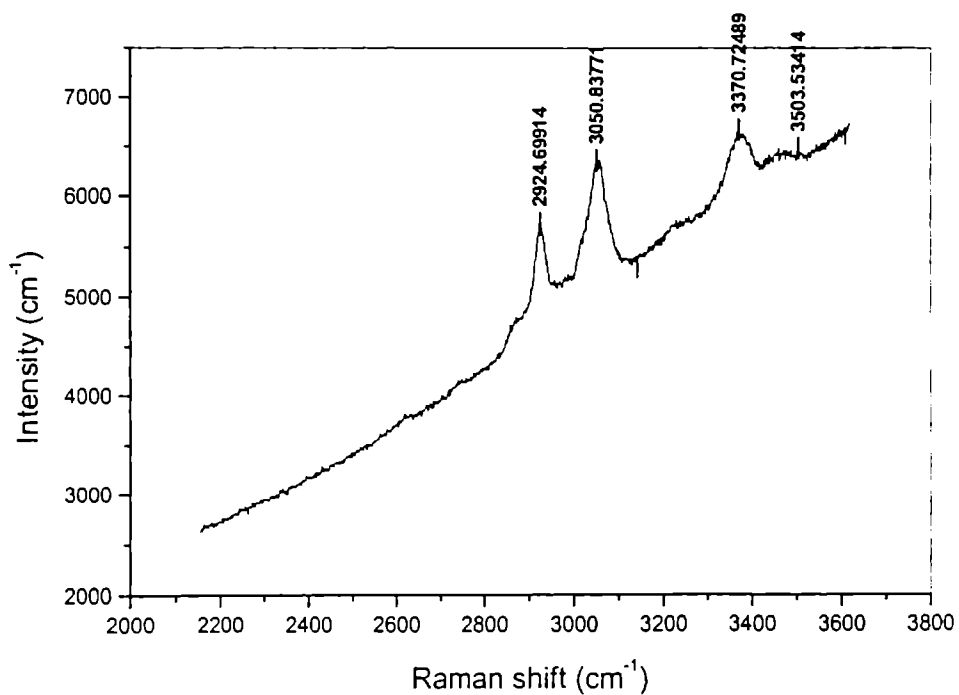


Fig.4.13 Pulsed laser Raman spectrum of *m*-toluidine in the range 2000-3800 cm^{-1}

Observed Raman shifts for *m*-toluidine and their assignments

Raman shift in cm^{-1}	Assignments
674	Ring deformation mode
743	Characteristic of <i>m</i> -substitution
875	<i>o.p.</i> δ CH
998	Ring deformation
1302	C-N stretching
1382	<i>i.p.</i> δ s(CH ₃)
1525	
1611	NH ₂ bending
2925	ν_{as} (CH ₃)
3051	ν (CH) Aromatic
3371	ν_{s} (NH)
3504	ν (NH)

In pulsed laser Raman spectrum of *m*-toluidine, both the NH stretch (3504 cm^{-1}) and aromatic CH stretch (3051 cm^{-1}) are observed. The peak at 2925 cm^{-1} is the methyl CH stretch and the peak at 1611 cm^{-1} is NH bending [39]. Methyl CH in plane bending is observed at 1382 cm^{-1} and ring deformation at 998 cm^{-1} . The peak 1302 cm^{-1} corresponds to C-N stretching and 875 cm^{-1} corresponds to aromatic CH out of plane bending. The peak at 743 cm^{-1} is characteristic of *m*-substitution and the peak at 674 cm^{-1} is ring deformation mode. Thus the characteristic Raman peaks for substituted aromatic ring, methyl and chlorine substituents are observed and well assigned.

4.11 conclusions

The excitation of samples of N,N diethylaniline and polymerized *o*-chloroaniline using Q-switched Nd:YAG laser at 532 nm results in fluorescence emission of these samples. The laser induced fluorescence spectra are assigned as due to the excitation transitions π , π^* in both the compounds. The excitation of samples of *p*-chlorotoluene, nitromethane, *o*-chlorophenol and *m*-toluidine resulted in Raman spectra of these compounds. The observed pulsed laser Raman spectra are properly assigned to the vibrational frequencies of these molecules. Some low-lying vibrational modes are also observed and are well assigned. The experiment demonstrates the advantages of pulsed laser-CCD system over conventional setups, for convenient recording and study of fluorescence and Raman spectra.

References

1. J.Amorim, G.Baravian and J.Jolly; *J.Phys.D:Apply.Phys.*, 33 (2000) R51.
2. C.S.Cooper and N.M.Laurendeau; *Meas.Sci.Technol.*, 11 (2000) 902.
3. A.Cessou, U.Meier and D.Stepowski ; *Meas.Sci.Technol.*, 11 (2000) 887.
4. K.Muraoka and M.Maeda; *Plasma. Phys. Control. Fusion*, 35 (1993) 633.
5. T.G.Spiro; *Current Science*, 74 (1998) 308.
6. A.Jayaraman and S.K.Sharma; *Current Science*, 47 (1998) 308.
7. “*Fluorescence Spectroscopy*”, Ed. A.J.Pesce, C.G.Rosen, and T.L.Pasby, Marcel-Dekker, Inc, New York, 1971.
8. W.Demtroder: “*Laser Spectroscopy: Basic concepts and instrumentation*”, Second edition, Springer, 1996.
9. B.B.Laud; “*Lasers and non-linear optics*”, Second edition, New Age International (P) Ltd., New Delhi, 2001.
10. A.B.F.Dungan, F.A.Matsen, W.Gordy, C.Sandorfy, R.N.Jones, and W.West; “*Chemical Applications of spectroscopy*” Ed. W.West, Interscience Publishers, Inc,New York,1956.
11. J.Michael Hollas; “*High Resolution Spectroscopy*”, Second edition,John Wiley and sons, New York, 1998.
12. B.K.Sharma; “*Spectroscopy*”, 11th edition, Goel publishing House, India, 195-96.
13. E.L.We hry; “*Fluorescence; Theory, Instrumentation and Practice*” ed. G.G. Gullbault, Marcel Dekker, INC, New york, 1967.
14. N.J.Turro; ‘*Molecular photochemistry*’, Benajamin, New York,1965
15. F.Wilkinson, *Quart. Rev. (London)*, 20 (1966) 403.
16. F.Wilkinson, *Adv.Photochem.*, 3 (1964) 241.
17. A.S.Cherkasov; *Doklady Akad. Nauk, SSSR*, 146 (1962) 716.
18. E.L.We hry and L.B.Rogers in “*Fluorescence and Phosphorescence Analysis*” ed. D.M.Hercules, *Interscience, New York*, 1966,p.125-135.
19. A.Weller; *Progr.Reaction Kinetics*, 1(1961) 189.
20. E.L.We hry and L.B.Rogers, *J. Am. Chem. Soc.*,87 (1965) 4234.

21. H.H.Jaffe and H.L.Jones; *J.org.Chem.*,30 (1965) 961.
22. E.L.We hry; *J. Am. Chem.*, 89 (1967) 41.
23. M.Heintxe and G.H.Bauer; *J. Phys. D: Appl. Phys.*, 28 (1995) 2470.
24. B.Kim, P.L.Hunter and H.S.Johnston; *J. Chem. Phys.*, 96 (1992) 4057.
25. M.Hertl and J.Jolly; *J. Phys. D: Appl. Phys.*, 33 (2000) 381.
26. P.Misra, X.Zhu and H.L.Bryant Jr.; *Pure Appl. Opt.*, 4 (1995) 587.
27. T.Lee, D.Shin, J.B.Jeffries and R.K.Hanson; *AIAA* (American Institute of Aeronautics and Astronautics) 2002, 0399, p.1.
28. J.E.Harrington and K.C.Smyth; *Chem. Phys. Lett.*, 202 (1993) 196.
29. R.J.H.Klein-Douw el, J.Laque, J.B.Jeffries, G.P.Smith and D.R.Crosley; *Appl. Opt.*, 39 (2000) 3712.
30. L.Santos, E.Martinez, B.Ballesteros and J.Sanchez; *Spectrochim. Acta part A* 56 (2000) 1905.
31. S.Lee, K.Arita and O.Kajimoto; *Chem. Phys. Lett.*; 265 (1997) 579.
32. B.J.Kirby and R.K.Hanson; *Appl. Phys. B.*, 69 (1999) 505.
33. P.Jungner and L.Halonen; *J. Chem. Phys.*, 107 (1997) 1680.
34. M. Metsaalaa, M.Nela, S.Yang O.Vattinen and L.Halonen; *Vib. Spectrosc.*, 29 (2002) 155.
35. D.Hayashi, W.Hoeben, G.Dooms, E.van Veldhuizen, W.Rutgers and G.Kroesen; *Appl. Opt.*, 40 (2001) 986.
36. J.W.Pepper, A.O.Wright and J.E.Kenny; *Spectrochim. Acta. A.*, 58 (2002) 317.
37. Z.Chen, D.L.Kaplan, K.Yang, J.Kumar, K.A.Marx and S.K.Tripathy; *Appl. Opt.*, 36 (1997) 1655.
38. E.G.Brame Jr. and J.G.Grasselli; *Infrared and Raman Spectroscopy, Part B*; Marcel Dekker Inc., New York, 1977.
39. K.Nakanishi and P.H.Solomon; "Infrared absorption spectroscopy", second edition , Holden-Day Inc., San Francisco, 1977.
40. D.L.Philips and A.B.Myers; *J.Phys.Chem.*,95 (1991) 7164.
41. T.D.Klots; *Spectrochim.Acta, Part A*54 (1998) 1481.
42. D.Bermejo, G.D.Lonardo, J.L.Domienech and L.Fusina; *J.Mol.Spectrosc.*, 219 (2003) 290.

43. K.Anand, V.Asundi and R.Vasudeva; *Paper presented in SAE 2000 World Congress*, Detroit, Michigan, 2000 –01 – 1336.
44. I.L.Town, M.Becucci, G.Pietraperzia, E.Castellucci and J.C.Oero; *J. Mol. Struct.*, 565-566 (2001) 421.
45. K.P.R.Nair and S.M.Eappen; *Indian J. Pure. Appl. Phys.*, 39 (2001) 750.
46. T.M.Kolev and B.A.Stamboliyska; *Spectrochim. Acta. A.*, 56 (1999) 119.
47. M.Becucci, E.Castellucci, L.Fusina, G.DiLonardo and H.W.Schrotter; *J. Raman. Spectrosc.*, 29 (1998) 237.
48. H.G.M.Edwards, F.G.Pichel, E.M.Newton and D.D.W.Williams; *Spectrochim. Acta. A.*, 56 (1999) 193.
49. J.P.Pinan, R.Quillon, P.Ramson, M.Becucci and S.Califano; *J. Chem. Phys.*, 109 (1998) 5469.
50. J.R.McCaffery and Y.G.Durant; *J. Appl. Polym. Sci.*, 86 (2002) 1507.
51. F.A.Beleze and A.J.G.Zarbin; *J. Braz. Chem. Soc.*, 12 (2001) 542.
52. A.Buzarovska, I.Arsova and L.Arsov; *J. Serb. Chem. Soc.*, 66 (2001) 27.
53. J.E.P.da Silva, S.I.C.de Torresi and M.L.A.Temperini; *J. Braz. Chem. Soc.*, 11 (2000) 91.
54. J.Ravi; “Photothermal and Photoacoustic investigations on certain polymers and semi conducting materials”, Ph.D Thesis, Department of Physics, Cochin university of Science and Technology, 2003.
55. S.B.Hansen;”*The application of Raman spectroscopy of multicomponent systems*”, Ph.D. Thesis, Department of chemistry, Technical university of Denmark,2000.
56. J.C.Deak, L.K.Iwaki and D.D.Dlott; *J.Phy.Che. A*,103 (1999) 97.

CHAPTER 5

HIGH-RESOLUTION TDL AND CONVENTIONAL SPECTROSCOPIC STUDY OF 2-PROPANOL IN THE NIR REGION

5.1 Tunable Diode laser Absorption Spectroscopy

The developments of tunable lasers and their use as light sources have materially increased the sensitivity of all known methods of spectroscopy both for atoms and molecules. High resolution absorption spectroscopy requires narrow-bandwidth excitation sources. Spectroscopic studies in the visible spectral region typically use a tunable dye laser and studies in the near ultraviolet and near infrared are becoming more common as frequency doubling and wave mixing methods improve. Quite new methods have been developed like multistep photoionization of atoms and molecules [1], intra cavity absorption [2] and coherent antiStokes Raman scattering [3]. Better accuracy in the measurement of frequency is achieved by eliminating the Doppler broadening of spectral lines using non-linear spectroscopic techniques like saturation spectroscopy and molecular beam spectroscopy [4-6].

A high resolution molecular spectrum denotes a well resolved rotational structure of the fundamental or overtone vibrational band [7-9]. Mid infrared and near infrared tunable diode lasers are widely used for high resolution vibrational rotational spectroscopy [4]. The important characteristics of TDLS, which make them so useful in molecular spectroscopy in the Doppler and sub-Doppler domains, are the following. The output wavelength can be tuned over a wide spectral range, and the output power can be modulated, by changing the operating conditions, for example by changing temperature or bias current. They provide a fairly monochromatic beam that guarantees high spectral resolution and high sensitivity, with detection of absorbance as low as 10^{-6} - 10^{-7} [10]. Typical line widths of absorbing molecules at low pressures (≤ 1 torr) are $0.1 - 0.5 \text{ cm}^{-1}$. Therefore the use of diode lasers with emission line widths of 10^{-4} - 10^{-5} cm^{-1} does

not distort the recorded spectrum; the line width is limited by the broadening mechanism and not the laser source. The high spectral brightness and high spatial coherence of Tunable Diode Lasers allow the use for long path length measurements with high degree of spatial resolution.

Tunable diode laser absorption method is used to study the fine structures in many molecules corresponding to interactions between different forms of molecular motion (electronic, vibrational and rotational). With the recent developments in near infrared tunable diode lasers, the high resolution spectroscopic investigations could be extended to the NIR region also where the overtone absorption bands of local mode X-H oscillators occur [11]. The NIR diode lasers have become a valuable addition to the relatively very short list of available NIR spectral sources.

This chapter describes the recording of near infrared TDL high-resolution spectrum of the second overtone band of the –OH group in 2-propanol. The observed high resolution spectrum shows features corresponding to the trans and gauche conformations of the molecule. To our knowledge, this is the first measurement of the high resolution TDL spectrum of OH overtone of this molecule, leading to an accurate measurement of the frequency separation between the OH band origins corresponding to the two isomers.

A local mode analysis of the methyl CH and OH overtone bands of liquid phase 2-propanol is also included in this chapter.

5.2 High resolution overtone spectroscopy – some reported works

Vaittinen et al recorded the high resolution overtone spectrum of H₂S using intracavity laser absorption technique in the region 12270 – 12670 cm⁻¹ [12]. The rovibrational analysis provided upper state rotational parameters for the three interacting vibrational states. A local mode type behavior is evidenced by the values of the rotational parameters. Coheur et al [13] reported new water vapor line parameters in the 26000 – 13000 cm⁻¹ region with a high resolution Fourier transform spectrometer combined with a long path absorption cell. Naus et al. reported the high resolution cavity ring down spectrum of water vapor in the range

555 – 604 nm. Douketis et al [14] used photoacoustic spectroscopy in high resolution vibrational overtone studies. The high resolution vibrational overtone spectrum of H₂O₂ vapor between 740 and 760 nm is recorded under both bulk gas and supersonic beam conditions. An absorption band corresponding to a $\Delta V = 4$ O-H stretch is observed in this spectral region. Rotational analysis indicated that it is a hybrid band with mainly parallel character. The spectral linewidths are found to be Doppler limited in all cases.

Held et al [15] examined the first overtone N-H stretching region and the fundamental C-H stretching region of gas phase pyrrole using high resolution FTIR spectra. The first overtone N-H stretch has been rotationally analyzed using an asymmetric top model and was found to exhibit two separate perturbations. These perturbations produce line splitting and anomalous intensity patterns in the spectrum. Luckhaus et al. [16] carried out a combined high resolution and theoretical study of the rovibrational spectrum of hydroxylamine. They reported the ro-vibrational spectrum of hydroxylamine (NH₂OH) recorded by interferometric Fourier transform spectroscopy with a resolution up to 0.004 cm⁻¹ close to the Doppler limit at room temperature from 800 cm⁻¹ up to the visible range of the spectrum.

Zhan et al [17] studied the fifth and the seventh stretching vibrational overtone bands of a mono-isotopic stannane sample recorded with Doppler limited resolution using intracavity photoacoustic technique using a titanium: sapphire ring laser, leading to the observation of rotational structure under local mode behavior. High resolution infrared emission spectrum of sodium monofluoride recorded with a high resolution Fourier transform spectrometer was reported by Muntianu et al [18]. They observed and assigned a total of 1131 vibration – rotation transitions from the V=1 → 0 to V= 9 → 8 vibrational bands.

5.3 Earlier measurements of OH overtone spectra in alcohols

Phillips et al. [19] measured the intensity for several OH vibrational overtone bands for vapor phase methanol, ethanol and isopropanol. Fang et al. [20] measured the overtone absorption spectra of gaseous 1-propanol, 2-propanol

and *tert*-butyl alcohol using ICL- PAS and FTIR spectroscopy. These workers also studied the temperature dependence of vibrational overtones in gas phase ethanol in the region 10150 – 19900 cm^{-1} measured by ICL-PAS technique. The observations were interpreted in terms of contributions from different molecular conformers. They found that the OH overtones are composed of two sub bands, which are assigned as the transitions of two conformers of OH bond in the *trans* or *gauche* position with respect to the methyl group. From the temperature dependence of the OH overtone intensity, the enthalpy difference between the conformers is determined to be 0.7 kcal/mole. Weibel et al. [21] reported the experimental and *ab initio* investigations for the OH overtone vibration of ethanol. They recorded the intracavity dye laser photoacoustic absorption spectra of ethanol, ethanol (1, 1- d_2) and ethanol (2, 2, 2- d_3) in the region 16550 – 16700 cm^{-1} , which contain the OH fourth overtone absorption bands. The distinct absorption bands are assigned to the *trans* and *gauche* conformational isomers. Fang et al. [22] studied the absorption spectra of gas phase methanol (10150 – 19900 cm^{-1}) and methanol - d (10150 – 17600 cm^{-1}) recorded using intracavity dye laser photoacoustic spectroscopy. The prominent features in the spectra were assigned as OH, OD and CH overtones within the local mode model of loosely coupled anharmonic vibrations. Relatively less intense peaks were assigned as combinations involving an LM overtone and lower frequency motions in the molecules. Eappen et al reported the well-resolved high resolution spectra of methanol in the second OH overtone region [23].

5.4 The Tunable diode laser experimental set up

The main components of the tunable diode laser high resolution spectrometer are:

- a. The near infrared tunable diode laser source
- b. A neutral density beam splitter.
- c. A multipass cell with a maximum path length of 36 m.
- d. Photodetector that gives a balanced detection with logarithmic output.
- e. Vacuum system for evacuation of the multipass cell, and to work at the required sample pressure.

5.4.1 Tunable Diode Laser

The tunable source used is a commercially available external cavity tunable diode laser (New focus, Model 6320). The diode laser is tunable in the wavelength range 936-976 nm with tunability of the order of 0.01 nm in single mode. The line width of the laser is < 300khz when operated in single longitudinal mode.

5.4.2 Beam splitter

A beam splitter (neutral density filter) with varying ratios splits the beam into two – one is the reflected beam and the other is the transmitted beam through neutral density filter. The reflected beam is used as the reference beam and the transmitted beam as the signal in the experimental set up.

5.4.3 Multipass cell

The main parts of the multipass cell (New Focus Inc Model 5611) are; base plate, glass tube, two housings and two mirrors. The base plate is a piece of anodized aluminum with three slots for mounting on optical tables. The glass tube is made of borosilicate glass and the tube is sealed to the housings with an O-ring that is held in place by an anodized aluminum O-ring retainer. The two housings are made of nickel-coated aluminum aside from the aluminum mirrors and the housings; the remaining metal parts inside the cell are made of stainless steel.

There are three couplings in the front and back plates for various applications such as sample intake, pressure checking etc. The mirrors are made of a nickel-plated aluminum substrate that is polished into desired toroidal shape. A protected silver coating is deposited onto its surface. The flat surface on the edge of the mirror is approximately aligned with one of the mirror is approximately aligned with one of the mirrors toroidal axes.

5.4.4 Detector

The detector used in this set up is the New Focus Model 2017 Nirvana photo receiver. This device consists of two photodiodes designated as signal and reference. There are three outputs Linear, Log and Signal monitor. This detector enables traditional balanced detection. In the balance mode the linear output provides a voltage proportional to the difference between the photocurrents of the signal and reference diodes. It also provides auto balance detection with zero DC voltage and noise suppressed AC signal proportional to received signal optical power. In this state the detection automatically balances the photocurrent from signal and reference diodes. The signal monitor output enables constant monitoring of the signal. The log output at auto-balanced state provides a convenient measurement of absorption present in the signal path. The log output voltage is given as

$$\text{Logoutput} \approx -\ln \left[\frac{P_{\text{Ref}}}{P_{\text{Sig}}} - 1 \right].$$

The log output is bandwidth limited up to the selected gain compensation cut-off frequency. A block diagram of the experimental set up is shown in figure 5.1.

5.5 Experimental procedure

The fine tunability of the external cavity tunable diode laser-of the order of 0.01 nm, temperature stability, single mode operation, constant power mode etc. makes it an ideal laser source for high resolution spectrometer. It can be operated in single mode at constant power of 3-4 mw is found suitable for most of the measurements. The laser beam is split into two – one reference beam that falls directly on the reference photodiode of the photodetector and the other signal beam which is fed into the multipass cell that contains the sample whose spectrum is to be recorded in gas phase (2-propanol). A rotary pump is used to evacuate the multipass cell below atmospheric pressure. The beam emerging from the multipass cell at a slightly different angle with the incident beam is deflected

using a mirror and is focused on to the signal photodiode of the balanced photodetector.

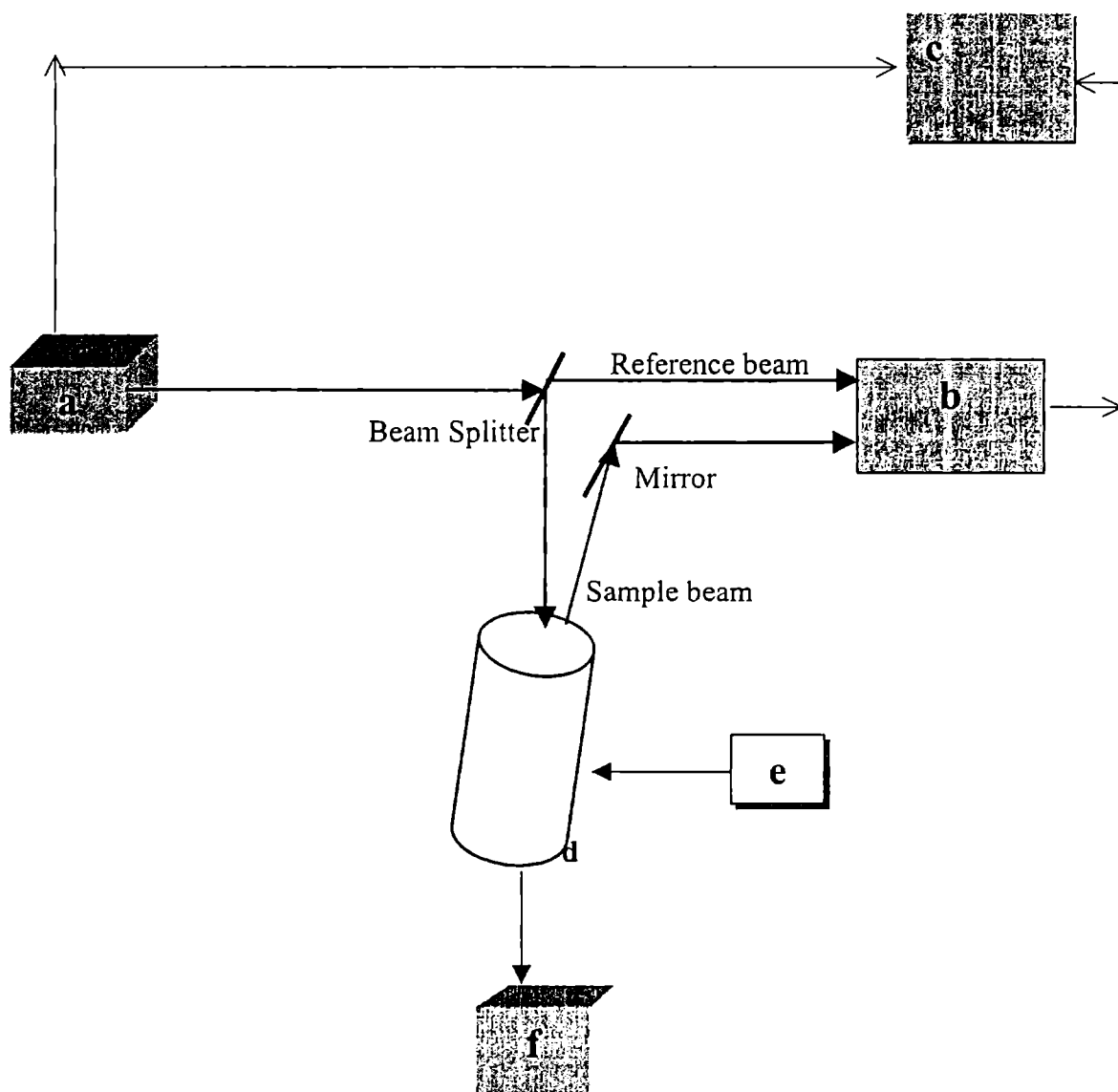
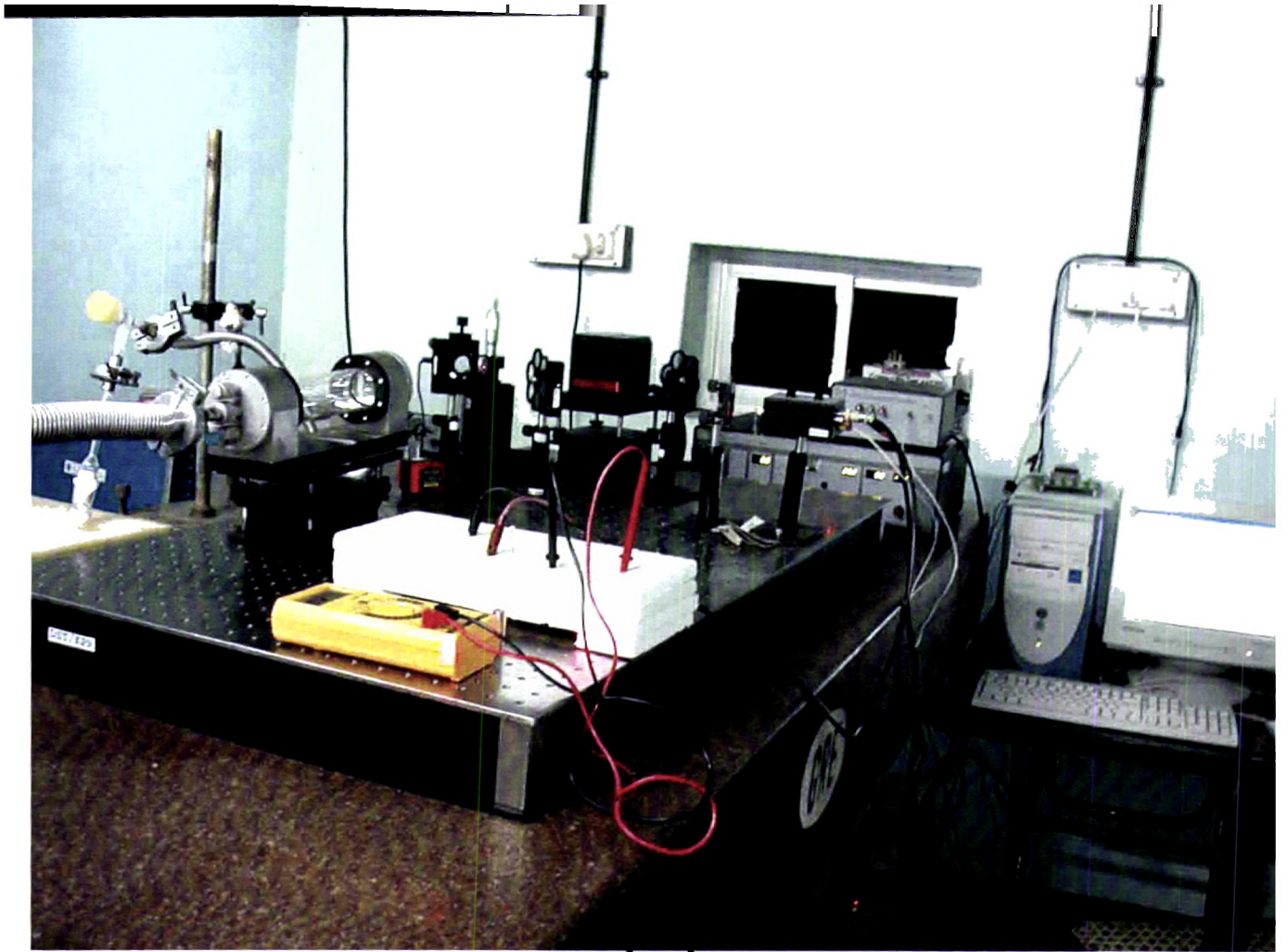
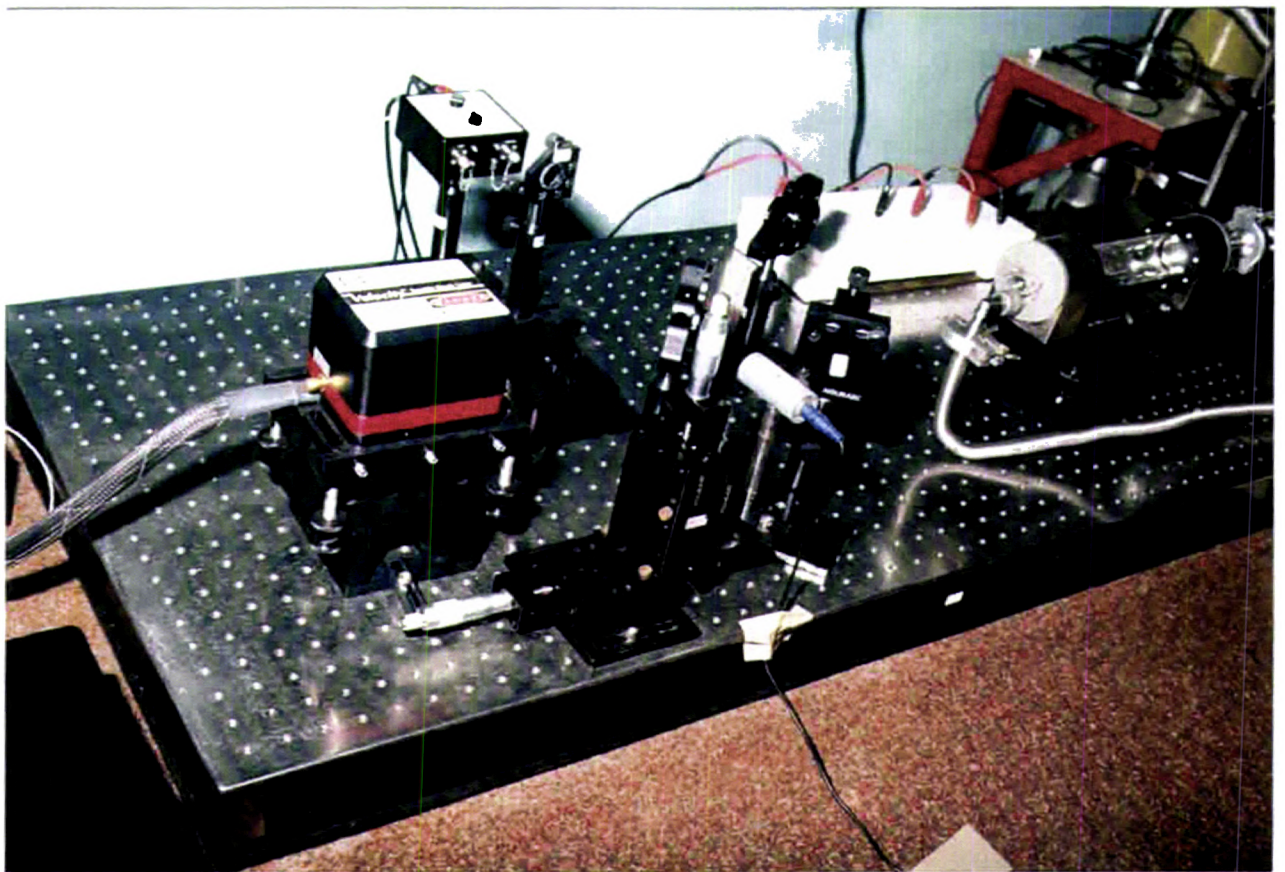


Fig.5.1 Schematic representation of the experimental setup; a-Tunable diode laser, b-photodetector, c-computer, d-multipass cell, e-sample holder, f-vacuum system

The log output from the photodetector is analog that is connected to ADC. This digital output is interfaced with the PC using Lab VIEW software. The multipass cell is evacuated and the sample is fed in to it. When the sample pressure becomes steady, the tunable diode laser wavelength is scanned in the region 940-970 nm.



(a)



(b)

Experimental Setup for TDLAS

The high resolution spectrum of –OH second overtone in 2-propanol is recorded. 2-propanol (> 99%) obtained from M/s MERCK, Mumbai is used for recording the spectrum without further purification. The experimental parameters are given below

Laser power - 2.7 mW
Scan speed - 0.02nm/sec
Temperature - 260C
Pressure - 0.05 mbar

The figures 5.2 and 5.3 show the spectrum obtained using the present high resolution spectrophotometer. The positions of conspicuous peaks obtained agree well with the values reported by Fang et al for the $\Delta V=3$ region of the –OH group in 2-propanol.

5.6 High resolution spectrum of 2-propanol in the second overtone region

The overtone bands for 2-propanol reveal the existence of two conformers [19]. Fang et al [20] had recorded the gas phase spectrum of 2-propanol in this region using intracavity photoacoustic technique. They could obtain two sub bands for each –OH overtone corresponding to the trans or gauche conformers. In the second overtone region, the OH stretching overtone of 2-propanol is a doublet containing a relatively broad high energy and a weaker low energy band. The high energy band is assigned as the transition of the gauche conformers and the low energy band as that of the trans conformer, which has the OH bond trans to one of the hydrogen atoms. The present experiment gives the well resolved rotational structure of these bands. The present TDL experimental values and the reported values of the band positions are given in table 5.1. To the best of our knowledge, this is the first high resolution study of 2-propanol OH overtone band in the second overtone region.

Table 5.1 The observed and reported transition frequency values for the OH stretching overtone spectra of gaseous 2-propanol

	Conformation	reported value	observed value
2-propanol	OH (3) Trans	10400 cm^{-1}	10414 cm^{-1}
	OH (3) gauche	10474 cm^{-1}	10471 cm^{-1}

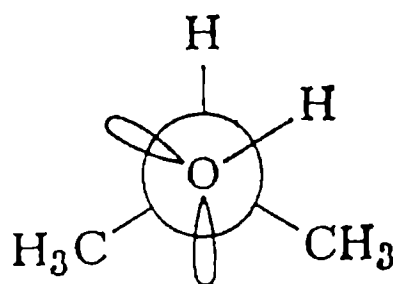
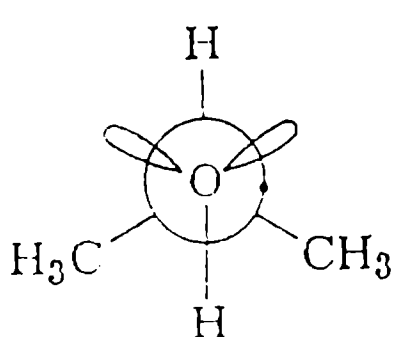


Fig. 5.2

Trans conformer

Gauche conformer

2-propanol

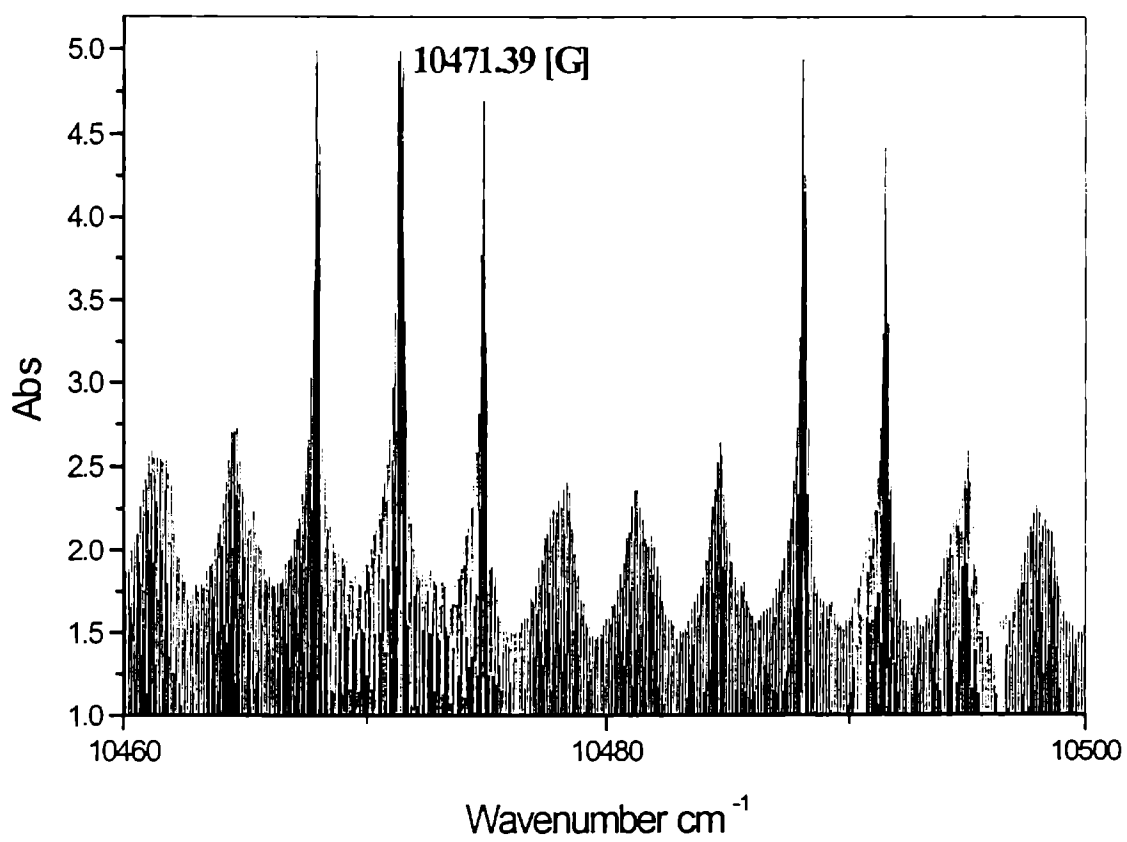


Fig.5.3 High resolution spectrum of 2-propanol in the second overtone region in the range 10460 cm⁻¹ - 10500 cm⁻¹

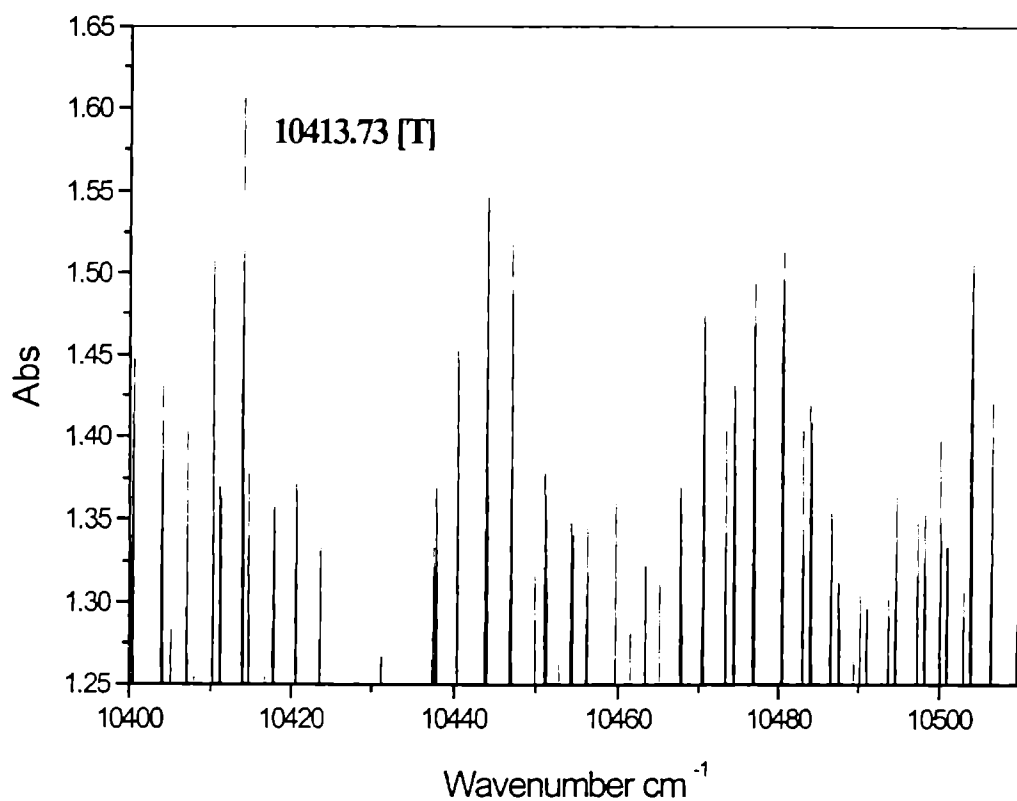


Fig.5.4 High resolution spectrum of 2-propanol in the second overtone region in the range 10400 cm^{-1} - 10500 cm^{-1}

5.7 Absorption spectrum of liquid phase 2-propanol in NIR region

As described in chapter 1, overtone absorption spectroscopy and the local mode model provide a valuable probe of molecular structure, inter and intra molecular interactions, conformational aspects and substituent effects in aliphatic and aromatic compounds [24-27]. The local mode parameters X_1 (mechanical frequency) and X_2 (anharmonicity) distinguish between both chemically nonequivalent X-H oscillators and conformationally nonequivalent X-H oscillators [28-31]. The absorption spectrum of liquid 2-propanol is recorded in the NIR region using a HITACHI Model U-3410 UV-Vis-NIR spectrophotometer as described in Chapter 2. The observed overtone spectra of 2-propanol are shown in figures 5.5-5.11

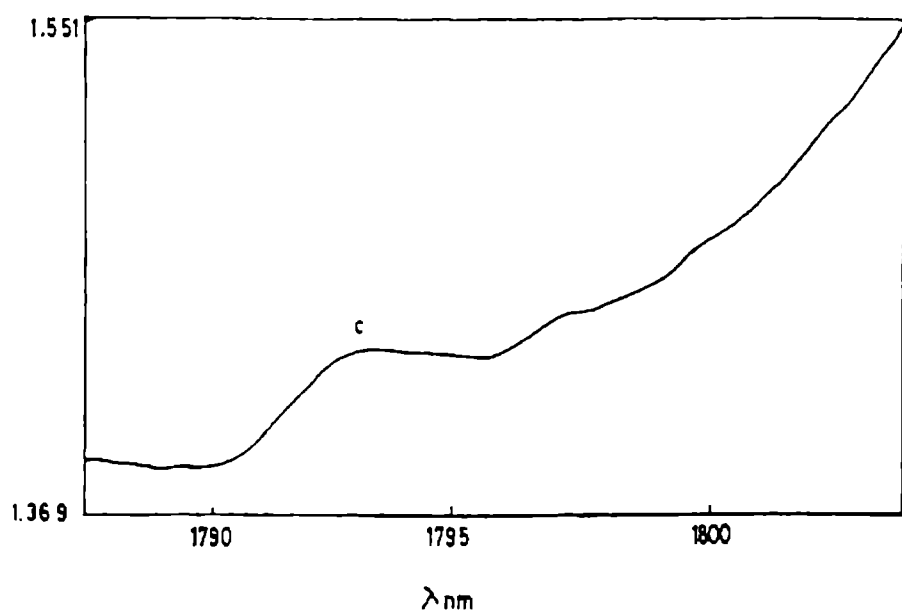


Fig. 5.5 The methynic CH overtone band of 2-propanol in the $\Delta V = 2$ region

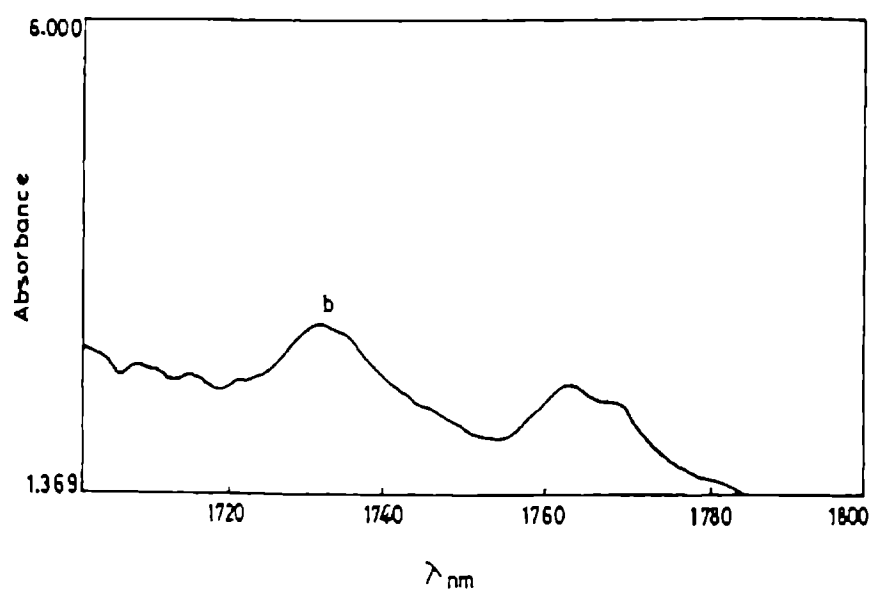


Fig. 5.6 The methyl CH overtone band of 2-propanol in the $\Delta V = 2$ region

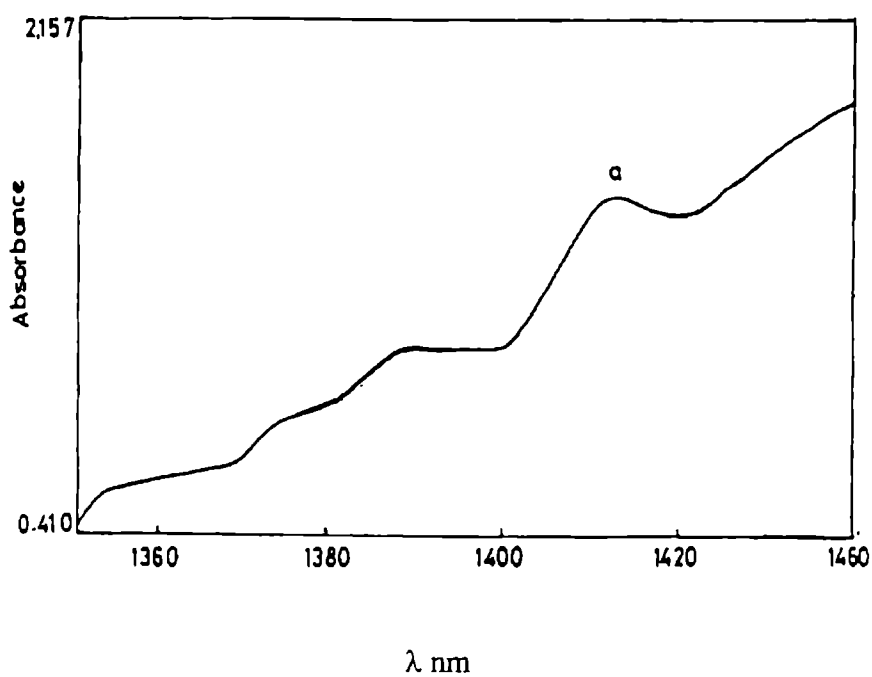


Fig. 5.7 The OH overtone band of 2-propanol in the $\Delta V = 2$ region

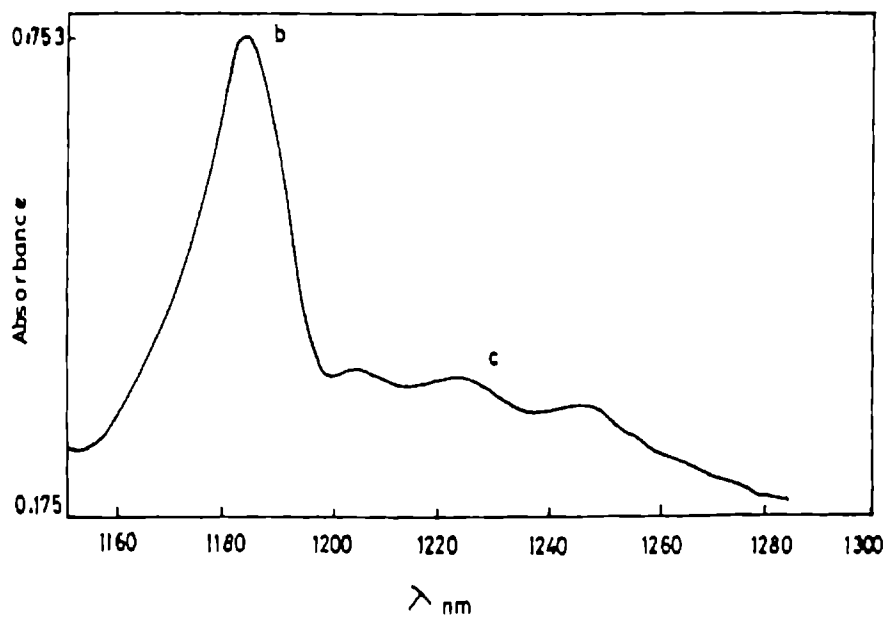
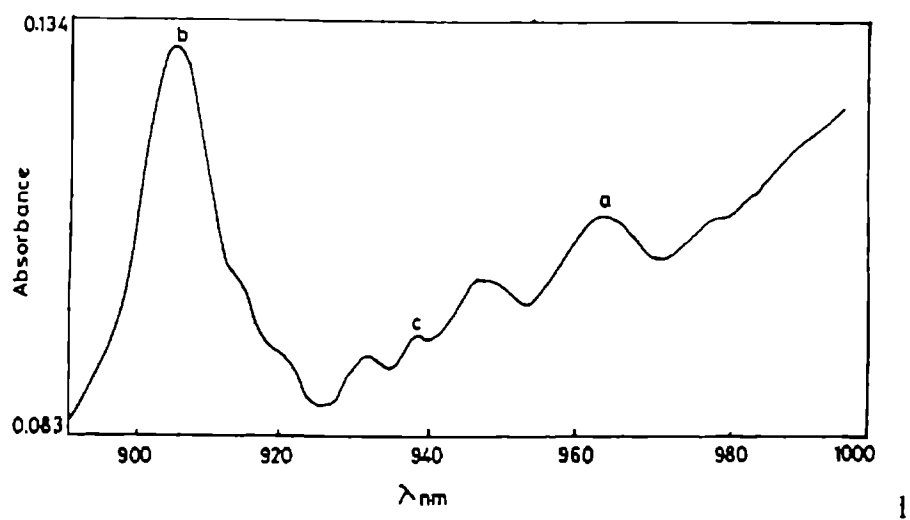


Fig. 5.8 The methyl CH and methynic CH overtone band of 2-propanol in the $\Delta V = 3$ region



methinic CH overtone bands of 2-propanol in the $\Delta V = 4$ region

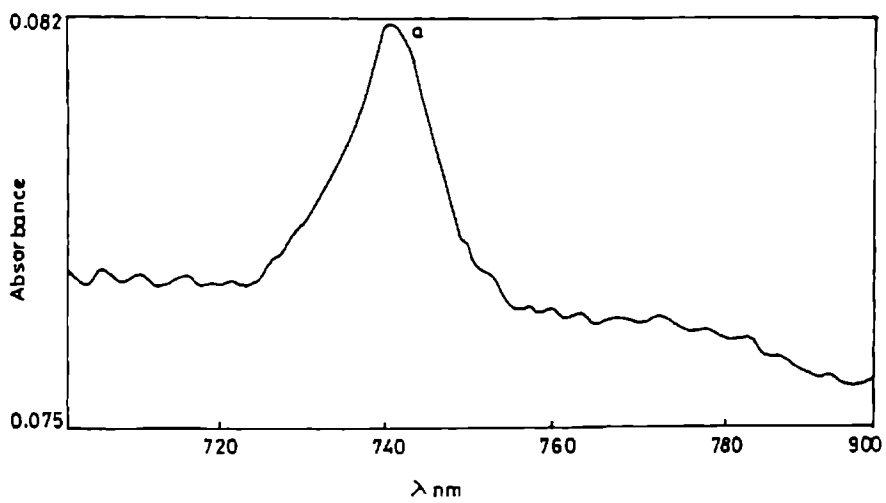


Fig.5.10 The OH overtone band in the $\Delta V = 4$ region of 2-propanol

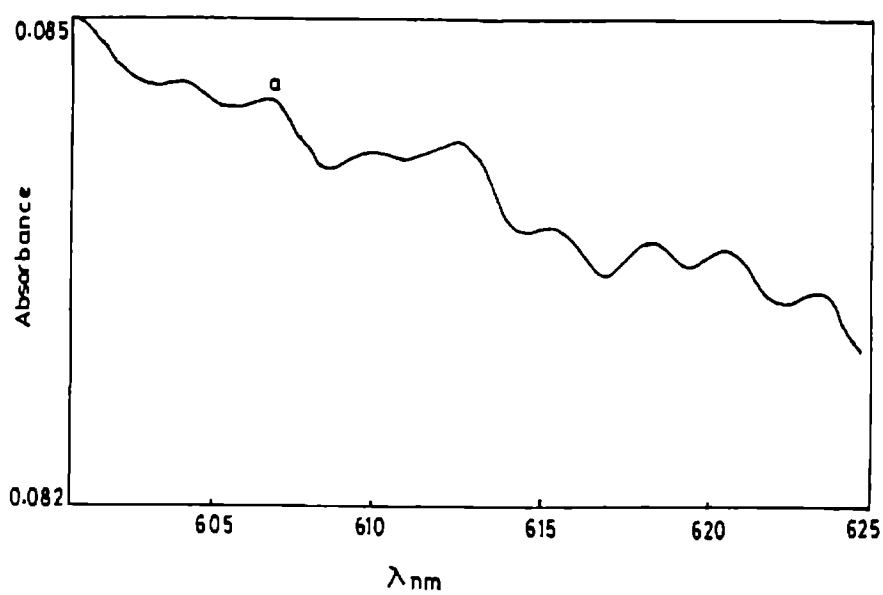


Fig.5.11 The OH overtone band in the $\Delta V = 5$ region of 2-propanol

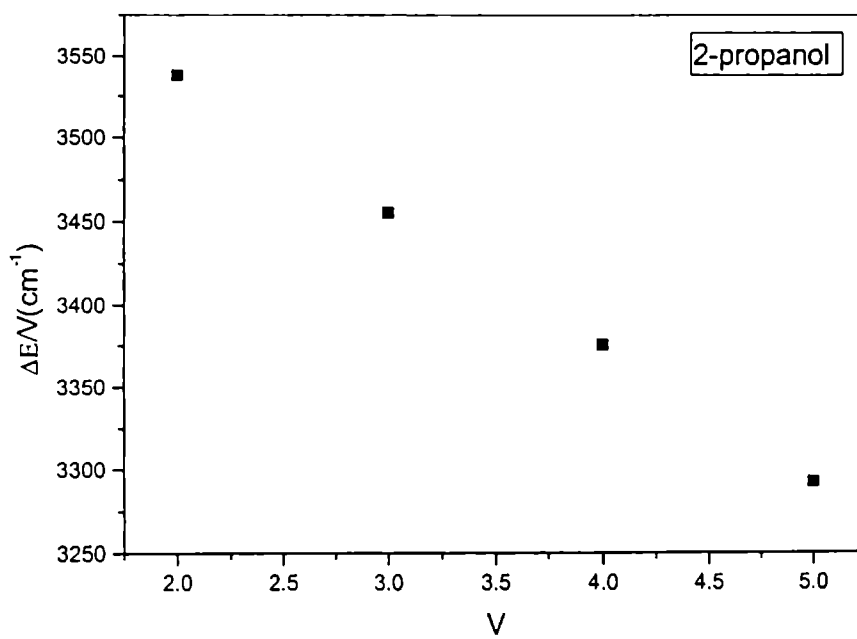


Fig. 5.12 Birge-Spinner plot for OH overtones in 2-propanol

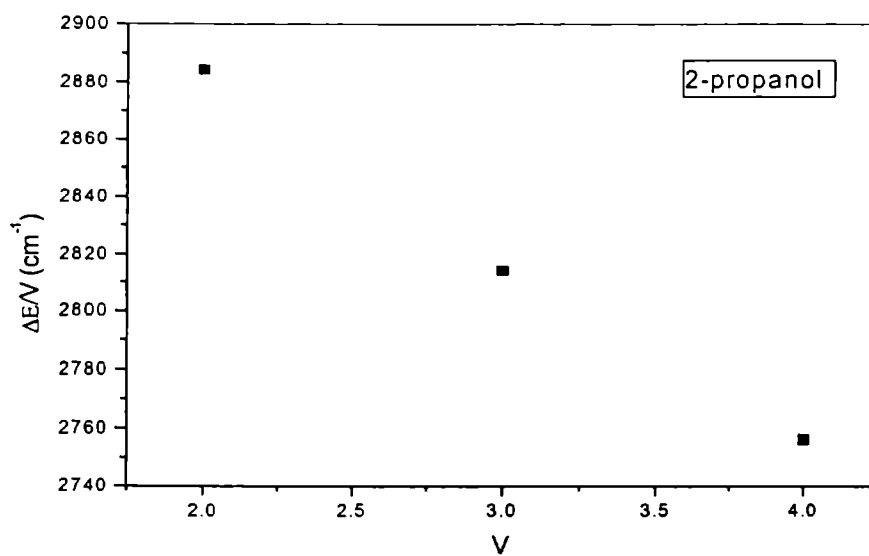


Fig.5.13 Birge-Sponer plot for methyl CH overtones in 2-propanol

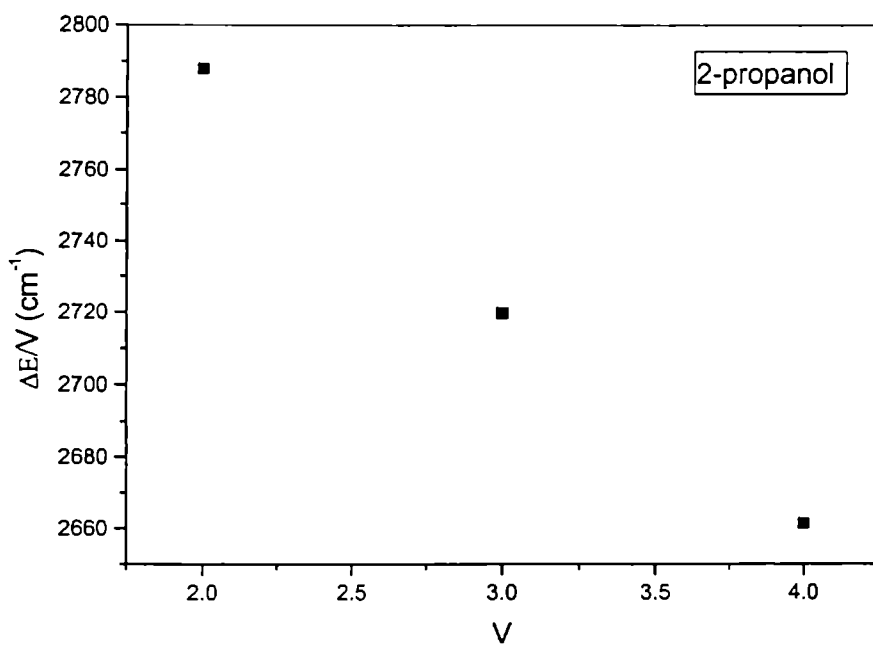


Fig. 5.14 Birge-Sponer plot for methynic CH overtones in 2-propanol

Table 5.2. Observed overtone transition energies (cm^{-1}), mechanical frequencies X_1 (cm^{-1}), and anharmonicities X_2 of OH, methyl CH and methynic CH in 2-propanol. The least square correlation coefficients (γ) are also given. The mechanical frequencies and anharmonicities of nitromethane are also given for a comparison.

Molecule	$\Delta V=2$	$\Delta V=3$	$\Delta V=4$	$\Delta V=5$	X_1	X_2	γ
2-propanol							
OH	7076.13	10365.91	13502.56	16460.9	3783	-81.73	-0.99996
Methyl CH	5768.67	8443.09	11024.14		3075	-64.15	-0.99904
Methynic CH	5576	8159.26	10645.09		2976	-58.12	-0.99901
Nitromethane							
Methyl CH					3143	-58	

The $\Delta V = 3$ region of OH in 2-propanol shows two well resolved peaks similar to those obtained in high resolution spectrum. The peaks 'a' represent OH overtones, 'b' represents methyl CH overtones and 'c' represents methynic CH overtones. The overtone peaks are assigned as those giving good least square fit for the Birge-Sponer plot with the pure overtone peaks in the other regions. The transition energies and local mode parameters of OH, methyl CH and methynic CH oscillators obtained from the Birge-Sponer relation are given in table 5.2. The methyl CH mechanical frequency in 2-propanol (3075cm^{-1}) is less than that in nitromethane (3143 cm^{-1} , chapter3). It is well established from overtone studies of substituted benzenes that an electron-withdrawing group causes an increase in mechanical frequency whereas an electron-donating group causes a decrease in mechanical frequency [32,33]. Since NO_2 is a withdrawing group, it increases the methyl CH mechanical frequency in nitromethane while in 2-propanol OH acts as a donating group and hence decreases the methyl CH mechanical frequency. The reported value of OH mechanical frequency in 2-propanol (trans conformer) in gas phase is 3805 cm^{-1} [20]. The OH mechanical frequency value obtained from the present liquid phase spectrum is 3783 cm^{-1} . The observed mechanical frequency value for CH_3 (methyl CH) is 3139 cm^{-1} , which is greater than that for CH (methynic CH) (3034 cm^{-1}). The relative energies of the peaks CH_3 , CH_2 , CH are observed to follow the familiar trend of decreasing CH bond strength from CH_3 to CH_2 to CH [34].

5.8 Conclusions

The high resolution spectrum of 2-propanol in the second OH overtone region is recorded for the first time using a NIR TDLAS setup. The spectrum shows two well –resolved peaks relating to trans and gauche conformations. The peak positions agree well with those reported earlier [20]. The liquid phase NIR spectrum also shows two peaks in the second OH overtone region. The decrease in methyl CH mechanical frequency in 2-propanol compared to nitromethane is explained as due to the substituent effect.

References

1. R.V.Ambartzumian and Lekhotov V.S *Appl. Opt.* 11 (1972) 354.
2. N.C.Peterson, M.J.Kurylo, W.Braun, A.M.Bass and K.A.Keller; *J.Opt. Soc. Am.* 61 (1971) 746.
3. P.D.Maker, R.W.Terhune, *Phys. Rev.* A137 (1965) 801.
4. W.Demtroder; "Laser Spectroscopy: Basic concepts and instrumentation", Second edition, Springer, 1996.
5. "An Introduction to Laser spectroscopy", Ed. D.L.Andrews and A.A.Demidov; Plenum press, New York, 1995.
6. B.B.Laud; "Lasers and non-linear optics", Second edition, New Age International (P) Ltd., New Delhi, 2001.
7. G.Herzberg; "Infrared and Raman spectra of polyatomic molecules", Van Nostrand, New York, 1995.
8. J.Michael Hollas; "High Resolution Spectroscopy", Second edition, John Wiley and sons, New York, 1998.
9. E.Hirota; "High Resolution Spectroscopy of transient molecules", Springer series in chemical Physics, 40 springer Verlag, 1985.
10. G.Winnewisser, T.Drascher, T.Giesen, I.Pak, F.Schmulling and R.Schieder; *Spectrochim.Acta. A* 55 (1999) 2121
11. V.S.Letokhov, "Laser Analytical Spectrochemistry", Adam Hilger, Bristol, 1986.
12. O.Vaittinen, L.Biennier, A.Camparge, J.M.Flaud and L.Halonen; *J. Mol. Spectrosc.*, 184 (1997) 288.
13. P.F.Coheur, S.Fally, M.Carleer, C.Clerbaux, R.Colin, A.Jenouvrier, M.F.Merienne, C.Hermans and A.C. Vandaele; *J. Quant. Spectrosc. Radiat. Trans.*, 74 (2002) 493.
14. C.Douketis and J.P.Reilly; *J. Chem. Phys.* 91 (1989) 5239.
15. A.Held and M.Herman, *Chem. Phys.*, 190 (1995) 407.
16. D.Luckhaus, *J. Chem. Phys.*, 106 (1997) 8409.
17. X.Zhan, M.Halonen, L.Halonen, H.Burger and O.Polanz; *J.Chem.Phys.*, 102 (1995) 3911.

18. A.Muntianu, B.Guo and P.F.Bernath; *J.Mol.Spectrosc.*, 176 (1996) 274.
19. J.A.Phillips, J.J.Orlando, G.S.Tyndall and V Vaida; *Chem. Phys. Lett.*, 296 (1998) 377.
20. H.L.Fang and D.A.C.Compton; *J. Phys. Chem.*, 92 (1988) 6518.
21. J.D.Weibel, C.F.Jackels and R.L.Swofford; *J. Chem. Phys.*, 117 (2002) 4245.
22. H.L.Fang, D.M.Meister and R.L.Swofford; *J. Phys. Chem.*, 88 (1984) 405.
23. S.M.Eappen, S.Shaji, T.M.A.Rasheed and K.P.R.Nair; (paper accepted for publication in *J. Quant.spectrosc.Radiat. Trans.*).
24. B R Henry; “*Vibrational spectra and structure*”, ed. J.R Durig (Elsevier Amsterdam.), 10 (1981) 269.
25. M S Child and L. Halonen; *Adv. Chem. Phys.*,57 (1984) 1.
26. R J Hayward, B R Henry; *J. Mol. Struct.* 57 (1975) 221.
27. B R Henry; *Acc. Chem. Res.*, 20 (1987) 429.
28. J.B. Birks; “*Photophysics of Aromatic molecules*” (Wiley, New York, 1970).
29. B.R.Henry and W.Siebrand; *J. Chem. Phys.*, 49 (1968) 5369.
30. E.W.Schlag, S.Schneider and S.F.Fischer; *Ann. Rev. Phys. Chem.*, 22(1971) 465.
31. B.R. Henry and M.Kasha; *Ann. Rev.. Phys. Chem.*,19 (1968) 161.
32. Y. Mizugai and M. Kattayama; *J.Am. Chem. Soc.*, 102 (1980) 6424.
33. S.Kuriakose, K.K. Vijayan, S.Shaji, S.M.Eappen, K.P.R.Nair and T.M.A.Rasheed; *Asian J.Phys.*, 11 (2002) 70.
34. W.R.A.Greenlay and B.R.Henry; *J.Chem.Phy.*, 69 (1978) 82.

SUMMARY AND CONCLUSIONS

The present work is mainly focused on the application of overtone spectroscopy for characterizing the CH, OH and NH bonds in some organic molecules. The NIR vibrational overtone spectra of the molecules from the first through fourth overtone levels are recorded by conventional spectrophotometric method using a commercial UV-Vis-NIR spectrometer, which uses a tungsten lamp as the light source. The observed NIR spectra of salicylaldehyde, benzaldehyde, phenyl hydrazine, phenol, o-chlorophenol, p-chlorophenol, formamide, nitromethane, allyl chloride and allyl alcohol are analyzed using local mode model.

The reduced value of aldehydic CH mechanical frequency value in benzaldehyde with respect to acetaldehyde is explained as due to the absence of indirect lone pair trans effect in that compound. The large value of aldehydic CH mechanical frequency observed in salicylaldehyde is due to the inhibition of donation of electron density from oxygen lone pair to the aldehydic CH bond. This inhibition of the direct lone pair trans effect is shown to occur due to the presence of the intramolecular hydrogen bonding between the OH and CHO groups. This observation gives an additional evidence for the originally present lone pair trans effect in aldehydes. The observed value of aryl CH mechanical frequency in salicylaldehyde agrees with the nature of substituent in the benzene ring. The presence of two NH bands in the overtone spectrum of phenyl hydrazine shows that the lone pair interaction between one of the NH and the adjacent nitrogen lone pair causes nonequivalent NH bonds. The large value of aryl CH mechanical frequency in phenyl hydrazine with respect to benzene is explained as due to the inductive electron withdrawal by the $-NH-NH_2$ group from the ring, in the absence of lone pair conjugation with the ring π electron system. The reduced value of NH mechanical frequency for both types of NH local modes in phenyl hydrazine is due to the existence of mutual lone pair interaction (the interaction between each one of the NH bond and the adjacent nitrogen lone pair) in hydrazine group as well as due to the inductive withdrawal of electrons by $-NH-NH_2$ group from the phenyl ring. A comparison of local mode parameters of

phenol, o-chlorophenol and p-chlorophenol shows that the OH local mode frequency in o-chlorophenol is much smaller than that in phenol due to the intramolecular hydrogen bonding between OH group and chlorine atom. In o-chlorophenol solution, as the concentration is decreased from high (saturated) values, the population of the trans form of the molecule increases, thus causing the formation of cis-trans dimer (due to intermolecular hydrogen bonding) to become dominant. This causes a decrease in the strength of the intramolecular hydrogen bonding originally present in the cis form. The weakening of intramolecular bonding causes a decrease in the electron density of the OH bond and hence an increase in the mechanical frequency value of the OH oscillator. This study shows that vibrational overtone spectroscopy can be used as a good diagnostic tool for probing even weak hydrogen bonding interactions existing in molecules.

The analysis of overtone spectrum of formamide shows that the lone pair trans effect is inhibited in formamide. The alkyl CH mechanical frequency in formamide is greater than the aldehydic CH mechanical frequency in salicylaldehyde. The large value of CH mechanical frequency occurs due to the binding of the lone pair of the NH_2 group by the carbonyl group and due to the presence of intermolecular hydrogen bonding, thereby inhibiting the lone pair trans effect. The local mode parameters of allyl alcohol show that one of the lone pair electrons of oxygen atom trans to CH bond of the CH_2OH group causes an interaction with CH bond and increases the electron density of methylene, which in turn reduces the mechanical frequency. In allyl chloride, CH_2Cl withdraws electrons from the vinyl group and increases the mechanical frequency of vinyl CH. The reduced value of mechanical frequency of vinyl CH in allyl alcohol is due to the electron donation by CH_2OH . The NIR CH vibrational overtone spectrum of liquid phase nitromethane is analyzed using the local mode picture. This approach uses a C_{3v} coupled oscillator Hamiltonian to predict the transition energies of pure CH local mode and local-local combination states of the methyl group. It is found that the observed transition energies generally agree with the calculated values.

The pulsed laser induced fluorescence /Raman spectra of some organic compounds are recorded using a Q-switched Nd:YAG laser-based setup. A

monochromator and a CCD detector are used for the spectral recording. The observed fluorescence emission for N,N diethyl aniline centred at 618 nm is assigned as due to π, π^* transition. Polymerized o-chloroaniline also shows a broad fluorescence emission centred at 625 nm with some sharp peaks. The fluorescence emission is due to π, π^* transition and the peaks arise from Raman scattering. The pulsed laser Raman spectra of some organic compounds are also recorded using the same experimental set up. The calibration of the set up is done using the laser Raman spectra of carbon tetrachloride and carbon disulphide. The characteristic peaks in the observed high quality laser Raman spectra for p-chlorotoluene, nitromethane, o-chlorophenol, and m-toluidine are unambiguously assigned as corresponding to aromatic ring, methyl CH and as the characteristic peaks due to the substituent groups in the compounds.

A NIR tunable diode laser absorption (TDLA) spectrometer is used for recording high resolution OH second overtone spectrum of 2-propanol. To our knowledge, this is the first measurement of the TDLAS overtone spectrum of 2-propanol. The spectrum gives the well-resolved fine structure corresponding to the two different conformers (trans and gauche) of the molecule. The observed band positions agree well with the low resolution spectral results reported earlier. The liquid phase spectrum of 2-propanol in the NIR region is spectrophotometrically recorded and analyzed using local mode model. The decrease in methyl CH mechanical frequency with respect to nitromethane is explained as due to the substituent effect.

List of papers published in journals

1. Overtone spectra of benzaldehyde and salicylaldehyde: Evidence for the inhibition of indirect and direct lone pair trans effects
Sunny Kuriakose, K. K. Vijayan, and T. M. A. Rasheed,
Asian Journal of Spectroscopy, Vol.1, No.1 (2001) 17-23.
2. Overtone spectra of allyl chloride and allyl alcohol in the near infra red Region
Sunny Kuriakose, K. K. Vijayan, S. Shaji, Shibu M Eapen, K. P. R. Nair and T. M.A. Rasheed, *Asian Journal of Physics, Vol.11, No.1 (2002) 70-74.*
3. Overtone spectrum of Phenyl hydrazine in the near infrared region
Sunny Kuriakose, K. K. Vijayan, K. P. R. Nair and T. M. A. Rasheed, *Asian Journal of Physics, (in press).*
4. Overtone spectrum of formamide in the near infrared region- evidence for the inhibition of lone pair trans effect
Sunny Kuriakose, K. K. Vijayan, Shibu M Eapen, S. Shaji, K. P. R. Nair and T. M. A. Rasheed,
Asian Journal of Spectroscopy, Vol.6 (2002) 43-46.
5. CH overtone spectrum of Nitromethane: a C_{3v} coupled oscillator analysis using local mode parameters
Sunny Kuriakose, K. K. Vijayan, K.P.R.Nair and T. M. A. Rasheed (communicated)
6. Overtone spectra of benzyl amine and furfuryl amine – a comparative study
K. K. Vijayan, **Sunny Kuriakose** and T. M. A. Rasheed,
Asian Journal of Physics, Vol.10, No.3, 2001.
7. Vibrational overtone spectrum of 2-furaldehyde in the NIR region,
K. K. Vijayan, **Sunny Kuriakose, S. Shaji and T. M. A. Rasheed,**
Asian Journal of Physics, Vol.11, No.1 (2002) 66-69.

8. Overtone spectrum of cinnamaldehyde in the NIR region- Evidence for indirect lone pair trans effect
K. K. Vijayan, **Sunny Kuriakose**, S Shaji, Shibu M Eapen, K. P. R Nair and T. M. A. Rasheed,
Asian Journal of Spectroscopy, Vol.5, No.4 (2001)185-189.
9. CH overtone spectrum of t-butyl amine: a C_{3v} coupled oscillator analysis using local mode parameters,
K. K. Vijayan, **Sunny Kuriakose**, K.P.R.Nair and T. M. A. Rasheed
Asian Journal of Spectroscopy, 6 (2002) 125-131.

Seminar

1. Overtone spectra of allyl chloride and allyl alcohol in the near infrared region
Sunny Kuriakose, K. K. Vijayan, S. Shaji, Shibu M Eapen, K. P. R. Nair and T. M.A. Rasheed,
National Symposium on Lasers, Spectroscopy and Laser Applications, 27-30 December 2001, Meerut.
2. Overtone spectrum of formamide in the NIR region
Sunny Kuriakose, K.K. Vijayan, Shibu M.Eapen, S. Shaji, K.P.R Nair and T.M.A Rasheed
National symposium on Atomic Molecular Structure, Interactions and Laser spectroscopy, 22-24 February 2002, Banaras Hindu University, Varanasi.
3. Vibrational overtone spectrum of 2-furaldehyde in the NIR region
K.K. Vijayan, **Sunny Kuriakose**, Shibu M.Eapen, S. Shaji, K.P.R Nair and T.M.A Rasheed
National Symposium on Lasers, Spectroscopy and Laser Applications, 27- 30 December 2001, Meerut.
4. Vibrational overtone spectrum of Cinnamaldehyde in the NIR region
K.K. Vijayan, **Sunny Kuriakose**, Shibu M.Eapen, S. Shaji, K.P.R Nair and T.M.A Rasheed
National symposium on Atomic Molecular Structure, Interactions and Laser Spectroscopy, 22-24 February 2002, Banaras Hindu University, Varanasi.
5. Aryl CH overtone Spectrum of liquid phase N, methyl aniline and N,N di-methylaniline – A conformational structural analysis using local mode model
Shibu M.Eapen, Venketeswara Pai. R, S. Shaji, **Sunny Kuriakose**, K.K.Vijayan, K.P.R Nair and T.M.A Rasheed
National symposium on Atomic Molecular Structure, Interactions and Laser Spectroscopy, 22-24 February 2002, Banaras Hindu University, Varanasi.